



**NTNU – Trondheim**  
Norwegian University of  
Science and Technology

# Dynamic Analysis and Design of Mooring Lines

**Michael Olivier Chrolenko**

Marine Technology

Submission date: June 2013

Supervisor: Carl Martin Larsen, IMT

Norwegian University of Science and Technology  
Department of Marine Technology



---

# Dynamic Analysis and Design of Mooring Lines

*Master Thesis*  
*Michael Chrolenko*  
*Marine Structures and Hydrodynamics*  
*Spring 2013*

---

NORWEGIAN UNIVERSITY OF SCIENCE AND TECHNOLOGY  
DEPARTMENT OF MARINE TECHNOLOGY

Supervisor MTS: Professor Carl M. Larsen  
Supervisor DNV: Erling Lone



## Preface

This master thesis concludes the Master Degree program of Marin Technology at the Norwegian University of Science and Technology (NTNU). This thesis has been carried out from January to June 2013 in cooperation with DNV.

First of all I would like to thank DNV, and especially my supervisor Erling Lone for guiding me through this semester. He has given me continues help, and pointed me in the right direction when getting of track. The help, time spent, and the lectures given are most appreciated. The effort and patience towards me has been outstanding, especially when repeating problems which were not fully understood.

Would also like to thank my supervisor here on MTS, Carl Marin Larsen. Apart from the scheduled appointments, his door has always been open for consultation on my master thesis. He has also taken initiative and signed me up for different program courses given by MARINTEK, as well as providing me with relevant articles. His help regarding RIFLEX problems are greatly appreciated.

A warm thank is also given to MARINTEK, especially Karl Erik Kaasen. He has been most helpful in discussing different topics related to MIMOSA by email and scheduled meetings throughout this semester. Elizabeth Passano and Knut Mo at MARINTEK are acknowledged for including me in the SIMA course, and for meeting me in person when help was needed. Would also like to thank MARINTEK for providing me with the programs and licenses used for this master thesis.

This master thesis has been quite interesting and very educational. Learning about all the different computation programs has been challenging, but very useful in preparing me for real life work. Overall I'm quite satisfied and pleased for choosing this task given by DNV.

MTS, Trondheim, 3rd June 2013



---

Michael Chrolenko





## M.Sc. thesis 2013

for

**Stud.tech. Michael Chrolenko**

### **DYNAMIC ANALYSIS AND DESIGN OF MOORING LINES**

Mooring line response may be calculated in frequency domain (FD) or in time domain (TD), and the choice of method is normally a compromise between accuracy and computational effort. FD methods are faster than the use of TD simulations, and in many cases provide satisfactory results. Due to the non-linear and dynamic behaviour of mooring lines, TD simulations provide the most accurate results, but are considerably more time-consuming and introduce statistical uncertainty to the calculations due to the stochastic nature of the response. For fatigue calculations, a large number of sea states must be considered, and FD is therefore the preferred choice given that the response properties are satisfactorily modelled.

At shallow water depths ( $\leq 100$  m), catenary moorings without buoyancy elements or clump weights are considered to have a quasi-static behaviour. This implies that the tension may be calculated from a static representation of the mooring line, and calculation methods as e.g. MIMOSA QS (FD) or SIMO (TD) are expected to yield satisfactory results. Whereas this is often the case for the *windward lines* (i.e. pointing towards the incoming waves), the response properties of the *leeward lines* (i.e. pointing away from the incoming waves) of turret moored FPSOs are different and not necessarily well captured by a quasi-static model.

In most cases, the windward lines are the critical lines with respect to extreme response for moored structures, due to both a high mean tension and a large dynamic contribution. For estimation of fatigue damage, on the other hand, only the dynamic contributions are considered. For turret moored structures the largest dynamic response is often seen in the leeward lines, and this effect increases with the longitudinal distance from COG to the turret. Thus, a study addressing the goodness for such units of the frequency domain methods (both QS and FEM) compared to fully dynamic time domain analyses would be of high value to the industry.

The main scope of the thesis will be to perform a comparison of results for mooring line analyses in frequency domain (FD) and time domain (TD), for a turret moored FPSO with catenary moorings at 100m water depth. The following software (all developed by MARINTEK) and analysis methods should be compared:

- MIMOSA QS method - Frequency domain, quasi-static
- MIMOSA FEM method - Frequency domain, dynamic (linearized)
- SIMO Time domain, quasi-static
- RIFLEX /3/ Time domain, dynamic and fully non-linear
- SIMA Program to take care of communication between programs

The main concern of the comparison will be to investigate differences in response calculations for leeward lines, for the purpose of estimating fatigue damage in a given short-term sea state.





The work may show to be more extensive than anticipated. Some topics may therefore be left out after discussion with the supervisor without any negative influence on the grading.

The candidate should in her/his report give a personal contribution to the solution of the problem formulated in this text. All assumptions and conclusions must be supported by mathematical models and/or references to physical effects in a logical manner.

The candidate should apply all available sources to find relevant literature and information on the actual problem.

The report should be well organised and give a clear presentation of the work and all conclusions. It is important that the text is well written and that tables and figures are used to support the verbal presentation. The report should be complete, but still as short as possible.

The final report must contain this text, an acknowledgement, summary, main body, conclusions and suggestions for further work, symbol list, references and appendices. All figures, tables and equations must be identified by numbers. References should be given by author name and year in the text, and presented alphabetically by name in the reference list. The report must be submitted in two copies unless otherwise has been agreed with the supervisor.

The supervisor may require that the candidate should give a written plan that describes the progress of the work after having received this text. The plan may contain a table of content for the report and also assumed use of computer resources.

From the report it should be possible to identify the work carried out by the candidate and what has been found in the available literature. It is important to give references to the original source for theories and experimental results.

The report must be signed by the candidate, include this text, appear as a paperback, and - if needed - have a separate enclosure (binder, DVD/ CD) with additional material.

The work will be carried out in cooperation with Det Norske Veritas, Trondheim

Contact person at DNV is Erling Neerland Lone  
Supervisor at NTNU is Professor Carl M. Larsen

Carl M. Larsen

Submitted: January 2013  
Deadline: 10 June 2013



## Abstract

This master thesis presents a comparison study, where the main focus has been to assess if simplified methods can be used for analysing mooring lines for a turret moored FPSO in shallow waters. The MIMOSA program applies frequency domain (FD) methods, which is categorized as a simplified method but with short computation time. Fully non-linear time domain (TD) analysis in RIFLEX, which is a time consuming process, accounts for all non-linear effects, and was assumed throughout this master thesis to yield the best results. It was also necessary to perform mooring line analysis in SIMO to be able to isolate different effects between the three computation programs. The results were then used to explain the differences between the finite element method in MIMOSA (MIM-FEM) and RIFLEX (RIF-FEM). The main focus throughout this master thesis has been on the leeward line because this line will experience large dynamics, and it will also be the critical line for fatigue damage. The windward line has mainly been used to compare with the leeward line. For fatigue damage the most important parameters are the standard deviation (STD) of low- and wave-frequency tension (LF and WF).

When performing a comparison study it is important to assure that the model in MIMOSA, SIMO, and RIFLEX are equivalent. This means that line characteristics, restoring force characteristics, environmental forces, motions, equilibrium positions, and pretensions are the same for all programs. In MIMOSA and SIMO all the 12 mooring lines were modelled, while only the windward and leeward lines were modelled in RIFLEX. Because RIFLEX needs to get prescribed motions from SIMO, most of the comparisons in verifying the model were made based on results from MIMOSA and SIMO.

Comparing the mean equilibrium position between MIMOSA and SIMO exceeded the acceptable range of 5% difference in the model verification process. This difference arises because the iteration process in SIMO did not find the exact equilibrium position. This resulted in a residual tension force. By performing simple hand calculations, this difference equaled the difference in mean equilibrium position between MIMOSA and SIMO and was therefore acceptable. In the end one could conclude that all the models were equivalent, and could thus be used for further analysis.

The programming part for this master thesis was quite time consuming. For every program (MIM,SIM,RIF) a batch script was made, which then was combined together with one main batch script. The various analyses could then be carried out from this main batch file automatically, and Matlab was then used to post process the results.

The results showed that a quasi-static representation is acceptable when calculating the STD of LF tension. The difference between MIM-FEM and RIF-FEM for STD of LF tension was 0,13% for the leeward line, and -3,58% for the windward line, meaning that MIM-FEM slightly under predicts the STD of LF tension for the windward line.

For the turret moored FPSO analysed in this master thesis, a quasi-static representation of the mooring lines is not recommended for the leeward and windward line because the STD of WF tension will be too conservative. The difference between the simplified FEM in MIMOSA and the fully non-linear TD analysis in RIFLEX was -22,48% for the leeward line, and -16,66% for the windward line. The difference here is mainly caused by the linearisation methods used in MIMOSA to account for geometrical stiffness and dynamic effects (drag and inertia forces acting on the mooring line). Using the simplified FEM in MIMOSA one will under predict the STD of WF tension for the windward and leeward line, and therefore under predict the results in the estimation of fatigue life in the mooring lines.

## Sammendrag

Denne master oppgaven presenterer en sammenlignings studie, hvor hoved fokuset er å estimere om forenklede metoder kan brukes til fortøynings analyse av turret forankret FPSO på grunt vann. MIMOSA programmet bruker frekvensplan (FD) metoder, som er kategorisert for å være forenklede metoder som bruker kort beregningstid. Full ikke-lineær tidsplan (TD) analyse i RIFLEX er tidkrevende fordi RIFLEX betrakter alle ikke-lineære effekter. Gjennom denne master oppgaven så antas det at RIFLEX gir de beste resultatene. Det var også nødvendig å gjennomføre fortøynings analysen i SIMO for å kunne skille mellom ulike effekter for disse tre nevnte programmene. Resultatene fra SIMO analysen ble brukt til å forklare forskjeller mellom element metoden i MIMOSA (MIM-FEM) og element metoden i RIFLEX (RIF-FEM). Hovedfokuset gjennom denne master oppgaven har vært å se på le-linen fordi denne fortøyningslinen vil oppleve stor dynamikk samt også være den kritiske linen for utmattingssskade. Lo-linen har hovedsakelig blitt brukt til sammenligninger med le-linen. De viktigste parameterne når man ser på utmattingssskade er standard avvik (STD) for lav- og bølgefrequent strekk (LF og WF).

Når en sammenlignings studie skal utføres er det viktig å forsikre seg om at alle modellene i de tre programmene; MIMOSA, SIMO og RIFLEX er ekvivalente. Dette innebærer at line karakteristikk, fjæringskraft karakteristikk, miljø krefter, bevegelser, likevekts posisjoner, og forspenninger er like for alle programmene. I MIMOSA og SIMO så er alle de 12 fortøyningslinene modellert, mens i RIFLEX er kun lo- og le-linen modellert. Fordi RIFLEX for bevegelsen sin fra SIMO så vil mye av sammenligningen i verifiserings prosessen være basert på resultatene fra MIMOSA og SIMO.

Når likevekts posisjonen mellom MIMOSA og SIMO ble sammenlignet i verifiserings prosessen så overgikk denne sammenligningen den akseptable grensen, hvor akseptabel grense er på mindre en 5% forskjell. Forskjellen oppstår fordi SIMO ikke klarte å finne den eksakte likevekts posisjonen. Dette resulterte i en restkraft. Ved å utføre en enkel håndberegning ble det vist at denne restkraft forskjellen er lik forskjellen i likevekts posisjonen mellom MIMOSA og SIMO. Konklusjonen i verifiserings prosessen ble at alle modellene er ekvivalente og kan brukes videre i prosjektet.

Programmerings delen i denne master oppgaven var meget tidkrevende. For hvert program (MIM, SIM, RIF) ble det laget et batch-skript, som videre ble koblet sammen med et hoved batch-skript. De forskjellige analysene kunne nå bli kjørt fra dette hoved skriptet automatisk. Når alle analysene er ferdige ble Matlab brukt for prosessering av resultatene.

Resultatene viste at en kvasi-statisk representasjon er akseptabel for beregningen av STD av LF strekk. Forskjellen mellom MIM-FEM og RIF-FEM for STD av LF strekk var på 0,13% for lo-linen, og -3,58% for le-linen. Dette betyr at MIM-FEM så vidt under estimerer STD av LF strekk for le-linen.

I denne master oppgaven ble en turret forankret FPSO analysert, og en kvasi-statisk representasjon av fortøyningslinene er ikke anbefalt. Dette er fordi en slik representasjon av lo- og le-linen vil gi for konservative resultater. Forskjellen mellom den forenklede element metoden i MIMOSA og full ikke-lineær TD analyse i RIFLEX var på -22,48% for lo-linen, og -16,66% for le-linen. Hoved forskjellen kommer av lineariserings prosessen som foregår i MIMOSA som skal betrakte geometrisk stivhet og dynamiske effekter (drag og masse krefter som virker på fortøyningslinen). Ved å bruke den forenklede element metoden i MIMOSA vil man under estimere STD av WF strekk for lo- og le-linen, som igjen vil under estimere utmattings levetiden til fortøyningslinene.



# Contents

Preface . . . . .	i
Abstract . . . . .	vii
Sammendrag . . . . .	ix
Nomenclature . . . . .	xvii
<b>1 Introduction</b>	<b>1</b>
1.1 Background for master thesis . . . . .	2
<b>2 Mooring System - General Theory</b>	<b>3</b>
2.1 Mooring/Anchor Lines . . . . .	3
2.1.1 Drag Forces and Damping . . . . .	5
2.1.2 Stiffness . . . . .	6
2.2 Separate and Coupled Analysis . . . . .	7
2.3 Fatigue Damage . . . . .	8
<b>3 Modelling Procedure</b>	<b>12</b>
3.1 Model Implementation . . . . .	12
3.2 Case Parameter Study . . . . .	14
3.3 Model Verification . . . . .	15
3.3.1 Mean Environmental Forces . . . . .	16
3.3.2 Anchor Coordinates and Pretension . . . . .	17
3.3.3 "Mean" Position (equilibrium) . . . . .	18
3.3.4 "Mean" tension . . . . .	19
3.3.5 Line Characteristics . . . . .	19
3.3.6 Restoring Force Characteristics . . . . .	20
3.3.7 Conclusion - Model verification . . . . .	21
<b>4 Program Structure</b>	<b>23</b>
4.1 MIMOSA, SIMO, RIFLEX (MSR) Script - Main batch script . . . . .	23
4.2 MIMOSA . . . . .	24
4.3 SIMO . . . . .	25
4.4 RIFLEX . . . . .	27
4.5 Post Processing - Matlab . . . . .	28
<b>5 Program Theory</b>	<b>29</b>
5.1 MIMOSA . . . . .	30
5.1.1 LF tension - Only Quasi-Staticly . . . . .	30
5.1.2 WF tension - General . . . . .	31

5.1.3	WF tension - QS . . . . .	32
5.1.4	WF tension - FEM . . . . .	32
5.1.5	Non-linear WF tension - FEM . . . . .	33
5.2	SIMO . . . . .	34
5.2.1	Mooring line tension . . . . .	34
5.3	RIFLEX . . . . .	34
5.3.1	Fully non-linear analysis . . . . .	35
5.3.2	Linearised FEM analysis . . . . .	35
5.4	Summary of program theory . . . . .	36
<b>6</b>	<b>Case Study</b>	<b>37</b>
6.1	System Description . . . . .	37
6.2	Environmental Condition . . . . .	39
6.3	Calculation Methods . . . . .	39
6.3.1	General . . . . .	39
6.3.2	Time Domain . . . . .	40
6.4	Filter Design . . . . .	40
6.5	Fatigue Analysis . . . . .	44
<b>7</b>	<b>Results and Discussions</b>	<b>46</b>
7.1	Results . . . . .	46
7.2	Windward vs. Leeward line . . . . .	49
7.3	Comparison differences between methods: STD of WF tension . . . . .	51
7.3.1	Importance of updated line characteristics . . . . .	51
7.3.2	Importance of dynamic effects . . . . .	52
7.3.3	STD of WF tension: MIM-QS vs MIM-FEM . . . . .	53
7.3.4	STD of WF tension: MIM-FEM vs RIF-FEM . . . . .	54
<b>8</b>	<b>Conclusion</b>	<b>55</b>
8.1	Conclusion from discussions and results . . . . .	55
8.2	Suggestions for further work . . . . .	56
8.3	Practical improvement . . . . .	56
<b>A</b>	<b>Information Retrieval</b>	<b>I</b>
<b>B</b>	<b>Programlist</b>	<b>II</b>
<b>C</b>	<b>Case Parameter Study in MIMOSA - Results</b>	<b>III</b>
<b>D</b>	<b>Plots of Main Results</b>	<b>XI</b>
<b>E</b>	<b>Matlab Script for Post Processing</b>	<b>XIII</b>
<b>F</b>	<b>Marginal Distribution for <math>H_s</math> Based on Joint Probability Distribution of <math>H_s</math> and <math>T_P</math> (from article)</b>	<b>XL</b>
<b>G</b>	<b>Attached CD: Description of content</b>	<b>XLI</b>



# List of Figures

1.1	Two main types of turret moored systems . . . . .	1
2.1	Example of a typical line segment composition . . . . .	3
2.2	Shows the 2D forces acting on an mooring line element [Faltinsen, 1990] . . . . .	4
2.3	Mooring line profile from fairlead to touch-down point showing drag forces on the line (red arrows). Y-axis is depth [m], x-axis is the distance from fairlead to touch-down point [m] . . . . .	5
2.4	Motion-to-tension transfer function calculated by MIMOSA . . . . .	7
2.5	Illustration of the separated and coupled analysis . . . . .	8
2.6	Example of an S-N curve with two fatigue damage components, $d_1$ and $d_2$ . . . . .	10
3.1	Turret mooring system modelled in SIMA, 3D view . . . . .	12
3.2	Turret mooring system modelled in SIMA, 3D view from the side . . . . .	13
3.3	Horizontal and vertical projection of mooring system from MIMOSA . . . . .	13
3.4	Comparing mean forces for surge component . . . . .	17
3.5	Line characteristics for MIMOSA, SIMO, and RIFLEX (line 1). Negative x-value: moving towards the anchor. Positive x-value: moving from the anchor. . . . .	19
3.6	Restoring Force Characteristics for MIMOSA and SIMO plotted from 0 to 2,50 m . . . . .	20
4.1	Float diagram with description for MIMOSA, SIMO, RIFLEX (MSR) Script . . . . .	24
4.2	MIMOSA script description . . . . .	24
4.3	MIMOSA float diagram - script procedure . . . . .	25
4.4	SIMO script description . . . . .	26
4.5	SIMO float diagram - script procedure . . . . .	26
4.6	RIFLEX script description . . . . .	27
4.7	RIFLEX float diagram - script procedure . . . . .	27
4.8	Matlab script description . . . . .	28
4.9	Matlab float diagram - script procedure . . . . .	28
5.1	Calculating the STD of LF tension using mooring line characteristics, where T-STD is STD of tension . . . . .	31
6.1	Original mooring line composition . . . . .	38
6.2	FFT on the time series for SIMO (upper) and RIFLEX (lower) - line 1 (left) and line 7 (right) . . . . .	41
6.3	Designed filter. 4th order Butterworth bandpass filter . . . . .	42
6.4	Original (WF&LF) and filtered WF and LF tension forces for line 1 (upper) and line 7 (lower) for SIMO . . . . .	43

6.5	Original (WF&LF) and filtered WF and LF tension forces for line 1 (upper) and line 7 (lower) for RIFLEX . . . . .	43
6.6	Fatigue damage graphs. Maximum stress line 1 (upper left), fatigue damage results using CS approach (upper right). Maximum stress line 7 (lower left), fatigue damage results using CS approach (lower right) . . . . .	45
7.1	Comparing the main results from MIMOSA, SIMO and RIFLEX in a barplot . . . . .	47
7.2	Illustration of a elliptical motion for a turret moored FPSO, and the resulting forces due to this motion (red arrows) . . . . .	49
7.3	Comparing filtered WF and LF tension forces for windward (line 1) and leeward line (line 7) from RIFLEX time series. Plot: 300 s - 1300 s. . . . .	50
7.4	Comparing WF tension between SIMO and RIFLEX for leeward line (upper graph). Lower plot is the surge motion for the same time series. Plot: 300 s - 500 s . . . . .	52
C.1	Bar-plot of the ratio for all cases . . . . .	IV
C.2	Matlab results Base Case . . . . .	V
C.3	Matlab results Case 1 . . . . .	V
C.4	Matlab results Case 2 . . . . .	VI
C.5	Matlab results Case 3 . . . . .	VI
C.6	Matlab results Case 4a . . . . .	VII
C.7	Matlab results Case 4b . . . . .	VII
C.8	Matlab results Case 5 . . . . .	VIII
C.9	Matlab results Case 6 . . . . .	VIII
D.1	Comparing WF and LF tension for RIFLEX and SIMO, 300 s - 5000 s. In both figures the upper graph compares LF tension, while the lower graph (around $y = 0$ ) compares WF tension. . . . .	XI
D.2	Line 1: Compares LF tension for SIMO and RIFLEX, 9 hour simulation . . . . .	XII
D.3	Line 7: Compares LF tension for SIMO and RIFLEX, 9 hour simulation . . . . .	XII

# List of Tables

2.1	Fatigue curve parameters proposed by the DNV rules . . . . .	9
3.1	Case Description . . . . .	14
3.2	Case parameter study . . . . .	14
3.3	Summary of the STD WF tension ratio between MIM-FEM and MIM-QS for windward and leeward line . . . . .	15
3.4	Program Comparison - Model Verification . . . . .	16
3.5	Mean environmental force comparison in initial position (MIMOSA and SIMO) . . . . .	16
3.6	Comparing calculated anchor coordinates . . . . .	17
3.7	Anchor coordinates and Pretension . . . . .	18
3.8	"Mean" Position (equilibrium) comparison . . . . .	18
3.9	"Mean" Tension comparison . . . . .	19
3.10	Restoring force comparison between MIMOSA and SIMO . . . . .	20
3.11	Conclusion table - Model Verification . . . . .	21
5.1	Advantages and disadvantages regarding the use of FD or TD methods . . . . .	29
5.2	Compares different effects that are included or not included in the calculation methods for all the three computation programs used. '√' - accounted for in the analysis method. 's' - accounted for in a simplified manner. . . . .	36
6.1	FPSO data given by Erling Lone, DNV . . . . .	37
6.2	Original and modified mooring system data . . . . .	38
6.3	Line segment properties given by Erling Lone, DNV . . . . .	38
6.4	Environment description. Used for all models . . . . .	39
6.5	Comparing calculated STD tension with the original STD tension force . . . . .	42
7.1	Description of calculation methods, explanation of abbreviations used in tables and graphs. For a more detailed description of computation methods see chapter 5 . . . . .	47
7.2	Main comparison results for line 1 and 7. All the values in the table are STD, and the table is sorted in the order of importance . . . . .	48
7.3	STD of WF tension difference for leeward line (line 7) . . . . .	54
C.1	Case parameter study . . . . .	III
C.2	STD tension ratio for Windward line . . . . .	IV
C.3	STD tension ratio for Leeward line . . . . .	IV
F.1	Marginal distribution for $H_s$ based on joint probability distribution of $H_s$ and $T_P$ , retrieved from [Larsen, 1987] . . . . .	XL



## Nomenclature

General rules:

- Parameters used in equations are explained after the equation has been used.
- Abbreviations are given after the first use of the term

## Roman Letters

$T_p$	Peak period
$H_s$	Significant wave height
$t_z$	Mean up-crossing period
$d_c$	Summarized load cycle for fatigue damage
$d_{CS}$	Fatigue damage for combined spectrum
$A$	Cross section area
$X_{Global}$	Global x-coordinate
$Y_{Global}$	Global y-coordinate
$k$	Mooring line stiffness
$k_{MIM}$	Mooring line stiffness for MIMOSA
$k_{SIM}$	Mooring line stiffness for SIMO
$r$	Projection of the horizontal distance
$wd$	Water depth
$xt$	Turret x position
$m$	Meters

## Greek Letters

$\beta$	Weight parameter used in the Newmark- $\beta$ method
$\gamma$	Weight parameter used in the Newmark- $\beta$ method
$\sigma$	Standard Deviation
$\nu_{Li}$	LF component for mean-up-crossing rate
$\nu_{Wi}$	WF component for mean-up-crossing rate
$\Delta F$	Force difference between two points
$\Delta x$	Displacement difference between two points
$\Delta t$	Time step

## Matrices

$\mathbf{M}$	Mass matrix
$\mathbf{C}$	Damping matrix
$\mathbf{K}$	Restoring matrix
$\mathbf{F}$	Force vector
$\mathbf{r}$	3 (surge, sway, yaw) or 6 DOF position vector

## Abbreviations

FPSO	Floating, Production, Storage and Offloading vessel
TD	Time domain
FD	Frequency domain
WF	Wave frequency
LF	Low-frequency
WF&LF	Combined wave- and low-frequency
DOF	Degree(s) of Freedom
FEM	Finite Element Method
QS	Quasi-static Method
SAM	Simplified Analytic model (also referred to as Simplified Analysis Method)
COG	Center of gravity
LCG	Longitudinal center of gravity
RAO	Response Amplitude Operator
CS	Combined Spectrum Approach
DNB	Dual Narrow-band Approach
RFC	Rain-Flow Counting
FEM-WF	WF analysis by using FEM
QS-WF	WF analysis by using QS-method
QS-LF	LF analysis by using QS-method
FFT	Fast Fourier Transform
TLP	Tension-leg Platform
MIM	MIMOSA computation program developed by MARINTEK, FD analysis
SIM	SIMO computation program developed by MARINTEK, TD analysis
RIF	RIFLEX computation program developed by MARINTEK, TD analysis
MSR	MIMOSA,SIMO,RIFLEX program
Env.dir.	Environmental propagating direction (180 degrees; propagates towards south)
T-STD1	Standard deviation of tension 1
T-STD2	Standard deviation of tension 2
F <sub>s</sub>	Sampling Frequency
MIM-FEM	MIMOSA Finite Element Method calculation
MIM-QS	MIMOSA Quasi-Static Method calculation
SIMO-QS	SIMO Quasi-Static Method calculation
SIMO-SAM	SIMO Simplified Analytic Model calculation
RIF-FEM	RIFLEX Finite Element Method calculation
Line 1	Windward line
Line 7	Leeward line

# Chapter 1

## Introduction

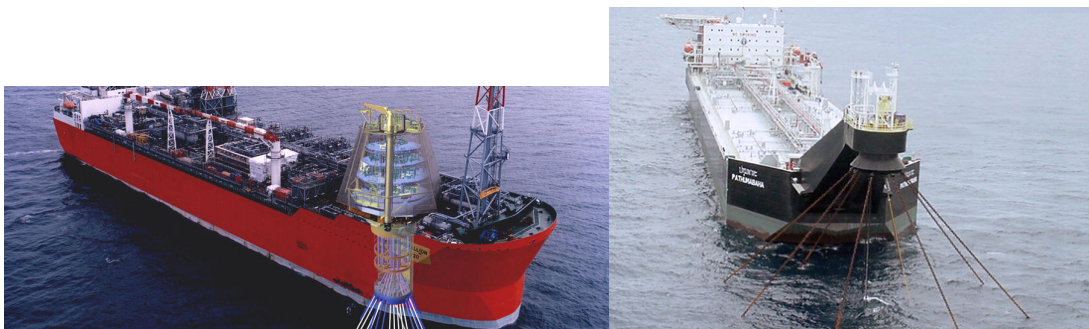
In marine operations it is important to keep a precise position. For instance, when conducting a drilling operation one wishes to minimize the movements of the drilling riser, because too much movement can cause the riser to fail. Thruster and mooring systems are used to withstand environmental loads which arise from waves, wind, and current.

A mooring system is composed of a number of cables which are connected to the floater. They are oriented in a radial fashion around the mooring point. The lower end of the cables are attached to the seabed with anchors. There are several mooring systems that exist, and the one that will be dealt with in this master thesis is a turret moored system [Faltinsen, 1990].

There are two main types of a turret moored system:

- Internal moored system
- External moored system

The internal moored system is integrated into the forward end of a vessel, where there is a large roller bearing which is either located within a moonpool or at deck level. An external moored system is situated outside the vessel's hull, and can be located close to the bow or close to the stern of the vessel. Figure 1.1a shows a picture of a FPSO which has an internal turret mooring system, while figure 1.1b shows an oil tanker with an external turret mooring system.



(a) Internal turret moored system

(b) External turret moored system

Figure 1.1: Two main types of turret moored systems

What makes a turret moored system special is that the vessel can rotate around the fixed turret. The vessel can then position itself in such a way that it minimizes the forces acting on the vessel from the environment. It is also easier to keep the desired position with such systems. Fewer chains and smaller anchors can then be used compared to a traditionally spread mooring system. This is one of the main advantages with a turret moored system. One of the advantages by using a internal turret moored system instead if a external one is that it can accommodate more risers. On the other hand, an external turret moored system can be used to moor in deeper waters. The mooring forces acting on the turret need to be transferred to the ships hull, which give rise to large mechanical challenges compared to a spread mooring system [SMB-Offshore, 2013], [Miedema, 2013].

## 1.1 Background for master thesis

The main goal in this master thesis is to assess if simplified computations methods can be used for an internal turret moored FPSO in shallow waters. The main focus will be on parameters that are important and governing for fatigue damage. The MIMOSA program is assumed to be the simplified computation method which used frequency domain (FD) methods. The RIFLEX program, which uses time domain (TD) methods, will be used to compare with the MIMOSA program.

MIMOSA, SIMO, and RIFLEX will be compared about each other in an attempt to isolate different effects. When performing a comparison study it is important that all the models in the different programs are equivalent, and in this master thesis a chapter deals with how all the models were verified for further use. It is also important to have knowledge about how the different programs calculate the parameters which are of interest for fatigue damage. This will be covered in the chapter dealing with program theory.

A lot of time will be spent on creating batch-scripts and sub-routines within all the three programs. Float diagrams for the different batch-scripts will therefore be presented in the main report.

In the end of the master thesis the case which was used will be presented followed by results and discussions.



## Chapter 2

# Mooring System - General Theory

### 2.1 Mooring/Anchor Lines

Mooring lines are usually composed of several segments which normally are a combination of chain (heavy cable at the mid section) and wire rope (lighter cable at the sea surface). This typical combination will increase the stiffness in the mooring system, meanwhile getting a much more lighter cable system [Faltinsen, 1990]. Figure 2.1 illustrates how a mooring line can be composed of several segments.

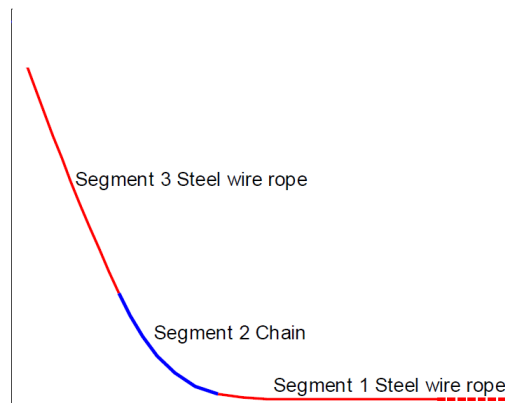


Figure 2.1: Example of a typical line segment composition

Mooring lines have to withstand forces that arise from the vessels static movements, and also the environmental loads that act on the mooring line itself. Current forces will induce drag forces on the line and could give dynamic amplification. This will give various tension forces in the anchor line [Fylling and Larsen, 1982] [Faltinsen, 1990]. The next figure shows a mooring line element and the force components that act on the element.

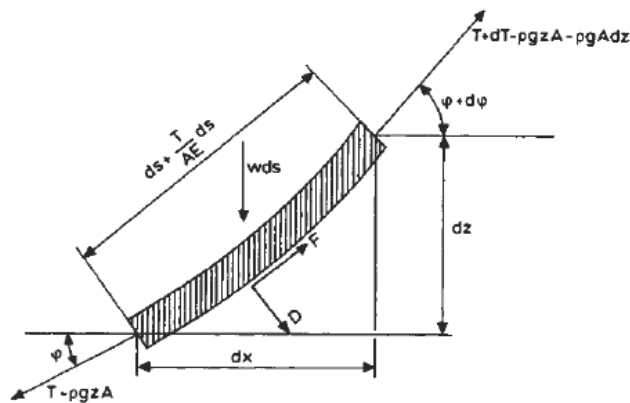


Figure 2.2: Shows the 2D forces acting on an mooring line element [Faltinsen, 1990]

$T$  - Axial tension [N],

$w$  - submerged weight of the unit length [N/m],

$AE$  - axial elastic stiffness [N], where  $A$  is the cross section [ $m^2$ ], and  $E$  is the Young's modulus [MPa],

$x, z$  - horizontal and vertical coordinates [m],

$s$  - arc length variable [m],

$\varphi$  - angle between tangential tension force and horizontal plane [rad],

$F$  - hydrodynamic force in tangential direction [N],

$D$  - hydrodynamic force in transverse direction [N].

When a floater is exposed to different sea states, the mooring lines will experiences three processes that occur simultaneously:

- Mean offset due to environmental forces (waves, wind, and current),
- Low-Frequency (LF) offset which arise from slow-drift motions (large amplitude),
- Wave-Frequency (WF) motions of the vessel (moderate amplitude).

These three points can cause rapid motions of the vessel, and give rise to instantaneous tensions in the anchor lines, especially in surge and sway for a moored system. FPSO vessels usually have a turret moored system which helps to weather vane. This means that the vessel positions itself so that the weather propagates towards the bow. This will minimize the forces acting on the vessel, which means that the tension in the mooring lines will also be minimized. The horizontal motion (surge) is therefore the most interesting motion when it comes to finding the mooring line tension. This is because of the turrets weather vane abilities will always result in a horizontal (surge) motion, which will give rise to the largest displacements.

### 2.1.1 Drag Forces and Damping

When a mooring line experiences rapid motions through the water, large flow velocities through the line, the mooring line will induce non-linear drag forces. The vessel will then *feel* this drag force as a damping force. From the drag term in Morrison's equation (eq. 2.1) the velocity will be squared, and this means that drag forces are highly dependent on the flow velocity. An illustration of how drag forces are induced on a mooring line due to rapid motions is given in figure 2.3.

$$dF = \rho\pi\frac{D^2}{4}C_M a_1 + \frac{\rho}{2}C_D D|u|u \quad (2.1)$$

$D$  - Line diameter [m],

$\rho$  - water density [ $\frac{kg}{m^3}$ ],

$C_M$  - mass coefficient [-],

$C_D$  - drag coefficient [-],

$u$  - flow velocity through the line [ $\frac{m}{s}$ ],

$a_1$  - horizontal acceleration (x-direction) [ $\frac{m}{s^2}$ ].

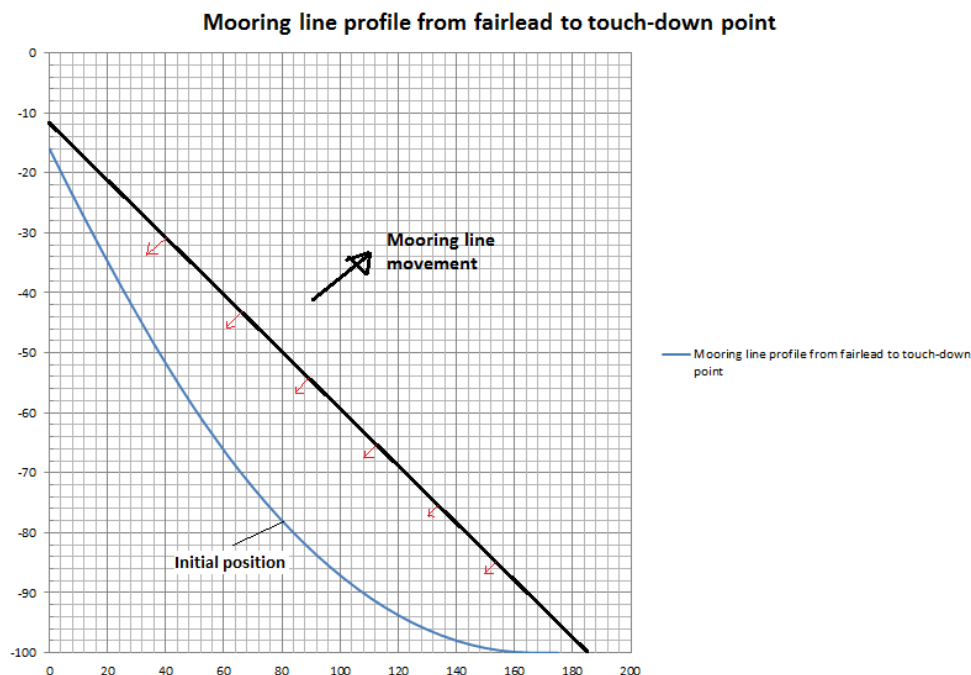


Figure 2.3: Mooring line profile from fairlead to touch-down point showing drag forces on the line (red arrows). Y-axis is depth [m], x-axis is the distance from fairlead to touch-down point [m]

William C. Webster [Webster, 1995] carried out a study showing how mooring lines induce damping for moored skip-like platform. In Webster's paper he focused on roll and surge motions, and the damping of the mooring lines in the fairlead position. Roll motions was studied because the magnitude of roll motions at resonance is governed by damping, and at severe seas surge motions is the most important motion which can lead to quite taut mooring lines. By looking at the energy absorbed by the moor, Webster performed a parameter study that showed the effect of scope (mooring line length and depth ratio), drag coefficient, excitation period, stiffness, and current. Two mechanisms were modelled, cross-flow drag and internal damping of the mooring lines. From Webster's study the following was concluded:

- Mooring-induced damping is complex, and that the transverse and longitudinal motions compete with each other. There is a balance between them for each response.
- Damping decreases when drag coefficients increase for high pretensions
- When increasing the mooring line stiffness there is a drastic increase in damping for horizontal and vertical motions.
- For low pretensions the damping increases with higher frequency excitations (horizontal motion). For higher pretensions the damping decreases for higher frequency excitations (horizontal motion).
- Increasing the current give small changes in damping. The difference between including and not including current forces acting on the mooring lines will give small changes in the horizontal motion. The difference in the vertical motion can for all practical purposes be neglected.

In a research article written by H. Ormberg and K. Larsen [Ormberg and Larsen, 1998], they investigate the coupled analysis of a turret-moored ship. In this article they illustrated how the current affects the static offset of the mooring lines. In practise, the current has often been neglected when running a mooring line analysis. The mean offset will be incorrect by neglecting the current forces completely, while the mean horizontal restoring force will be correct. On the other hand, if the current forces are included as a fixed forces on the vessel the mean horizontal restoring force will be overestimated, while the static offset will be correct. The inaccuracy will increase with increasing water depth, increasing current velocity, or increasing number of mooring lines. Meanwhile the line tension calculated with or without current is basically unchanged. The unchanged line tension force is due to the fact that current will only change the top end angle of the line, and the tension experience will be the same. The LF damping from mooring lines and risers are established by performing a linear damping procedure.

### 2.1.2 Stiffness

Mooring line stiffness is governed by geometrical and elastic stiffness. The elastic stiffness arise from the cables elastic properties, while the geometrical stiffness is due to the change in mooring line geometry [Faltinsen, 1990]. When simply summarizing these flexibilities we get an effective stiffness as shown in the following equation:

$$\frac{1}{k_{Effective}} = \left( \frac{1}{k_{Geometric}} + \frac{1}{k_{Elastic}} \right) \quad (2.2)$$

From equation 2.2 we see that, when  $k_G \rightarrow \infty$  the total stiffness is governed by elastic elongation. Physically this means that the mooring line is totally stretched out, and material properties will govern the total stiffness. If  $k_E \rightarrow \infty$  then we see that the total stiffness is governed by geometrical properties, which is non-linear geometry stiffness and is dependent on the mooring line characteristics. Non-linear geometrical stiffness is one of the most important non-linear effects regarding mooring lines, and need to be properly accounted for when performing a mooring line analysis.

Figure 2.4 shows the motion-to-tension transfer function calculated by MIMOSA. This transfer function illustrates what stiffness contributions are governing for the line tension for various frequencies. For low frequencies, when drag forces are almost negligible due to slow drift motions, the line tension is governed by the effective stiffness or quasi-static stiffness. For high frequencies, where drag forces contribute significantly due to rapid motions, the line tension is governed by elastic stiffness.

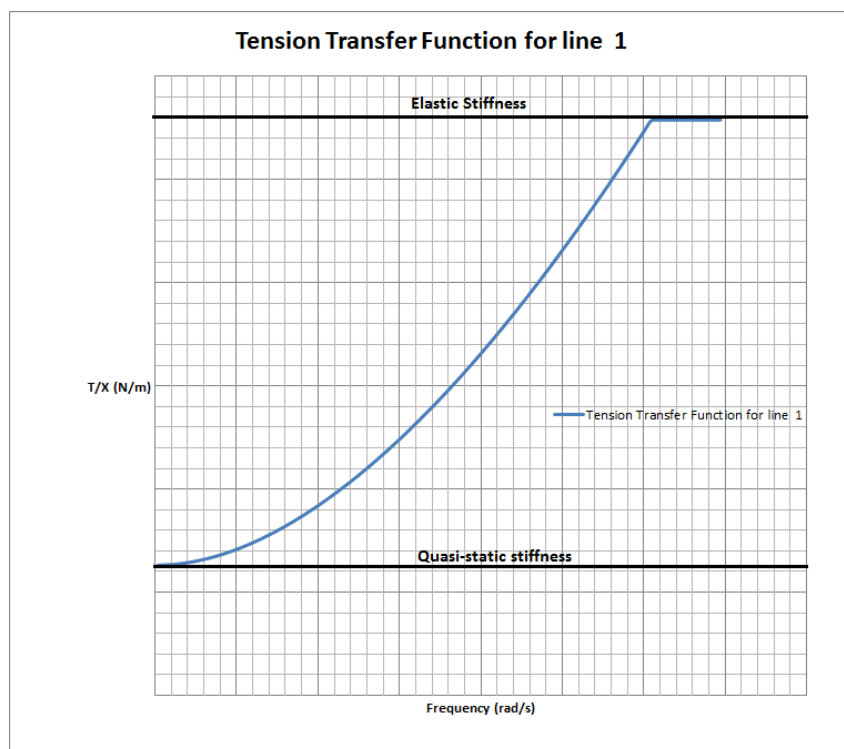


Figure 2.4: Motion-to-tension transfer function calculated by MIMOSA

## 2.2 Separate and Coupled Analysis

Separate analysis is usually referred to as a vessel motion analysis. This is because of the technique used in obtaining the dynamic response of the mooring lines and risers. Articles and conference papers are published that compare separate and coupled analysis with each other. In some articles these two methods are also compared with model tests. The next figure gives a good illustration of the differences between performing a separate and coupled analysis. The next figure and the content of this section is taken from the conference paper, [Ormberg et al., 1997], and article, [Ormberg and Larsen, 1998].

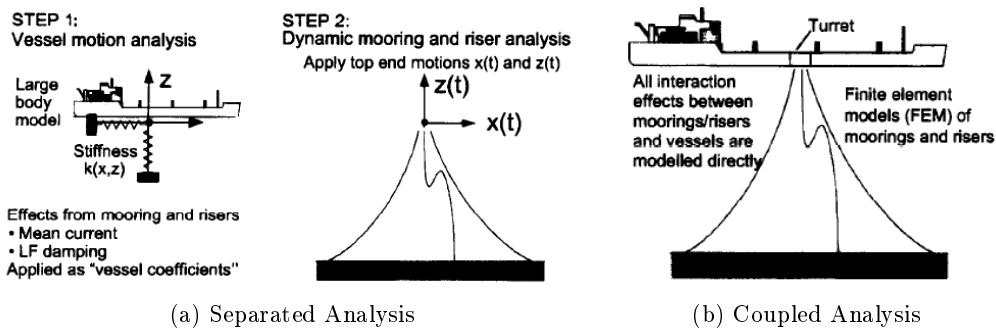


Figure 2.5: Illustration of the separated and coupled analysis

In a separated analysis vessel motion analysis is carried out first. Mean current, LF damping and mass are applied as vessel coefficients in the vessel motion analysis. In the dynamic mooring line and riser analysis the motion carried out in step 1 is applied. Due to this simplification, there are some shortcomings:

- Mean loads on risers and mooring lines are not sufficiently accounted for,
- for weakly damped systems, such as moored ships, LF response is important. The damping effect from the mooring and riser systems need to be included in a simplified way.

For a coupled analysis these effects listed above are accounted for, and is the main reason for performing a coupled analysis. All interaction between mooring lines/risers and vessel are modelled directly. In other words, to sufficiently account for mean offset and LF motions a coupled analysis is preferable, especially for increased water depths, when the mean offset and LF motions govern the total motion.

One of the main conclusions made in the research article written by Ormberg and Larsen were that the coupled analysis give quite good results compared with experiment tests. For a separated analysis without LF damping and mean current forces, the total surge motion will be over predicted. Including the LF damping and mean current forces in the separated analysis will under predict the total surge motion. The case study (in the article) for a turret moored ship at 2000 m water depth gave some interesting results. At this water depth 62 % of the surge damping is due to the mooring lines and risers. Due to this high percentage, the LF damping coefficients that are implemented in the floater coefficients need to be dealt with care if the separated analysis is to be the chosen method. In deep waters it is therefore preferable to perform a coupled analysis even though it might be more time consuming.

## 2.3 Fatigue Damage

The content of this section is based on DNVs offshore standard [DNV, 2010].

The characteristic fatigue damage summarizes the cycle loading on the mooring line:

$$d_c = \sum_{i=1}^{i=n} d_i, \quad (2.3)$$

where  $d_i$  is the fatigue damage in the component arising from sea state  $i$ . If the LF stress components from the analysis are small, and can therefore be neglected, then a narrow-band assumption may be used. Because of this assumption, the following equation may be used:

$$d_{NBi} = \frac{v_{0i} T_i}{a_D} (2\sqrt{2}\sigma_{Si})^m \Gamma\left(\frac{m}{2} + 1\right) \quad (2.4)$$

$v_{0i}$  - Mean-up crossing rate of the tension process [Hz],

$T_i$  - duration of the environment state  $T_i = P_i * T_D$  [s],

$P_i$  - probability of occurrence for state  $i$  [-],

$T_D$  - design lifetime of the mooring line component in seconds [s],

$\sigma_{Si}$  - standard deviation of the stress process [MPa],

$a_D$  - intercept parameter of the S-N curve [-],

$m$  - S-N curve slope parameter [-],

$\Gamma(.)$  - gamma function [-].

$a_D$  and  $m$  are parameters that can be found from the S-N curves which are proposed by the DNV rules for sea water. The two parameters are given in table 2.1 and depend on what kind of cable is used.

Fatigue Curve Parameters		
	$a_D$	$m$
Stud chain	$1.2 * 10^{11}$	3.0
Studless chain (open link)	$6.0 * 10^{10}$	3.0
Stranded rope	$3.4 * 10^{14}$	4.0
Spiral rope	$1.7 * 10^{17}$	4.8

Table 2.1: Fatigue curve parameters proposed by the DNV rules

If however, the wave-frequency (WF) and low-frequency (LF) stress components give significant contributions to the tension process, a narrow-band process assumption can no longer be used. The recommended practice is then to use one of these approaches:

- Combined Spectrum approach (CS), which can be used in the FD and TD. Considered as a conservative approach.
- Dual Narrow-Band approach (DNB), which can be used in the FD and TD.
- Rain-Flow Counting (RFC) (provides more accurate results), only used for TD.

The combined spectrum approach is an conservative approach, and the fatigue damage for  $i$  sea states is denoted  $d_{CSi}$ :

$$d_{CSi} = \frac{v_{yi}T_i}{a_D} (2\sqrt{2}\sigma_{Yi})^m \Gamma\left(\frac{m}{2} + 1\right) \quad (2.5)$$

The main difference compared to the narrow-band approach discussed earlier is that mean-up-crossing rate,  $v_{yi}$ , and standard deviation of the stress process,  $\sigma_{yi}$ , now include both WF ( $\sigma_{Wi}$ ) and LF ( $\sigma_{Li}$ ) stress components.

$$\sigma_{yi} = \sqrt{\sigma_{Li}^2 + \sigma_{Wi}^2} \quad (2.6)$$

$$v_{yi} = \sqrt{\lambda_{Li}v_{Li}^2 + \lambda_{Wi}v_{Wi}^2} \quad (2.7)$$

The dual narrow-band approach uses the results from the combined spectrum approach and multiplies it by a correction factor  $\rho_i$ .

$$d_{DNBi} = \rho_i * d_{CSi} \quad (2.8)$$

Normalised variance of the stress component,  $\lambda_{Li}$  and  $\lambda_{Wi}$  are found by:

$$\lambda_{Li} = \frac{\sigma_{Li}^2}{\sigma_{Li}^2 + \sigma_{Wi}^2}, \quad \lambda_{Wi} = \frac{\sigma_{Wi}^2}{\sigma_{Li}^2 + \sigma_{Wi}^2}, \quad (2.9)$$

and the correction factor,  $\rho_i$ , is shown how to obtain in the DNV rules.

This master thesis is a comparison study of different computation programs, and to be aware of what we want to compare is important. The S-N curve used in the DNV rules are independent of the different computation programs. If there are any differences between the programs which will be used in this thesis, we will then get two points on the S-N curve, which represent two different fatigue damage components,  $d_1$  and  $d_2$ . A example is shown in figure 2.6:

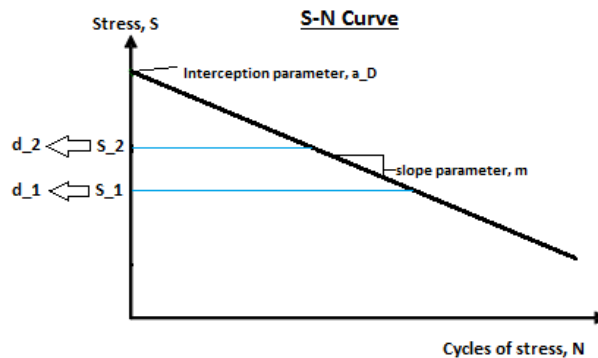


Figure 2.6: Example of an S-N curve with two fatigue damage components,  $d_1$  and  $d_2$



If we now, as an example, look at the difference in fatigue damage for the narrow band approach, the following equation can be derived if  $a_D$  and  $m$  have the same values, meaning that they use the same S-N curve independently for the two fatigue damage results:

$$\frac{d_{NB2}}{d_{NB1}} = \frac{\frac{v_{02}T_2}{a_D}(2\sqrt{2}\sigma_{S2})^m\Gamma(\frac{m}{2} + 1)}{\frac{v_{01}T_1}{a_D}(2\sqrt{2}\sigma_{S1})^m\Gamma(\frac{m}{2} + 1)}, \quad (2.10a)$$

$$= \frac{v_{02}T_2(\sigma_{S2})^m}{v_{01}T_1(\sigma_{S1})^m}. \quad (2.10b)$$

The standard deviation of the stress process, and the mean-up crossing rate of a sea state  $i$  can be written as:

$$\sigma_{Si} = \frac{\sigma_{Ti}}{A}, \quad (2.11a)$$

$$v_{0i} = \frac{1}{t_{zi}}, \quad (2.11b)$$

where  $\sigma_{Ti}$  is the standard deviation of the tension process, and  $t_{zi}$  is the mean-up crossing period of the tension process.

By inserting eq. 2.11a and 2.11b into eq. 2.10b and introducing sea states  $i=1$  and  $2$ , respectfully we get:

$$\frac{d_{NB2}}{d_{NB1}} = \frac{\frac{1}{t_{z2}}T_2(\frac{\sigma_{T2}}{A})^m}{\frac{1}{t_{z1}}T_1(\frac{\sigma_{T1}}{A})^m}. \quad (2.12)$$

The models which give rise to two different fatigue damages ( $d_1$  and  $d_2$ ) are equivalent, meaning that the cross-sectional area ( $A$ ), environment durations ( $T_{1,2}$ ) are the same for the two fatigue damage cases. The slope parameter ( $m$ ) will also be the same for the two cases since they both use the same S-N curve. Eq. 2.12 can now be reduced to:

$$\frac{d_{NB2}}{d_{NB1}} = \frac{t_{z1}}{t_{z2}} \left( \frac{\sigma_{T2}}{\sigma_{T1}} \right)^m \quad (2.13)$$

So, the point of all this is to show what parameters are of interest when comparing the results from different programs. Eq. 2.13 shows that the mean-up crossing period and the standard deviation of the tension process are the two interesting parameters. It can also be seen that a small difference in the ratio of the standard deviation will give rise to large difference in the fatigue damage ratio, since the standard deviation ratio is multiplied to the power of  $m$ . It is therefore important that the models which are going to be used in the comparison study are equivalent for all the programs, so that the difference only is due to computation methods within the programs.

## Chapter 3

# Modelling Procedure

When performing a comparison analysis of different computation programs it is important that the models are the same in each program. Likewise it is important to ensure that the environmental loads are equal, and that they act on the system in the same manner for all the programs used in this master thesis. When the comparison analysis is conducted we want to be sure that the differences only arise from the computational differences within the programs, and not caused by modelling errors. This chapter deals with how the models are verified for further use for MIMOSA, SIMO, and RIFLEX.

### 3.1 Model Implementation

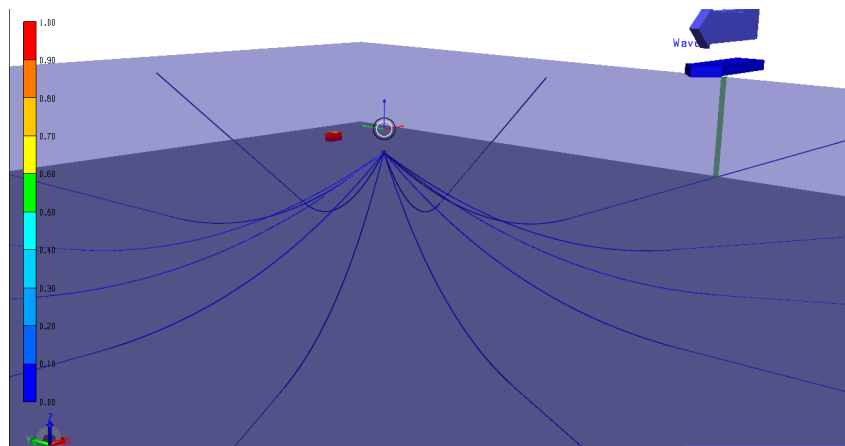


Figure 3.1: Turret mooring system modelled in SIMA, 3D view

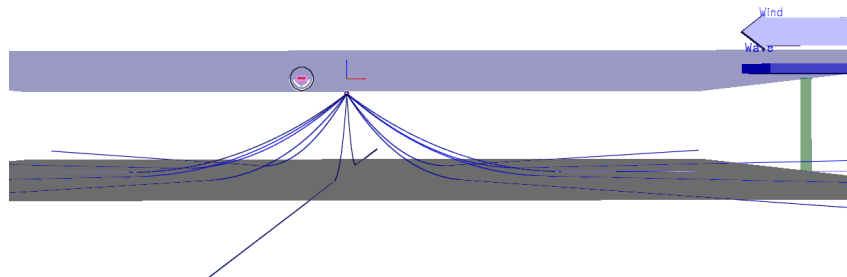


Figure 3.2: Turret mooring system modelled in SIMA, 3D view from the side

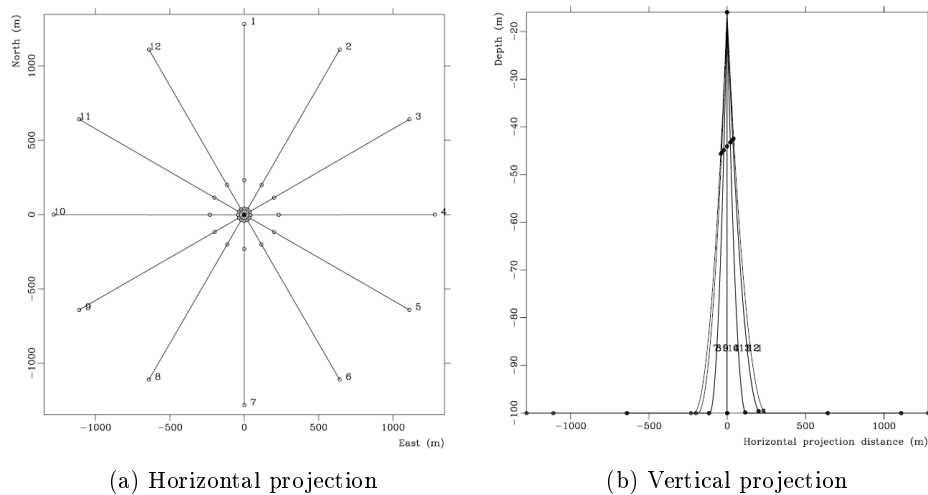


Figure 3.3: Horizontal and vertical projection of mooring system from MIMOSA

The input files for the model that was going to be used throughout this master thesis were given by Erling Lone. Input file description can be found in appendix G. These input files were directly implemented into MIMOSA, while some manipulation had to be done when using these input files in SIMO. RIFLEX and SIMO can be used through SIMA which is a new program developed by MARINTEK. SIMA is a more user friendly program, and this program makes it easier to perform a RIFLEX and SIMO analysis. Other programs can also be used in SIMA, but for this study only RIFLEX and SIMO were used. MIMOSA is not implemented in SIMA, so it had to be handled in batch mode.

Even though SIMA is a more user friendly program, it was mainly used to check (graphically) that the modelling was done correctly. Batch scripts were made for all the program; MIMOSA, SIMO, RIFLEX separately to achieve maximum learning, and to have full control over all the different procedures.

### 3.2 Case Parameter Study

A base case was initially supposed to be used throughout this whole master thesis. The parameters used in the base case were the following:

Case	Pretension [kN]	Wd [m]	xt [m]	Env.dir. [deg]
Base Case	1200	100	48,32	180

Table 3.1: Case Description

*wd* - water depth

*xt* - turret *x* position

*Env.dir.* - environmental propagating direction (180 degrees: propagates towards south)

After conduction the analysis in MIMOSA the results showed that the leeward line in the base case was highly dominated by LF motion, which means that slow-drift motions dominate the total motion for the leeward line. By also looking at the ratio between the standard deviation (STD) of WF tension calculated by the finite element method (FEM) and the quasi-static (QS) method in MIMOSA (MIM-FEM and MIM-QS respectfully), we get an idea of the differences between these methods. Since the ratio between these methods for the leeward line are almost equal to one for the base case, meaning that they are almost equal, the desired effects may not be seen when later conducting the main comparison study.

For this reason we want to find a idealized model to better suite this study. Idealized model in this case only mean that the model is slightly changed to emphasize the desired effects. Since the base case did not give satisfactory results, ratio between MIM-FEM and MIM-QS almost equal to one, a parameter study was conducted. This was done to make this master thesis more interesting, and later on see if the linearisation methods in the MIM-FEM analysis is a *problem* for certain systems. It is therefore desired to increase the MIM-FEM and MIM-QS STD of WF tension ratio, and in the meantime not changing the model to much compared to the base case. The next table shows all the cases which were analysed:

Case Description

Case	Pretension [kN]	Wd [m]	xt [m]	Env.dir. [deg]
Base Case	1200	100	48,32	180
1	1000	100	48,32	180
2	800	100	48,32	180
3	1000	120	48,32	180
4a	1000	100	60,00	180
4b	1000	100	60,00	170
5	1000	100	70,00	180
6	1000	120	70,00	180

Table 3.2: Case parameter study

The case parameter study results can be found in appendix C. A summary table of the STD tension ratio results is presented in the next table:

Case	Windward [-]	Leeward [-]
Base Case	0,84	1,06
1	0,88	1,08
2	0,90	0,92
3	1,10	1,23
4a	0,98	1,17
4b	0,96	1,18
5	1,05	1,20
6	1,48	1,42

Table 3.3: Summary of the STD WF tension ratio between MIM-FEM and MIM-QS for windward and leeward line

From table 3.3 we see that case 3, 5, and 6 give the largest ratio for both the windward and leeward line. Even though these three cases are good candidates, case 4a was selected for further analysis. The reason for this is because we do not want to change the model too much compared to the base case. Increased water depth will increase drag forces, which will increase the ratio. Since we want to investigate the importance of line dynamics at a 100 m, the water depth needs to be kept constant. Changes made in case 4a compared to the base case is the turret position and pretension. We also see that case 4a is less dominated by LF motions than the base case (see appendix C). It is therefore case 4a that is going to be used throughout this master thesis, and compared with the other computation methods in SIMO and RIFLEX.

Explaining why FEM and QS give different results within MIMOSA is actually one of the main purposes of the thesis, and will be dealt with later on. The content of this section emerged from discussions with Erling Lone, [Lone, 2013].

### 3.3 Model Verification

As mentioned, it is important that the models are equivalent for each program. It is therefore wise to compare models to each other and check that the models react equally when exposed to the same environmental conditions. A rule of thumb is that if the comparison results deviate more than 5% it needs to be investigated more thoroughly [Lone, 2013], otherwise it is acceptable for further use. The comparison between the three programs was done early in the modelling process, and static results are mainly used for this particular comparison. Table 3.4 shows what can be compared directly between the different programs.

Program Comparison - Model Verification

	MIMOSA	SIMO	RIFLEX
Mean current force <sup>a</sup>	x	x	
Mean wind force	x	x	
Mean wave drift force	x	x	
Anchor coordinates	x	x	x
Pretension	x	x	x
Mean position (equilibrium) <sup>b</sup>	x	x	
Mean tension	x	x	x
Line characteristics	x	x	x
Restoring force characteristics	x	x	

Table 3.4: Program Comparison - Model Verification

<sup>a</sup>all the mean environmental forces are found in initial position

<sup>b</sup>"mean" = static

A lot of the same things can be compared between MIMOSA and SIMO, as it is seen from the table above. The input files to SIMO are basically the same as for MIMOSA, but some modifications had to be done. One important difference between MIM/SIM and RIFLEX is that in RIFLEX the motion of the vessel has been extracted from SIMO. This means that the vessel motion (top motion) that occur in SIMO due to environmental loads is extracted and implemented as top motion in the RIFLEX model. This is done to exclude motion variations between SIMO and RIFLEX that would occur if a coupled analysis between SIMO and RIFLEX had been conducted. It is therefore no need to compare mean environmental forces and mean equilibrium position from SIMO and MIMOSA with RIFLEX.

### 3.3.1 Mean Environmental Forces

	MIM	SIM		MIM	SIM		MIM	SIM	
	Surge [kN]	Fx [kN]	Diff [%]	Sway [kN]	Fy [kN]	Diff [%]	Yaw [kNm]	Mz [kNm]	Diff [%]
Mean WIND force	-465,80	-465,80	<b>0,00</b>	-13,50	-13,48	<b>0,15</b>	505,00	505,00	<b>0,00</b>
Mean WAVE force	-468,50	-481,00	<b>2,67</b>	0,00	0,03	<b>0,03</b>	4,10	4,24	<b>3,37</b>
Mean CURRENT force	-33,00	-33,01	<b>0,03</b>	0,00	0,00	<b>0,00</b>	0,00	0,00	<b>0,00</b>
TOTAL	-967,30	-979,81	<b>1,29</b>	-13,50	-16,45	<b>0,37</b>	509,10	509,24	<b>0,03</b>

Table 3.5: Mean environmental force comparison in initial position (MIMOSA and SIMO)

Table 3.5 shows a comparison between the mean environmental forces for MIMOSA and SIMO in initial position. The total difference for each component (surge, sway, and yaw) that occur are within the acceptable range which was mentioned in the beginning of this section [Lone, 2013]. A 3-degree of freedom (DOF) system is the lowest DOF that can be modelled in MIMOSA. The surge component is the one that is of main interest, and is therefore the reason for only choosing the 3-DOF system. It must be noted that the SIMO sway and yaw components have changed signs from positive to negative in the represented table above. This is done because the axis

system are defined differently in MIMOSA and SIMO, and it is simpler to compare results when they have the same sign.

The surge components from the table above are now illustrated in a bar plot. It can now be seen more clearly that the mean wave force is slightly larger in SIMO than in MIMOSA.

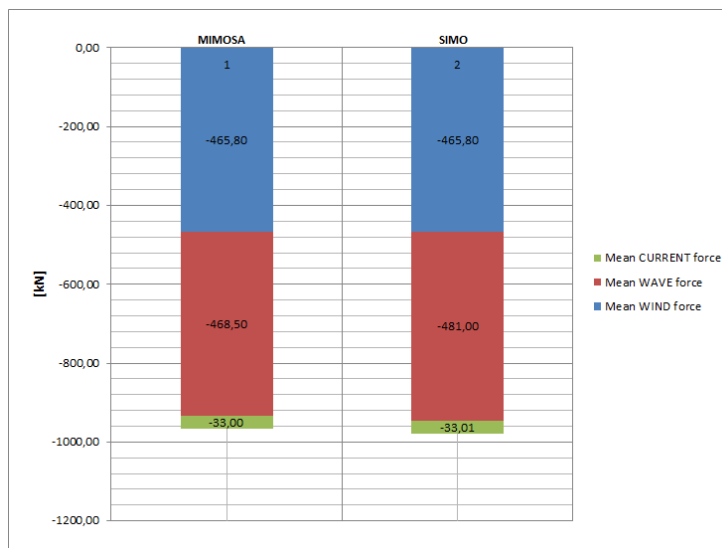


Figure 3.4: Comparing mean forces for surge component

### 3.3.2 Anchor Coordinates and Pretension

Line no.	MIMOSA		SIMO	
	$X_{global}$ [m]	$Y_{global}$ [m]	$X_{global}$ [m]	$Y_{global}$ [m]
1	1279,31	0,00	1279,31	0,00
2	1107,92	639,66	1107,92	-639,66
3	639,66	1107,92	639,66	-1107,92
4	0,00	1279,31	0,00	-1279,92
5	-639,66	1107,92	-639,66	-1107,92
6	-1107,92	639,66	-1107,92	-639,66
7	-1279,31	0,00	-1279,31	0,00
8	-1107,92	-639,66	-1107,92	639,66
9	-639,66	-1107,92	-639,66	1107,92
10	0,00	-1279,31	0,00	1279,31
11	639,66	-1107,92	639,66	1107,92
12	1107,92	-639,66	1107,92	639,66

Table 3.6: Comparing calculated anchor coordinates

Because the axis systems are defined differently in MIMOSA and SIMO it is seen from table 3.6 that the  $Y_{global}$  in SIMO have different sign then for MIMOSA. Other than that, there is

no difference in the calculated anchor coordinates. MIMOSA and SIMO calculate the anchor coordinates given the pretension, meanwhile RIFLEX calculates the pretension given the anchor coordinates. So, to get the same pretension in RIFLEX the anchor coordinates have to be slightly changed, see table 3.7. As mentioned previously, the main focus is on the windward and leeward lines (line 1 and 7) and in RIFLEX only these two lines have been modelled.

Program	Anchor coor. [m]	Pretsnion [kN]
MIM	1279,31	1000
SIM	1279,31	1000
RIF-1	<b>1279,31</b>	<b>984,8</b>
RIF-2	<b>1279,52</b>	<b>1000</b>

Table 3.7: Anchor coordinates and Pretension

To get the same pretension in RIFLEX the anchor coordinates in x-direction have to be change by  $\pm 0,21\text{m}$  depending on if it is the leeward or windward line. The difference in anchor coordinates is only 0,016%, which is relatively small and within acceptable range.

### 3.3.3 "Mean" Position (equilibrium)

Mooring position in global x-axis: 60,00m

	MIMOSA			SIMO			Diff		
	X [m]	Y [m]	Yaw [deg]	X [m]	Y [m]	Yaw [deg]	[%]	[%]	[%]
Eq. position	-62,20	-0,06	0,04	-62,03	0,03	-0,02	-	-	-
Change in turret pos.	-2,20	-0,03	0,04	-2,03	0,03	-0,02	<b>7,73</b>	<b>0,00</b>	<b>50,00</b>

Table 3.8: "Mean" Position (equilibrium) comparison

Table 3.8 shows that there are differences in the calculated equilibrium position, notably in the surge (x-direction). The difference in yaw is negligible since the values are small. In the conclusion at the end of this section the difference in the surge component will be investigated more thoroughly since the deviation is larger then 5%.



## 3.3.4 "Mean" tension

Line no.	MIMOSA [kN]	SIMO [kN]	Diff [kN]	Diff [%]
1	1180,10	1180,00	0,10	<b>0,01</b>
2	1153,70	1150,00	3,70	<b>0,32</b>
3	1084,90	1080,00	4,90	<b>0,45</b>
4	999,90	1000,00	-0,10	<b>0,01</b>
5	925,10	930,00	-4,90	<b>0,53</b>
6	876,80	877,00	-0,20	<b>0,02</b>
7	859,00	860,00	-1,00	<b>0,12</b>
8	875,20	875,00	0,20	<b>0,02</b>
9	922,30	928,00	-5,70	<b>0,62</b>
10	996,10	999,00	-2,90	<b>0,29</b>
11	1081,30	1080,00	1,30	<b>0,12</b>
12	1151,30	1150,00	1,30	<b>0,11</b>

Table 3.9: "Mean" Tension comparison

From table 3.9 we see that all the static ("mean") tension forces deviate less than 1%, which is quite good and acceptable.

## 3.3.5 Line Characteristics

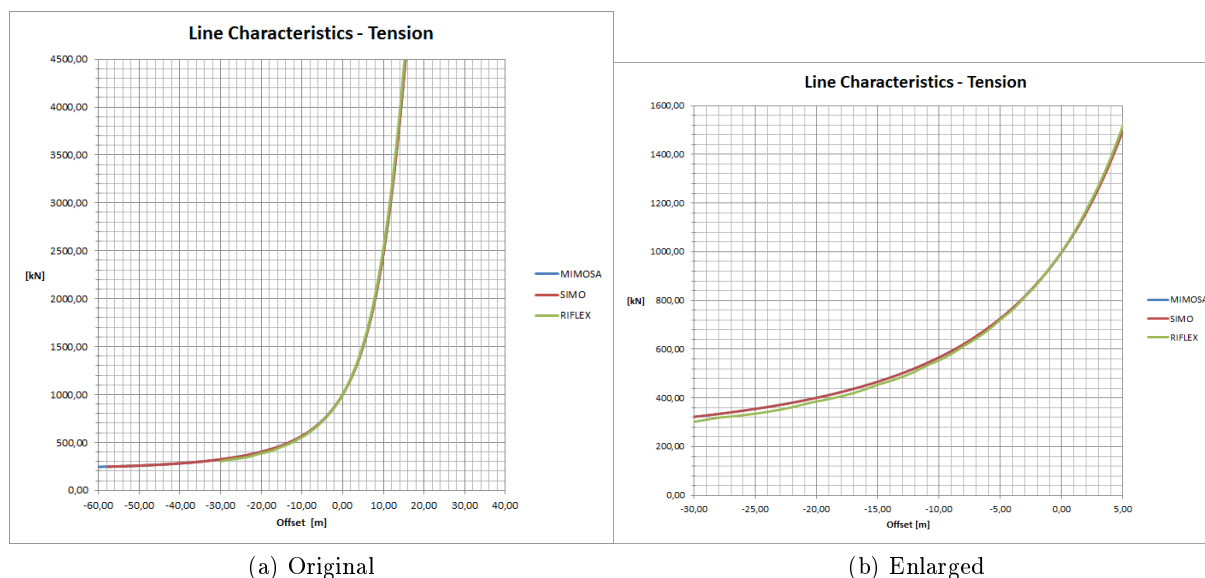


Figure 3.5: Line characteristics for MIMOSA, SIMO, and RIFLEX (line 1). Negative x-value: moving towards the anchor. Positive x-value: moving from the anchor.

The two graphs above show that the line characteristics for the three programs; MIMOSA, SIMO, and RIFLEX follow each other quite well. The line characteristics in MIMOSA and SIMO are identical, but deviate slightly from RIFLEX. These small differences are acceptable due to the rule of thumb criteria mentioned in the beginning of this section. We can also see that the pretension (in  $X = 0,00$ ) is equal for all the programs due to the modification made to the anchor coordinates in RIFLEX. Since all the mooring lines are identical, and we only need to look at the line characteristics for one mooring line, see figure 3.5.

### 3.3.6 Restoring Force Characteristics

Forcing the vessel in surge direction and stepwise finding the resistance in mooring line 1, we can obtain the restoring force characteristics for the line. The differences between MIMOSA and SIMO are within 5% as it can be seen from the figure and table below.

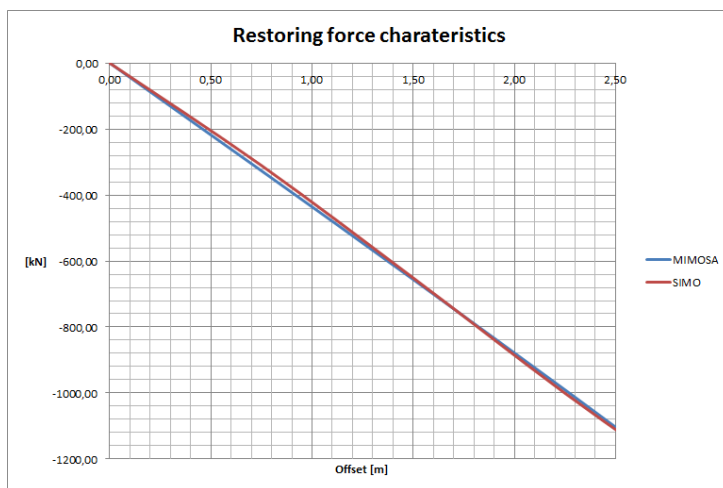


Figure 3.6: Restoring Force Characteristics for MIMOSA and SIMO plotted from 0 to 2,50 m

Offset [m]	MIMOSA [kN]	SIMO [kN]	Diff [%]
0,00	0,00	0,00	0,00 %
1,50	-655,80	-651,10	0,72 %
3,00	-1332,20	-1328,60	0,27 %
4,50	-2047,00	-2050,20	0,16 %
6,00	-2826,10	-2824,10	0,07 %
7,50	-3693,80	-3685,70	0,22 %
9,00	-4671,30	-4668,20	0,07 %
10,50	-5791,80	-5793,00	0,02 %
12,00	-7086,90	-7088,60	0,02 %
13,50	-8574,20	-8566,20	0,09 %
15,00	-10280,70	-10285,20	0,04 %

Table 3.10: Restoring force comparison between MIMOSA and SIMO

### 3.3.7 Conclusion - Model verification

Comparing the static results for all models was done early in the modelling procedure, and it is important for further analysis. A conclusion table is made to illustrate, and to summarize the different comparisons that have been done in the process of verifying the different models.

	MIMOSA	SIMO	RIXLEX	
Mean current force	x	x		✓
Mean wind force	x	x		✓
Mean wave drift force	x	x		✓
Anchor coordinates	x	x	x	✓
Pretension	x	x	x	✓
"Mean" position (equilibrium)	x	x		✓
"Mean" tension	x	x	x	✓
Line characteristics	x	x	x	✓
Restoring force characteristics	x	x		✓

Table 3.11: Conclusion table - Model Verification

✓ - *within acceptable range*

✓ - *some modifications had to be made (mainly in RIFLEX). May affect the final result*

✓ - *exceeds the acceptable range, need to be clarified*

The mean equilibrium position exceeds the acceptable range when comparing MIMOSA and SIMO, and needs to be investigated. The difference in mean equilibrium position is because SIMO does not obtain static equilibrium throughout the iteration process. This can be seen from the SIMO result file for static analysis, which is found on the attached CD (see appendix G). SIMO stops looking for the mean equilibrium position when a satisfactory error limit is reached. The residual force in surge for SIMO is -74.08 kN, while in MIMOSA the equilibrium position is found. By simple hand calculations we can check what the actual difference in mean equilibrium position is suppose to be. We know that mooring line stiffness can be found by:

$$k = \frac{\Delta F}{\Delta x}. \quad (3.1)$$

By using the restoring force table (table 3.10) and finding the mooring line stiffness around the mean equilibrium position (between 1,50 - 3,00 meters) the stiffness for MIMOSA and SIMO then becomes,

$$k_{MIM} = \frac{1332,20kN - 655,80kN}{3,00m - 1,50m} = 450,93 \frac{kN}{m}, \quad (3.2)$$

$$k_{SIM} = \frac{1328,60kN - 651,10kN}{3,00m - 1,50m} = 451,67 \frac{kN}{m}. \quad (3.3)$$

The difference in stiffness is only 0.16 % and they are considered to be relatively equal. By dividing the static residual force with the calculated stiffness for SIMO, the residual static offset becomes:

$$x_{residual} = \frac{F_{residual}}{k_{SIM}} = \frac{74,08kN}{451,67\frac{kN}{m}} = 0,164m. \quad (3.4)$$

The residual static offset ( $x_{residual}$ ) is almost the same as the difference in mean equilibrium position (0,17m) between MIMOSA and SIMO (see table 3.8). This means that the difference arises because of the residual static force from SIMO, which occurs because SIMO does not obtain the exact mean equilibrium position.

## Chapter 4

# Program Structure

MIMOSA, SIMO, and RIFLEX are the programs used in this master thesis. As mentioned in the previous chapter, SIMO and RIFLEX can be used in SIMA. The graphical interface in SIMA makes it easy to use and it is much simpler to visualize the model. A choice was made quite early in the master thesis to also run all the programs in batch mode. This was done because all the input files had to be created and read, and one then gets full control over the whole analysis process. It was also simpler to interpret the error messages when using the programs in batch mode. Another reason for creating individual scripts for each program and then combining them with one batch script was to make everything automatic. Typing in all the necessary files for each program, for every analysis is quite time consuming. So, by spending some time on creating one batch file that combines every single batch file for all the individual programs was time saving in the long term.

Appendix G gives a description of structure and content of the attached CD. On that CD all the files used and created can be found. In appendix G there is also a table explaining all the different file types that were created and used.

### 4.1 MIMOSA, SIMO, RIFLEX (MSR) Script - Main batch script

By creating a small batch script that was called MSR program, was quite time saving in the long run. All the individual programs; MIMOSA, SIMO, and RIFLEX could then be executed at the same time, or individually depending on the users choice. This combined script was useful when the turret position was changed in the parameter study (section 3.2), and all the programs needed to be executed once again. The float diagram below illustrates how the MSR script works. Note that in the float diagram the MSR script is called MSR Program.

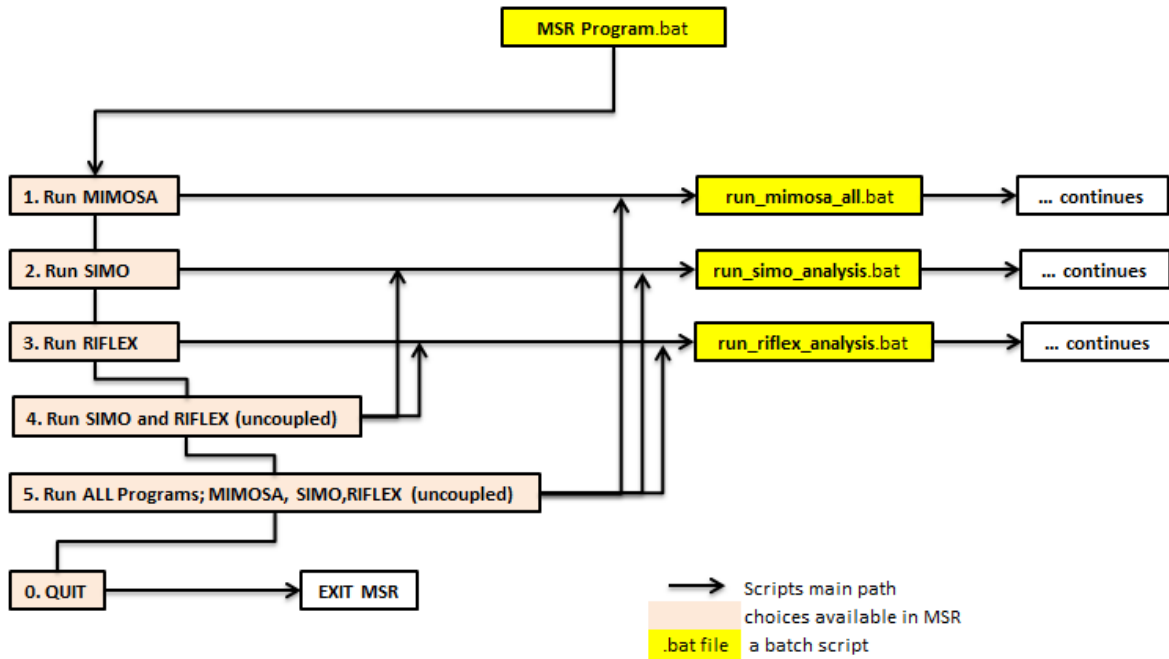


Figure 4.1: Flow diagram with description for MIMOSA, SIMO, RIFLEX (MSR) Script

Figure 4.1 shows how all the batch scripts are combined together, and the continuity of every sub-batch script will be shown later on with flow diagrams of their own.

## 4.2 MIMOSA

The flow diagram below shows how different scripts within MIMOSA are coupled together for running multiple analysis, i.e. FEM-WF, QS-WF, and QS-LF. Figure 4.2 describes the different colors and arrows, and all the self-made scripts can be found on the attached CD (see appendix G). The MIMOSA user's manual has been used as help for creating the MIMOSA scripts and routines [MIM, 2012].

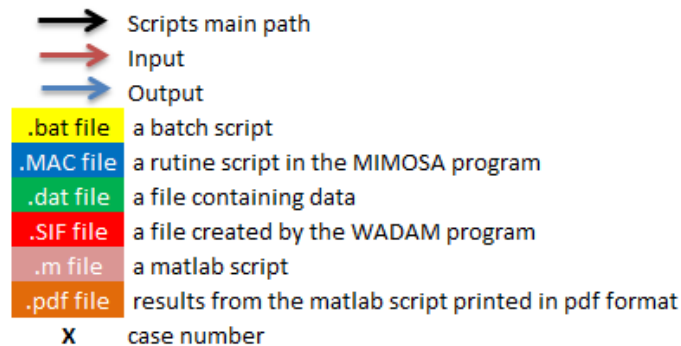


Figure 4.2: MIMOSA script description

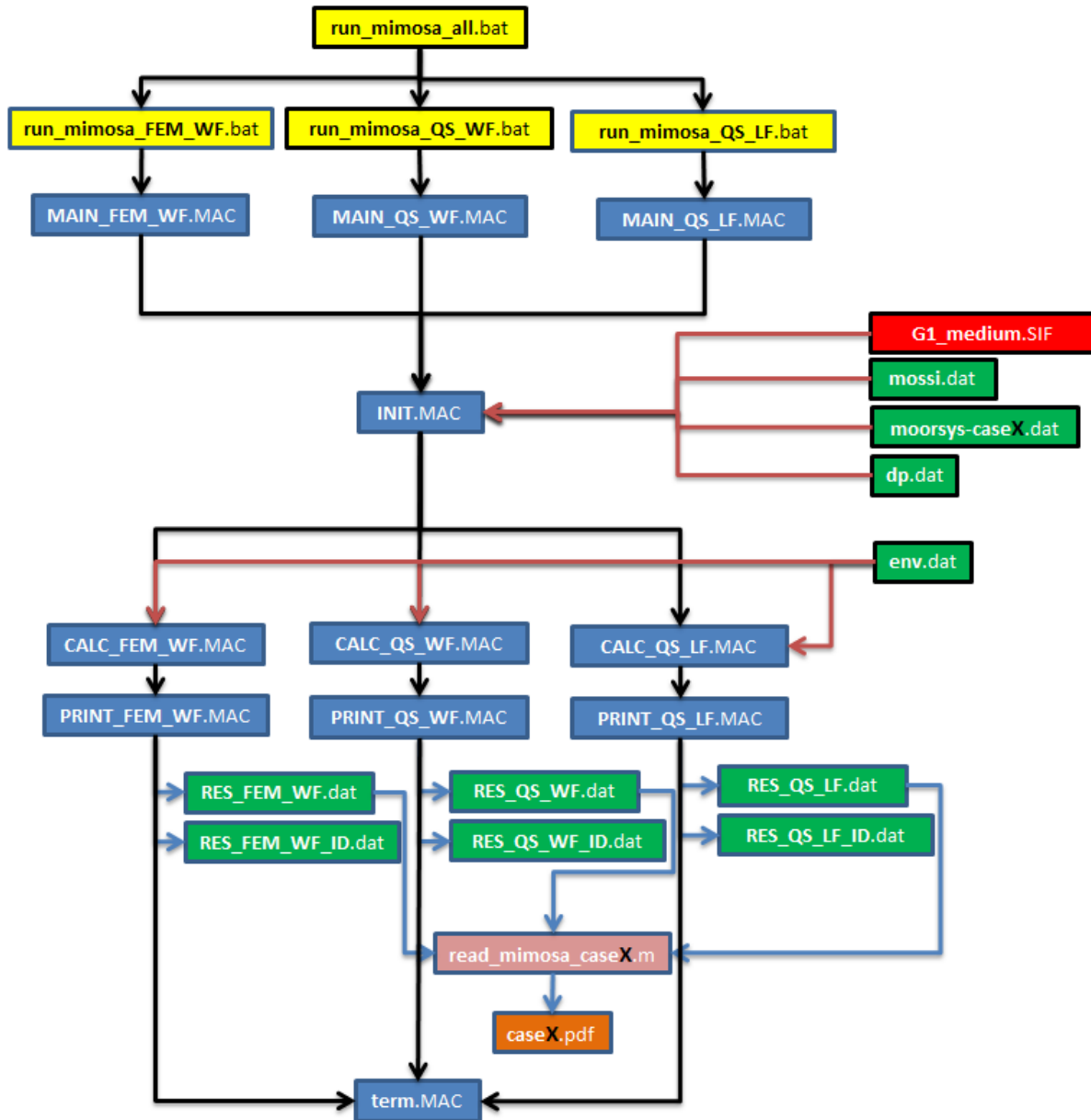


Figure 4.3: MIMOSA float diagram - script procedure

### 4.3 SIMO

The SIMO user’s manual has been used as help for creating the scripts and routines in SIMO, [SIM, 2012b].

SIMO was used in SIMA and in batch mode. This following section will only go through the SIMO script in batch mode. SIMO is similar to MIMOSA in many ways, and here one could also create routines within the program and coupling them together with a batch script. The scripts structure and coupling is visually explained in the float diagram below.

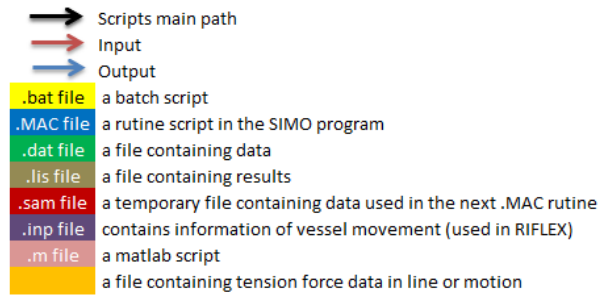


Figure 4.4: SIMO script description

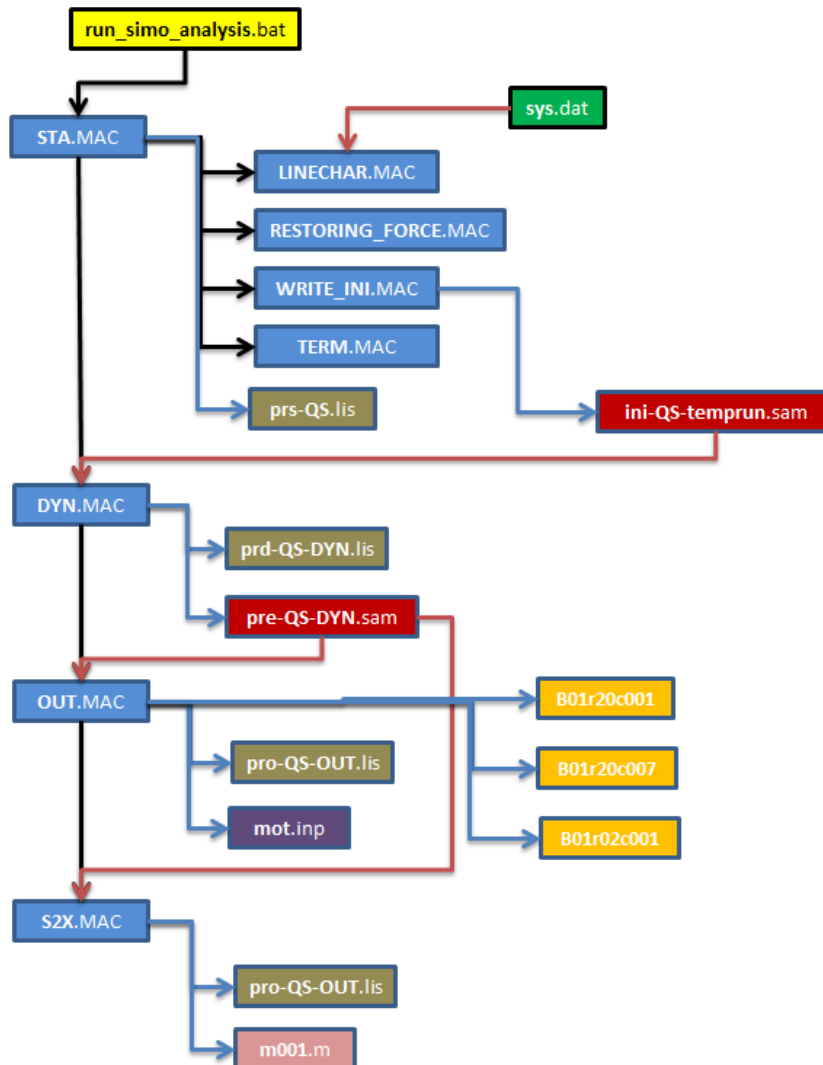


Figure 4.5: SIMO float diagram - script procedure



### 4.4 RIFLEX

RIFLEX has a totally different interface than SIMO and MIMOSA, and needs to be dealt with differently. A batch script was made to run the different modules automatically as it can be seen from the flow diagram below. The RIFLEX user's manual was frequently used when creating the input files for all the modules used in RIFLEX, [RIF, 2012b].

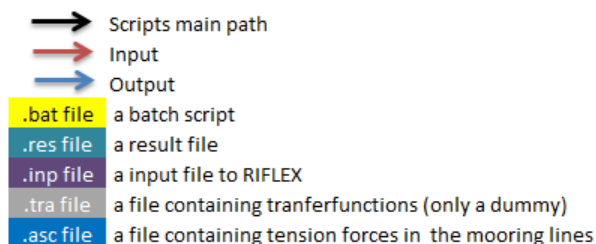


Figure 4.6: RIFLEX script description

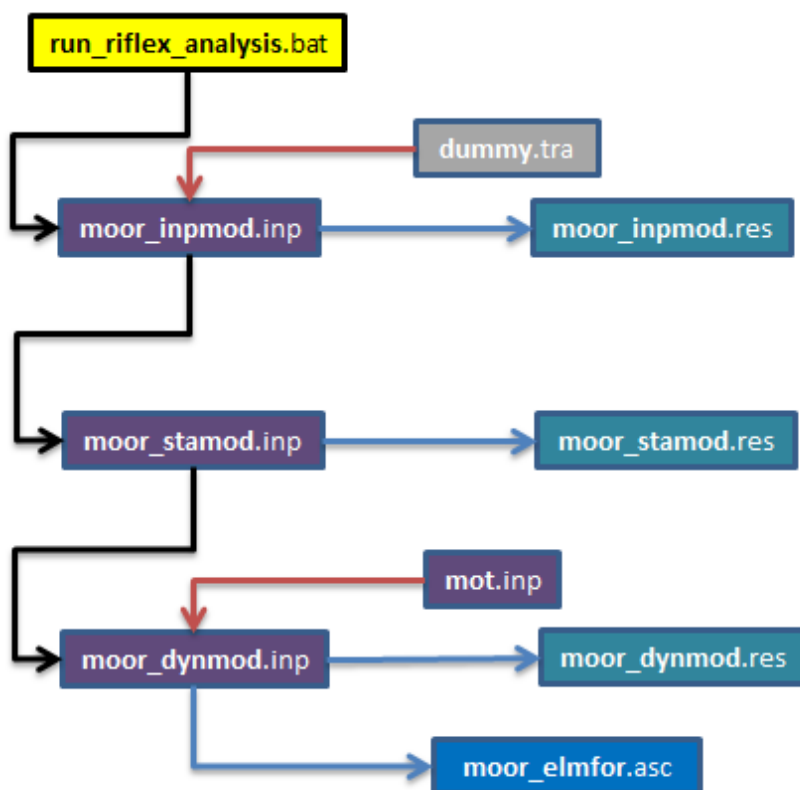


Figure 4.7: RIFLEX flow diagram - script procedure

### 4.5 Post Processing - Matlab

This Matlab script was made for processing the results given from MIM, SIM, and RIF. The coding can be found in appendix E, and on the attached CD (see appendix G).

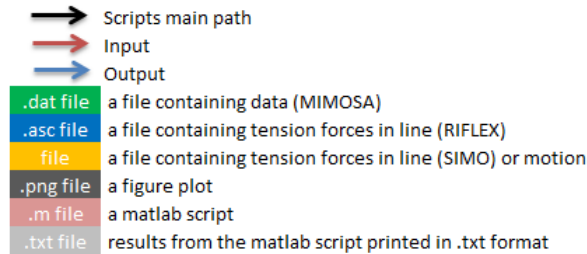


Figure 4.8: Matlab script description

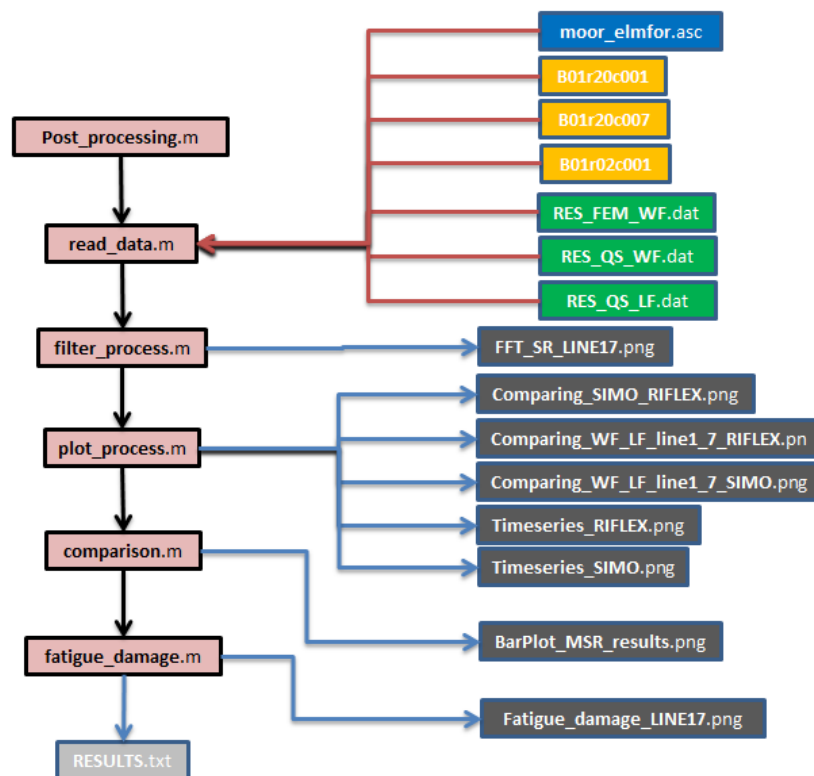


Figure 4.9: Matlab float diagram - script procedure

Note that every file and every script can be found on the attached CD, and it is recommended to read through appendix G before accessing the CD. The post-processing scripts will be referred to a lot throughout this master thesis and is therefore included in appendix E.

# Chapter 5

## Program Theory

Several programs exist that can perform mooring line analysis. MIMOSA, SIMO and RIFLEX are all developed by MARINTEK and are the main programs that will be used for this master thesis. Ariane and DeepC are examples of other programs that also can be used for analysing moored systems. When using a computation program one must be aware of how the program works. Every program has some advantages and disadvantages, and to have knowledge about this will provide good reliable results and discussions. This chapter will cover a small amount of general theory for each program being used in this master thesis, and the main focus will be on how the different programs calculate the standard deviation of tension forces in the mooring lines. The reasoning for mainly looking at STD of tension forces is discussed in section 2.3.

Mooring line response can be calculated in the frequency domain (MIMOSA) or in the time domain (SIMO and RIFLEX). The following table summarizes the advantages, and disadvantages between performing a frequency and time domain analysis. [Lone, 2009]

<b>Frequency domain (FD)</b>	<b>Time Domain (TD)</b>
<i>Advantages</i>	
Calculations are fast. No loss of statistical properties	Non-linearities are accounted for.
<i>Disadvantages</i>	
Non-linear systems are linearised Only steady-state response	For strong non-linear system many simulation are required. Time-demanding
<i>Program</i>	
MIMOSA	SIMO and RIFLEX

Table 5.1: Advantages and disadvantages regarding the use of FD or TD methods

The three programs that are used can all model a 6-DOF system. Note that for this master thesis only a 3-DOF system is modelled in MIMOSA, mainly because the surge motion is of interest and because the effects we are after appear for this motion.

## 5.1 MIMOSA

The content for this section is based on the MIMOSA course given by MARINTEK [Kaasen, 2012] and the MIMOSA User’s manual [MIM, 2012]. Karl E. Kaasen has also been helpful with clarifying unclear subjects within the MIMOSA theory section [Kaasen, 2013].

Throughout this section we denote  $r$  as the projection of the horizontal distance from anchor to top end (farilead) of the line.

### 5.1.1 LF tension - Only Quasi-Statically

Two options are available for computing the LF tension:

1. A linearised model, which is non-Rayleigh based method developed by Carl Trygve Stansberg,
2. Rayleigh based method.

The procedure for calculating LF tension is only done quasi-statically. It can be seen from the equation below, that the STD of LF tension is computed by using the LF vessel motion. LF motions are computed with linearised models if option 1 is chosen from the list above. If we now denote  $r_s$  as the static position of the mooring line, the STD of LF tension is in MIMOSA found by:

$$\sigma_T^{LF} = T(r_s + \sigma_r^{LF}) - T(r_s). \tag{5.1}$$

$\sigma_T^{LF}$  - STD of LF tension,

$r_s$  - static position, or mean offset,

$\sigma_r^{LF}$  - STD of LF offset (computed from response spectrum).

The interpretation of equation 5.1 is that MIMOSA uses the static position and the STD of LF offset directly in the line characteristics to find the STD of LF tension. If the mooring line characteristics is non-linear, MIMOSA will choose the value which obtains the largest STD of LF tension. The next figure illustrates this by showing that T-STD 1 is smaller then T-STD 2 for the the same STD of LF offset.

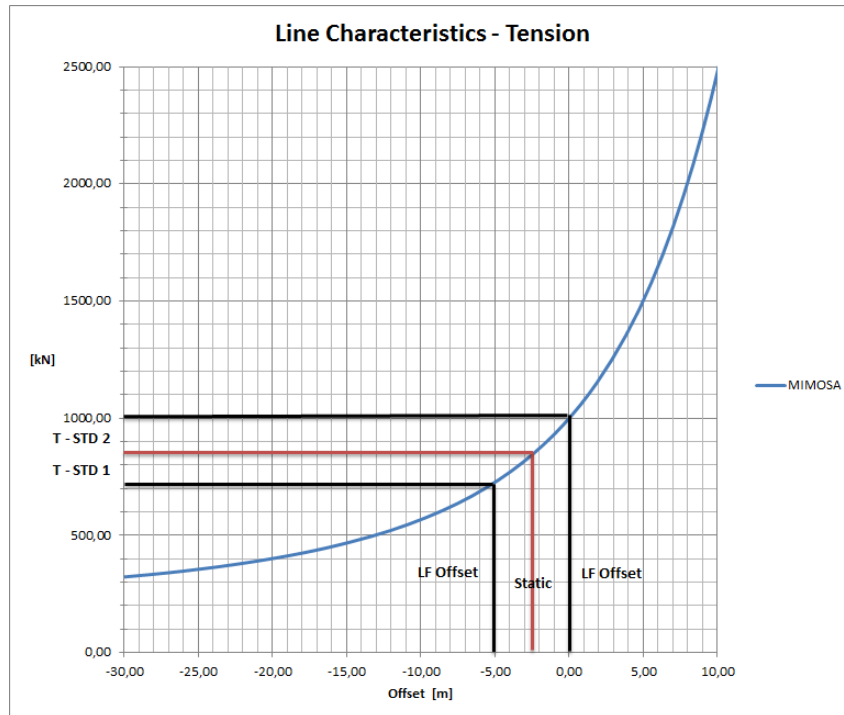


Figure 5.1: Calculating the STD of LF tension using mooring line characteristics, where T-STD is STD of tension

It is written in the MIMOSA user's manual that the STD of WF and LF tension calculations are not true standard deviations, unless the displacement-tension characteristics are linear. This means that if the mooring line characteristics curve in figure 5.1 was linear, T-STD 1 and T-STD 2 would be equal and therefore would represent the true STD of LF tension. This indicates that for non-linear line characteristics there is a certain inaccuracy in the computed STD of LF tension.

### 5.1.2 WF tension - General

In MIMOSA there are three options for calculating the WF tension.

1. Quasi-static (QS) method
2. Simplified Analytic Method (SAM)
3. Finite Element Method (FEM)

The SAM method will not be handled in this master thesis and the theory behind this calculation method is therefore not included. QS and FEM both use the base offset,  $r_b$ , when computing the STD of WF tension for combined WF and LF motions. The base offset is computed individually for every line as a projection of the fairlead motion in the line plane (xz-plane). STD of WF and LF tensions are for this master thesis computed separately, and the use of base offset is included here to show that there are differences in performing a separate and combined analysis for obtaining the STD of WF tension.

$$r_b = \begin{cases} r_s + r_{extr}^{LF} + (2\sigma_r^{WF} - r_{extr}^{WF}), & r_1 < r_2 \\ r_s + 2\sigma_r^{LF}, & r_1 \geq r_2 \end{cases} \quad (5.2)$$

where  $r_1$  and  $r_2$  are found by:

$$r_1 = (2\sigma_r^{LF} + r_{extr}^{WF}), \quad (5.3a)$$

$$r_2 = (r_{extr}^{LF} + 2\sigma_r^{WF}). \quad (5.3b)$$

$r_{extr}^{LF}$  - Extreme LF response (based on Rayleigh assumptions),

$\sigma_r^{WF}$  - STD of WF response (response spectrum),

$r_{extr}^{WF}$  - Extreme WF response (based on Rayleigh assumptions),

$\sigma_r^{LF}$  - STD of LF response (response spectrum).

### 5.1.3 WF tension - QS

Inertia and damping forces are neglected when using the QS-method. As previously described, there is a difference between a separate (WF only) and coupled (WF&LF) analysis. This section describes the procedure for WF only.

This method uses the mean offset (not the base offset) and adding the STD of WF position directly in the mooring line characteristics in obtaining the STD of WF tension. Drag forces and other non-linearities acting on the line are not accounted for, but current forces acting on the cable can be included in a simplified manner. The STD of WF tension for the QS-method is found similarly as for the STD of LF tension:

$$\sigma_T^{WF} = T(r_s + \sigma_r^{WF}) - T(r_s). \quad (5.4)$$

### 5.1.4 WF tension - FEM

The FEM accounts for inertia and drag forces. Current forces can be included in the same manner as for the QS-method. In this computation method there is a procedure that accounts for non-linearities. The aim is to find a estimate of dynamic WF tension. The mooring cable is now modelled as multi-degree-of-freedom dynamical system and solved in the FD:

$$\mathbf{M}\Delta\ddot{\mathbf{r}} + \mathbf{C}\Delta\dot{\mathbf{r}} + \mathbf{K}\Delta\mathbf{r} = \mathbf{K}_0\mathbf{r}_{WF} + \mathbf{F} \quad (5.5)$$

$\Delta\mathbf{r}$  - Contains nodal displacement in (x,y,z) from the mean offset,  $r_s$ ,

$\mathbf{K}$  - builds up a stiffness matrix based on the line configuration dependent on  $r_s$ ,

$\mathbf{K}_0\mathbf{r}_{WF}$  - a given force from the WF motion at fairlead, where the motion ( $\mathbf{r}_{WF}$ ) is found from the response spectrum,

$\mathbf{M}$  - mass and added mass matrix are constant,

**C** - average linear damping coefficient. Stochastic linearisation of the displacements at every node. Creates coefficients for every node. Iteration process in finding the drag forces acting on every node is included in the damping coefficient,

**F** - wave force vector that acts on the mooring line.

This method can also perform a separate and coupled analysis as for the QS-method, but here we only have considered a separate analysis meaning that WF only has been used. The difference would be that for the separate analysis, in our case WF only, the *mean offset* is used. While for the combined analysis the *base offset* is used.

$\Delta r$  will now be used in computing the STD of WF tension,  $\sigma_T^{WF}$ , using the FEM. The FEM model can only be used for long-crested waves because short-crested waves are not implemented in the MIMOSA program.

### 5.1.5 Non-linear WF tension - FEM

MIMOSA has a procedure that attempts to capture the effect of the non-linear nature of the dynamic cable model. This method is based on the assumption that the response spectrum is narrow banded. The procedure for including the non-linear effects are as following:

1.  $\sigma_T^{WF}$  will be found by the procedure described in the previous section.
2. MIMOSA finds the max tension ( $T_{max}$ ) from Rayleigh calculations, and assumes that close to the max tension top the amplitudes around this top are of equal magnitude.
3. Finds  $R = \frac{T_{max}}{\sigma_T^{WF}}$ , which is a constant relationship between max tension and STD of WF tension.
4. From point 2 MIMOSA then assumes a stationary sinusoidal response curve around the extreme top ( $T_{max}$ ). Because of this stationary sinusoidal assumption, the relationship between  $\sigma_r^{WF}$  and  $T_{max}$  becomes;  $\sigma_r^{WF} = \frac{T_{max}}{\sqrt{2}}$ .
5. The wave spectrum will now be scaled up by  $0,5R^2$  so that the amplitude between the stationary sinusoidal response curve and the calculated Rayleigh max value ( $T_{max}$ ) are of equal magnitude. A new response including the non-linear effects will now be calculated once again;  $\hat{\sigma}_r^{WF} = \frac{1}{\sqrt{2}} * R * \sigma_r^{WF}$ .
6. This new calculated  $\hat{\sigma}_r^{WF}$  will be multiplied by  $\sqrt{2}$  because of the sinusoidal response curve assumption. The iteration process for solving eq.5.5 will be repeated, but now the  $\sigma_r^{WF}$  is replaced by  $\hat{\sigma}_r^{WF}$ .  $\hat{\sigma}_T^{WF}$  will now be the new STD of WF tension including non-linear effects.

In the new iteration process (point 6) MIMOSA will find a new damping coefficient to account for the new drag forces, while the mass and stiffness matrix will remain unchanged. The linearised stiffness matrix is kept constant and the touch down point is fixed at the sea-floor. Retaining the touch-down point is done so by fitting a hinge pin at this node [Leira, 2013].

There was some confusions around the usage of non-Rayleigh and Rayleigh based method, and if this would affect the STD of WF tension calculations. This issue was clarified by conversations

with Karl Kaasen [Kaasen, 2013]. The STD is an average measurement and will not be affected by the choice of non-Rayleigh or Rayleigh method. On the other hand, the max tension value will depend on the choice of method.

## 5.2 SIMO

The content of this section is taken from SIMO theory and user's manual [SIM, 2012a], [SIM, 2012b].

SIMO uses a similar calculation procedure as MIMOSA for analysing mooring lines, and in SIMO there are two methods which can be used:

1. Quasi static (QS) analysis
2. Simplified dynamic analysis (SAM)

### 5.2.1 Mooring line tension

SIMO performs the analysis in the TD, and every mooring line is handled separately. Friction at the bottom is neglected and the line can rotate freely about the anchor. For the QS method the transverse drag on the lines are neglected. The procedure for calculating the total line tension is similar as for MIMOSA, and the top tension is determined by the location of the upper end relative to the anchor. This is done in a two dimensional plane (vertical plane/xz-plane).

The QS method uses the mooring line characteristics to find the line tension at the top end. In doing so SIMO uses a quadratic interpolation function to obtain the tension through the time simulation [Mo, 2013]. This interpolation method will now be denoted as *updated line characteristics*. The updated line characteristics means that geometrical stiffness will be properly accounted for. The geometrical stiffness is linearised in MIMOSA.

The SAM method that is available in SIMO accounts for dynamic effects in a simplified way. A method that considers these effect has been developed by Larsen and Sandvik [Larsen and Sandvik, 1990]. This simplified method does not account for mass forces on the line, and is therefore a method which only includes transverse drag forces.

Current forces acting on the mooring lines are not included in the QS and SAM in the SIMO program.

## 5.3 RIFLEX

The content for this section is taken from the RIFLEX theory and user's manual [RIF, 2012a], [RIF, 2012b].

RIFLEX was originally created for analysing flexible risers and other slender structures. RIFLEX is fully capable of conducting analysis of mooring lines in the TD. The general dynamic equilibrium equation that RIFLEX solves for dynamic TD analysis is:

$$\mathbf{R}^I(\mathbf{r}, \ddot{\mathbf{r}}, \mathbf{t}) + \mathbf{R}^D(\mathbf{r}, \dot{\mathbf{r}}, \mathbf{t}) + \mathbf{R}^S(\mathbf{r}, \mathbf{t}) = \mathbf{R}^E(\mathbf{r}, \dot{\mathbf{r}}, \mathbf{t}) \quad (5.6)$$



- $\mathbf{R}^I$  - inertia force vector,
- $\mathbf{R}^D$  - damping force vector,
- $\mathbf{R}^S$  - internal structural reaction force vector,
- $\mathbf{R}^E$  - external force vector,
- $\mathbf{r}, \dot{\mathbf{r}}, \ddot{\mathbf{r}}$  - structural displacement, velocity and acceleration vectors.

Eq. 5.6 is solved by step-by-step numerical time integration with equilibrium iteration at each time step. Available analysis methods in RIFLEX are:

1. Fully non-linear analysis,
2. Linearised FEM analysis.

The most important non-linear effects that have to be considered in a dynamic analysis are: (i) geometrical stiffness of mooring line, and (ii) contact problems. Other types of non-linear effects can be found in T. Moan's booklet given in the advanced finite element course [Moan, 2003]. Since this master thesis handles mooring lines the two listed effects above are the most important non-linear effects.

Contact problems are modelled as springs at the seabed. Geometrical stiffness depends on the mooring line configuration. For slack mooring lines the non-linear geometry need to be properly accounted for. For both these computation methods, current forces acting on the mooring lines can be included.

### 5.3.1 Fully non-linear analysis

A fully non-linear analysis handles all non linearities properly and is rather time consuming compared to MIM-FEM and SIM-QS method. This is because a fully non-linear analysis in RIFLEX establishes system matrices (mass, damping and stiffness) repeatedly. Drag, current and inertia forces acting on the mooring lines are accounted for. This method account for all the desired effects with we are after, and this method is therefore considered to give the most accurate results.

### 5.3.2 Linearised FEM analysis

Linearised TD analysis is much less time consuming then a fully non-linear TD analysis. The step-by-step time integration now linearises the mass, damping and stiffness matrix. These matrices are kept constant throughout the analysis. Keeping the stiffness matrix constant means that this method linearises the geometrical stiffness, and will not have a updated line characteristics which is the case for the fully non-linear analysis. Non-linear hydrodynamics are accounted for which makes this linear analysis appealing when non-linear hydrodynamic effects are governing.

## 5.4 Summary of program theory

Table 5.2 summarizes what kind of non-linear dynamic effects are accounted for in the different computations methods within MIMOSA, SIMO, and RIFLEX.

Method	Updated . line char	Current loads	Drag and inertia loads
MIMOSA-QS	-	s	-
MIMOSA-FEM	-	s	s
SIMO-QS	✓	-	-
SIMO-SAM	✓	-	s
RIFLEX-linear	-	✓	✓
RIFLEX-Nonlinear	✓	✓	✓

Table 5.2: Compares different effects that are included or not included in the calculation methods for all the three computation programs used. '✓' - accounted for in the analysis method. 's' - accounted for in a simplified manner.

# Chapter 6

## Case Study

System description, environmental loads that have been used throughout this master thesis will in this chapter be dealt with properly. The main goal is to find the differences between the three programs; MIMOSA, SIMO and RIFLEX that are of importance for fatigue damage analysis. These results are presented and discussed in chapter 7. The procedure in finding these results have somewhat been covered in earlier chapters, meanwhile here some specific details are reviewed in how the results were found such as filter design and calculation methods used within the three programs.

### 6.1 System Description

The case is a turret moored FPSO vessel at 100 m water depth. Table 6.1 presents the data for the Aasgard FPSO T900s which was used throughout this master thesis.

<b>FPSO DATA</b>			
Variable	Value	Unit	Comment
T (draught)	16,50	m	"medium" loading condition
$L_{pp}$	258,00	m	Distance from Ap to Fp
$L_{pp}/2$	129,00	m	
LCG	113,58	m	In front of Ap
RAO reference point	117,12	m	
RAO ref. - LCG	3,54	m	Distance from LCG to RAO ref. point

Table 6.1: FPSO data given by Erling Lone, DNV

In chapter 3.2 we discussed the reason for modifying the original model to enhance the final results. Reducing the pretension in the mooring lines and positioning the turret further away from the COG (positive x-direction), were the only two changes made to the original model. The table below shows a column with the original data and one column with the modifications made to the original model.

Mooring System			
Description	Original Value	Modified Value	Unit
Distance from COG to turret center	48,32	60,00	m
Vertical position of fairlead	15,97	15,97	m
Number of lines	12	12	[-]
Segments per line	3	3	[-]
Pretension (all lines)	1200	1000	kN

Table 6.2: Original and modified mooring system data

The model consists of 12 identical mooring lines (for MIMOSA and SIMO) numbered in a clockwise direction, beginning with the one pointing towards north (see figure 3.3). In RIFLEX only the windward and leeward line have been modelled. Each mooring line consist of 3 segments, which were originally divided like shown in figure 6.1.

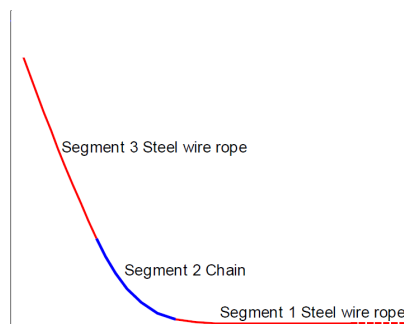


Figure 6.1: Original mooring line composition

In the modelling process we found that the mooring system was too heavy and gave too much stiffness to the system [Lone, 2013], so the chain segment was changed to steel wire rope. One segment could just as well be modelled for the whole line, but since the modelling process was well under way the three segments were kept, even though all the segments have the same properties.

Line Segment Properties						
Segment no <sup>a</sup>	Diameter	Length	No. of elements	$C_D$	$C_L$	Type
	[m]	[m]	[m]	[-]	[-]	
1	0,13	1050	70	2,40	1,15	Wire
2	0,13	200	20	2,40	1,15	Wire
3	0,13	50	10	2,40	1,15	Wire

Table 6.3: Line segment properties given by Erling Lone, DNV

<sup>a</sup>Numbered from anchor

Compared to general mooring systems, the system used here is still a stiff system even though measures have been made to make this particular mooring system less stiff [Lone, 2013].

The models for all the computation programs are restricted against rotations in yaw. This is done because the surge motion will give rise to the largest tension forces in the mooring lines [Faltinsen, 1990]. This restricting is obtained by introducing an artificial stiffness in the yaw motion.

## 6.2 Environmental Condition

As mentioned throughout this whole master thesis, it is important that every model is exposed to the same environment. Wind, waves and current are propagating towards south (from north), and the windward line is line 1 and leeward line is line 7.

**Environmental Condition for MIMOSA, SIMO, RIFLEX<sup>a</sup>**

Waves:	$H_S = 8,0m, T_P = 12,5s$ . Double Peaked Spectrum.
Wind velocity:	20 m/s, 1 hour average 10m above surface. ISO 19901-1 (NPD) spectrum.
Current velocity:	0,60 m/s at the surface.

Table 6.4: Environment description. Used for all models

<sup>a</sup>Prescribed motion from SIMO

In the RIFLEX model there is no actual environment that act on the model since RIFLEX has a prescribed vessel motion from SIMO. This is for instance the reason for not checking the mean environmental forces from MIMOSA and SIMO with RIFLEX in section 3.3.

## 6.3 Calculation Methods

The MIMOSA, SIMO and RIFLEX theory manuals are used for this section [MIM, 2012], [SIM, 2012a], [RIF, 2012a].

### 6.3.1 General

The FD calculations for obtaining the STD of WF tension are performed in MIMOSA by the QS and FEM. A simplified method (SAM) is also available but is not used in this master thesis. The FEM divides the cable in to elements, and the accuracy increases with increased number of elements.

Current forces that act on the mooring lines can be included in the calculations in the MIMOSA program, but is disregard for all models. This is because SIMO is a program for motion simulations and station keeping, and for a quasi-static analysis in SIMO the transverse drag force component is neglected and current is mainly included for calculating mean current forces and static offset of the vessel. By neglecting the current forces acting on the mooring line we minimize the differences between the different models, and this is acceptable since we are interested in other effects. Regarding or disregarding the current effects on the mooring lines will not influence the line tension significantly as it was described in section 2.1.1.

Body type 2 is chosen in SIMO, which means that the WF motions are pre-calculated in the FD, and LF motions are calculated in the TD throughout the whole simulation. By choosing this body type in SIMO, the WF calculations will be more equal to the calculations done in MIMOSA because they use the same RAO's.

### 6.3.2 Time Domain

TD simulations are first performed in SIMO and prescribed vessel motions are then implemented in RIFLEX. RIFLEX then runs a TD analysis with the same simulation length as in SIMO. The simulation time was 9 hours and 300 seconds. The first 300 seconds of the simulation is removed because it takes some time before the simulation stabilizes, and 300 seconds were chosen just to be on the safe side. Usually, TD analysis are simulated for 3 hours. By running a 9 hour simulation, statistical uncertainties are reduced.

For wave generation, Fast Fourier Transform (FFT) method was chosen. Cooley-Tukey Fourier transform algorithm is used to pre-generate waves in SIMO. The FFT method is less time consuming then performing a simulation by summations of harmonic components for each time step.

For TD analysis in SIMO and RIFLEX the *Newmark* –  $\beta$  procedure is used for numerical time integration, see [Langen and Sigbjörnsson, 1999] for more detailed description of this method. The chosen parameters used for this procedure were:

- $\gamma = 0,50$  weighting parameter which gives no numerical damping
  - $\beta = 0,25$  weighting parameter which gives constant acceleration (the trapezoidal method) that is unconditionally stable
- SIMO:  $\Delta t = 0,5s$
- RIFLEX:  $\Delta t = 0,5s$  Vessel motion (Irregular time series)  
 $\Delta t = 0,1s$  Line elements (Irregular response analysis)

## 6.4 Filter Design

When conducting a TD analysis in SIMO and RIFLEX the total tension force is calculated for the total duration of 9 hours. For analysing the WF and LF tension forces separately, filtering the total tension result is necessary. Digital signal processing is a huge subject and some basic knowledge is required for designing a good filter. There is a lot of literature that can be found on digital signal processing, and the book written by Steven Smith [Smith, 1999] was particularly useful in this master thesis. Signal processing tools in Matlab include a lot of different filter models, and these filters need to be tailored for filtering WF and LF tension forces. The mathematics behind these filters can be quite complex and will not be dealt with here. Only the terminology and the specific parameters are handled for creating a filter that performs well for the desired purpose.

Filtering out the WF and LF tension forces requires a good filter. A optimal filter has:

- Good stop band attenuation
- Flat passband with small or none attenuation

- Fast roll-off

In the process of designing a low and highpass filter a FFT was performed on the total tension force time series for line 1 and 7. This was done to transform the tension forces from the TD to the FD [Myrhaug, 2005], [Newland, 1993]. The following figure shows the result of the FFT for the time series in SIMO and RIFLEX. Built in Matlab function was used for performing an FFT, and the FFT procedure can be found in the Matlab code, appendix E (filter\_process.m).

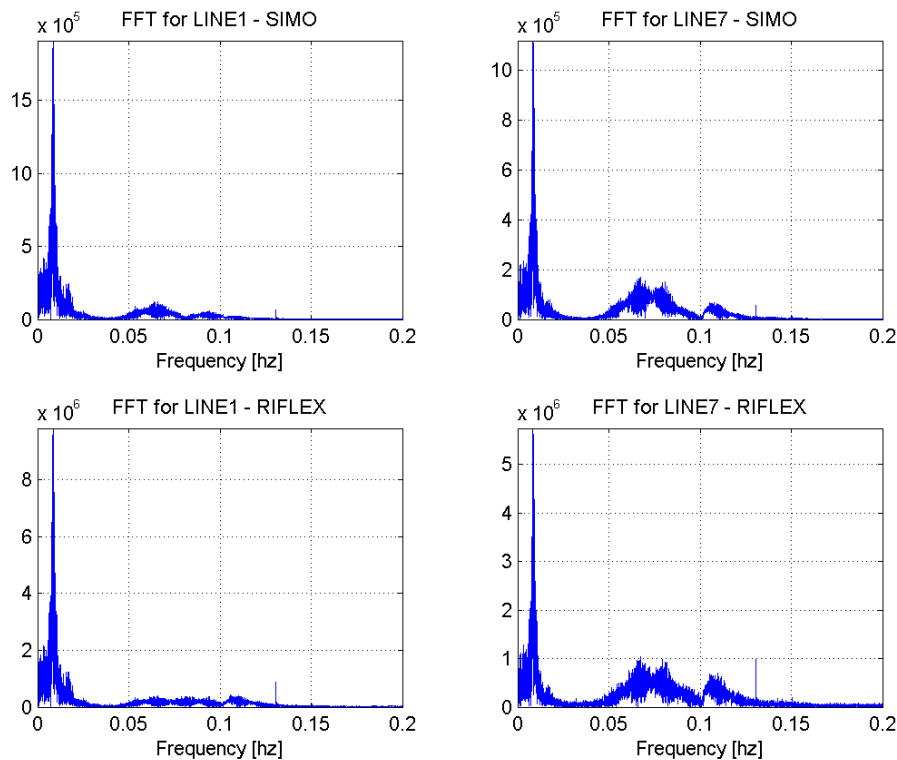


Figure 6.2: FFT on the time series for SIMO (upper) and RIFLEX (lower) - line 1 (left) and line 7 (right)

From figure 6.2 we see the tendency of a double peak spectrum. For line 7 (right) in both SIMO and RIFLEX the WF and LF peaks can clearly be seen. For the lowpass filter we want to damp out all the high frequency contributions. So a cut-off frequency was set to 0.03 Hz, which is a period of 33.33 s. The cut-off point is the point between the LF and WF peaks, and this will now become the basis for the designed filter.

For minimum passband attenuation a Butterworth filter was chosen. This filter is based on Chebyshev polynomials and the filter order. After some attempts the optimal filter order was found to be 4. As it will be shown later on, this order gave good filtering performance and avoided overflow. As most filter, also this filter introduces a phase shift of the output signal relative to the input signal. This was not corrected for because this will not have any influence on the final result since the goal is to find the STD of WF and LF tension forces. The sampling frequency ( $F_s$ ) was set to 2 Hz for SIMO and 10 Hz for RIFLEX, and this  $F_s$  must be equal to the time step given in the SIMO and RIFLEX analysis. Figure 6.3 shows the constructed Butterworth filter

used for filtering LF and WF tension forces from the total tension force time series.

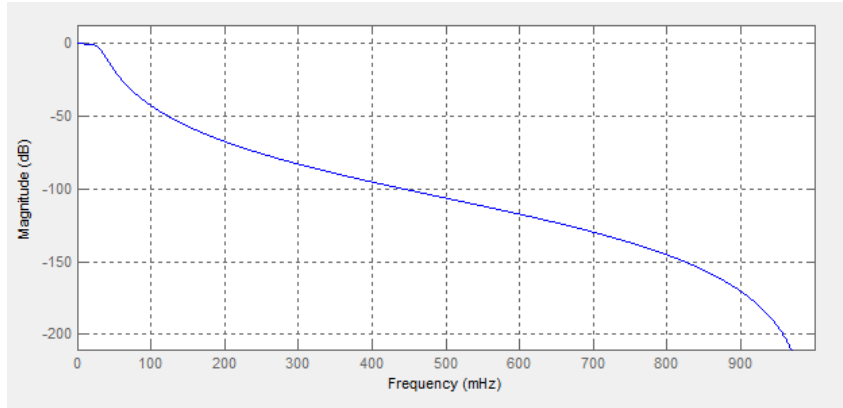


Figure 6.3: Designed filter. 4th order Butterworth bandpass filter

After the filtering process was done a simple test was performed to check if the designed filter was accurate enough. Since we have a double peaked spectrum and the fact that WF and LF tension forces are separable as seen from figure 6.2, the total STD of tension forces for line 1 and 7 can simply be calculated by using the filtered STD of WF and LF tension forces:

$$\sigma_{TOTFilter} = \sqrt{\sigma_{LFFilter}^2 + \sigma_{WFFilter}^2} \tag{6.1}$$

The next table shows a comparison between the calculated total STD tension force ( $\sigma_{TOTFilter}$ ) and the original unfiltered STD tension force ( $\sigma_{TOTOriginal}$ ):

	$\sigma_{TOTFilter}$ [kN]	$\sigma_{TOTOriginal}$ [kN]	Diff [%]
SIMO - $\Delta t = 0,5s = 2Hz$			
Line 1	187.38	188.27	0.47
Line 7	117.86	117.92	0.05
RIFLEX - $\Delta t = 0,1s = 10Hz$			
Line 1	192,69	193,61	0.47
Line 7	136.68	132,72	0.03

Table 6.5: Comparing calculated STD tension with the original STD tension force

The data for this table can be found in appendix E under section RESULTS.txt. From these results we see that the difference between the calculated total STD tension force ( $\sigma_{TOTFilter}$ ) and the original unfiltered STD tension force ( $\sigma_{TOTOriginal}$ ) deviate less then 0,50 % for both lines. This basically means that the designed filter is quite good, and can be used to filter out the LF and WF tension forces from the total tension force time series.

The next two figures will show how the filtered WF and LF tension forces corresponds to the original tension forces, which include both WF and LF tensions (WF&LF). From these figures it is seen that the filtered tension forces are phase shifted. As mentioned previously this will not affect the results since we are interested in STD of WF and LF tension forces.



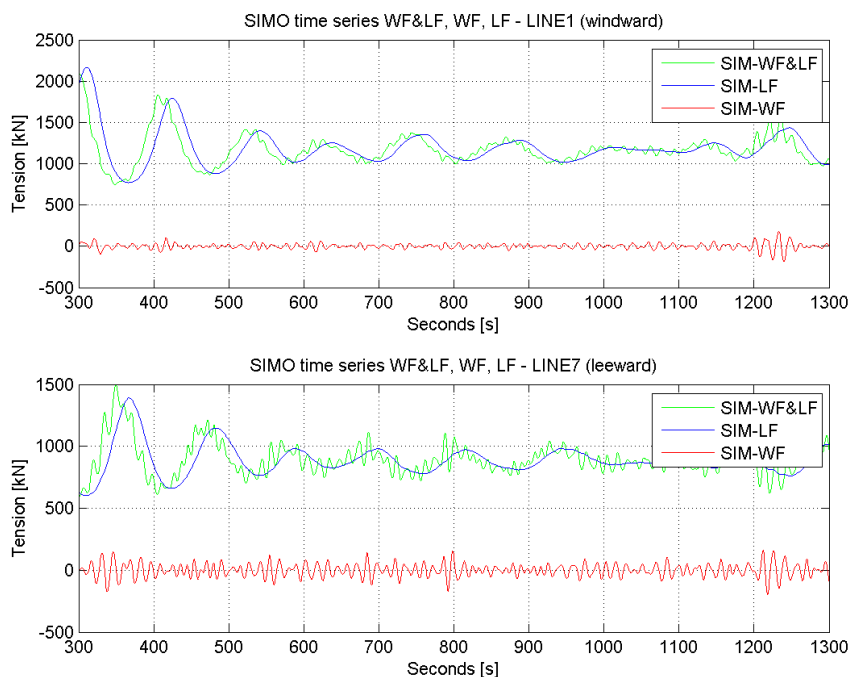


Figure 6.4: Original (WF&LF) and filtered WF and LF tension forces for line 1 (upper) and line 7 (lower) for SIMO

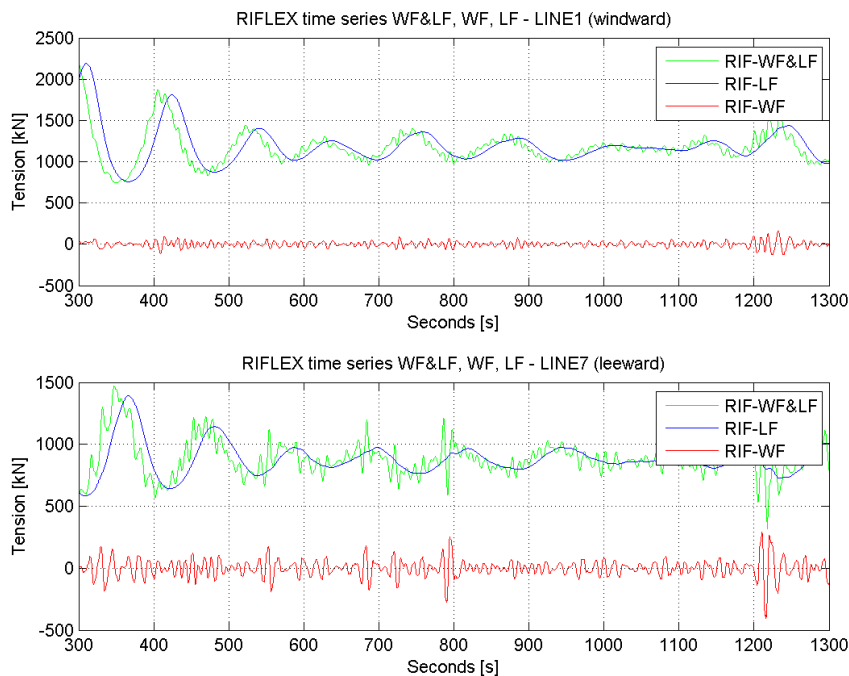


Figure 6.5: Original (WF&LF) and filtered WF and LF tension forces for line 1 (upper) and line 7 (lower) for RIFLEX

For illustrative purposes the time series is plotted from 300 s - 1300 s. From figure 6.4 and 6.5 we see that the filtered WF and LF tension forces follow the original (WF&LF) tension series quite well. For our case we have a pretension of 1000 kN, and it can be seen that the original tension forces for line 1 (windward line) fluctuates between a mean tension above the set pretension. The original tension forces for line 7 (leeward line) does the same except that the mean tension value is beneath the set pretension. This confirms that the mooring lines behave as expected, meaning that it is expected that line 1 is experiencing larger and line 7 is experiencing less tension forces than the set pretension.

## 6.5 Fatigue Analysis

A small fatigue analysis was carried out in this master thesis. This is done because it is interesting to show how the fatigue damage is affected for different sea-states. Simplified methods have been used and will be explained in this section.

In an article written by C.M. Larsen [Larsen, 1987], he performed a long-term fatigue analysis of risers on a tension-leg platform (TLP). The conclusion from this article was that for extreme sea-states,  $H_s$  larger than 10 m, can be neglected when it comes to fatigue damage because the probability for this sea-state to occur is small. Inspired by this, a similar fatigue analysis was performed on the mooring lines to see what sea-states contribute to fatigue damage.

For calculating the fatigue damage, the same sea-states has been used as in the article, and the combined spectrum (CS) approach was used for these calculations. The sea-states used can be found in appendix F. The equations used can be found in section 2.3 or in the DNV rules, [DNV, 2010]. This small fatigue damage analysis is done just to illustrate how the STD WF and LF tensions can be used directly in the fatigue analysis.

Even though the calculation performed here are simplified compared to the calculations done in the article, the same conclusion can be drawn here.  $H_s$  larger than 10 m will contribute minimally for the fatigue damage on line 1 and 7. Even though the maximum stresses are large for  $H_s$  larger than 10 m the probability for this sea-state to occur is small. When conducting the fatigue analysis only MIM-FEM was used. MIMOSA computes in the FD and is less time consuming than for instance conducting this analysis in SIMO or RIFLEX.

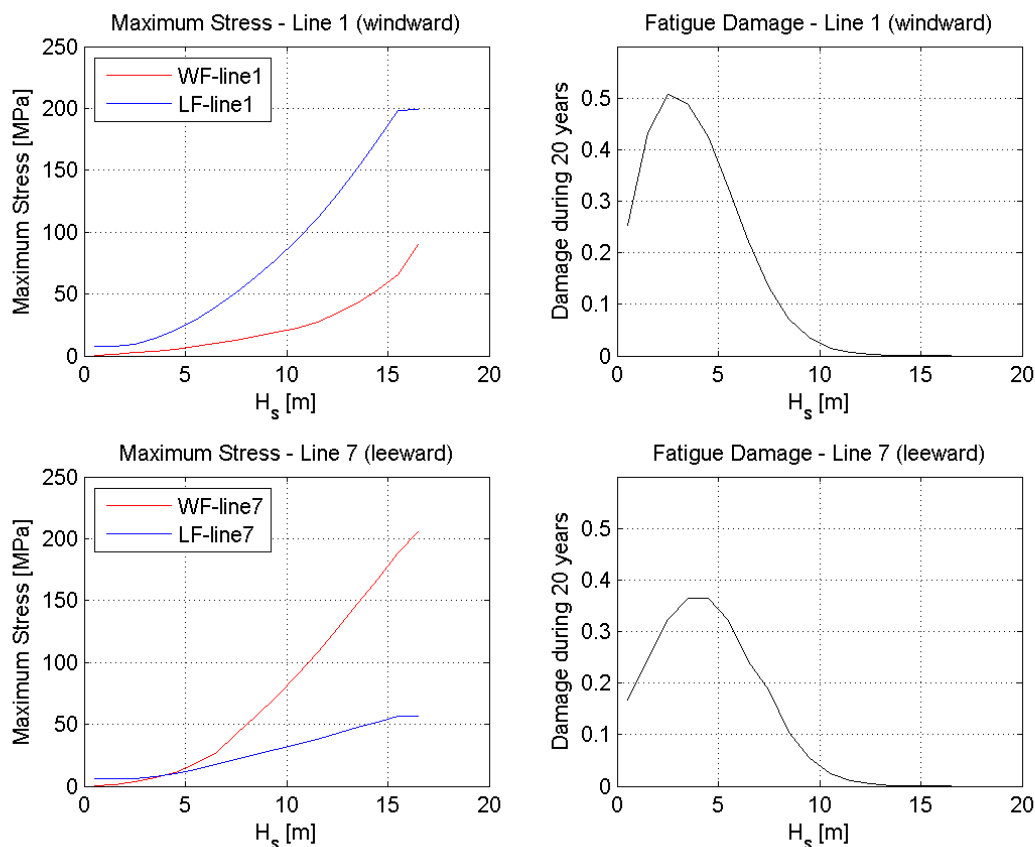


Figure 6.6: Fatigue damage graphs. Maximum stress line 1 (upper left), fatigue damage results using CS approach (upper right). Maximum stress line 7 (lower left), fatigue damage results using CS approach (lower right)

Note that by looking at the maximum stress curve for both cases, we see that the windward line is dominated by LF motion, while leeward line is dominated by WF motion. This will be discussed more thoroughly later on.

# Chapter 7

## Results and Discussions

It is important to keep in mind that the system which was described in the previous chapter and then analysed, is a modified system. These modifications are made to enlarge and isolate different effects that occur when analysing a turret moored FPSO. Even though it is not a completely real system these effect will be present for cases which are similar to the case used in this master thesis, which was a turret moored FPSO in shallow waters.

### 7.1 Results

In the process of computing the results the following must be kept in mind:

- Separate analysis was carried out for all computation methods in MIMOSA (see section 2.2), which means that WF only and LF only options have been used,
- wind, waves and current propagate in the same direction for MIMOSA and SIMO (towards south) hitting the vessels bow,
- current forces acting on the mooring lines are not included in the analysis,
- contact forces (friction) between the mooring lines and sea-floor is also not included because all the programs; MIMOSA, SIMO, and RIFLEX model this differently,
- the vessel has restricted rotations in yaw (see section 6.1),
- static offset is due to mean environmental loads acting on the floating vessel for MIMOSA and SIMO while RILFEX has a prescribed motion from SIMO with the same static offset (see section 3.3),
- in MIMOSA and SIMO all the mooring lines were modelled, while in RIFLEX only the windward (line 1) and leeward line (line 7) were modelled (see chapter 3),
- filtering was necessary to separate WF and LF tension forces for the time series simulations performed by SIMO and RIFLEX (see section 6.4),
- due to combined response spectrum the total STD tension in MIMOSA was calculated by using STD of WF and LF tension. In section 6.4 we verify that this approach is acceptable to use,

- STD of WF and LF tension was calculated by using Matlab for SIMO and RIFLEX based on filtered TD tension series, while these were given results from the MIMOSA analysis output file due to calculations made in the FD.

Abbreviation	Description (*)= <b>WF or LF</b>
MIM_FEM_(*)	MIMOSA: Computes STD of WF or LF tension using FEM.
MIM_QS_(*)	MIMOSA: Computes STD of WF or LF tension using the QS method.
SIM_QS_(*)	SIMO: Filtered and calculated STD of WF or LF tension using body type 2, QS method.
RIF_FEM_(*)	RIFLEX: Filtered and calculated STD of WF or LF tension for a fully non-linear FEM analysis.
DIFF	Percent difference between value 1 og value 2. A negative DIFF means that value 1 is smaller then value 2, while a positive DIFF means that value 2 is larger then value 1.
Ratio	Ratio between value 1 and value 2.

Table 7.1: Description of calculation methods, explanation of abbreviations used in tables and graphs. For a more detailed description of computation methods see chapter 5

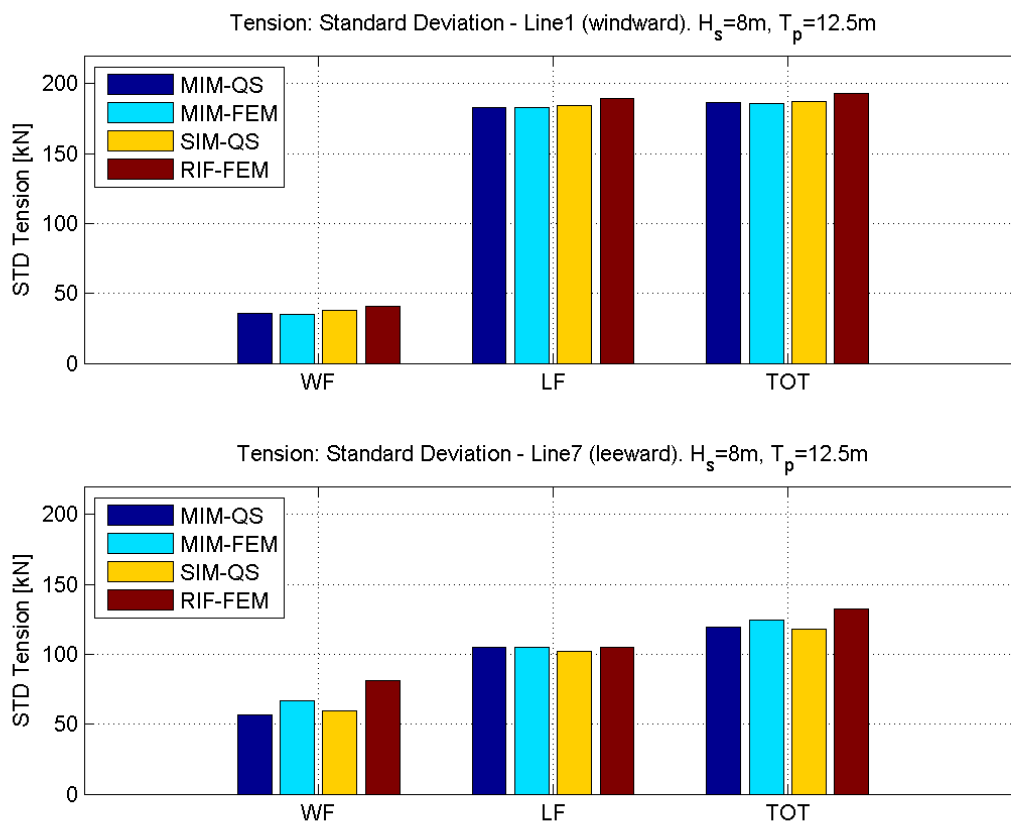


Figure 7.1: Comparing the main results from MIMOSA, SIMO and RIFLEX in a barplot

LINE 7 - Leeward						
	Value 1	[kN]	Value 2	[kN]	DIFF	Ratio
1	MIM_QS_WF	<b>56,64</b>	SIM_QS_WF	<b>59,33</b>	-4,75 %	0,95
2	SIM_QS_WF	<b>59,33</b>	RIF_FEM_WF	<b>81,44</b>	-37,27 %	0,73
3	MIM_QS_WF	<b>56,64</b>	RIF_FEM_WF	<b>81,44</b>	-43,79 %	0,70
4	MIM_QS_WF	<b>56,64</b>	MIM_FEM_WF	<b>66,49</b>	-17,39 %	0,85
5	MIM_FEM_WF	<b>66,49</b>	RIF_FEM_WF	<b>81,44</b>	-22,48 %	0,82
6	MIM_QS_LF	<b>104,94</b>	SIM_QS_LF	<b>101,90</b>	2,90 %	1,03
7	SIM_QS_LF	<b>101,90</b>	RIF_FEM_LF	<b>104,80</b>	-2,85 %	0,97
8	MIM_QS_LF	<b>104,94</b>	RIF_FEM_LF	<b>104,80</b>	0,13 %	1,00
9	MIM_QS_LF	<b>104,94</b>	MIM_FEM_LF	<b>104,94</b>	0,00 %	1,00
10	MIM_FEM_LF	<b>104,94</b>	RIF_FEM_LF	<b>104,80</b>	0,13 %	1,00
LINE 1 - Windward						
	Value 1	[kN]	Value 2	[kN]	DIFF	Ratio
1	MIM_QS_WF	<b>35,61</b>	SIM_QS_WF	<b>37,87</b>	-6,35 %	0,94
2	SIM_QS_WF	<b>37,87</b>	RIF_FEM_WF	<b>40,61</b>	-7,24 %	0,93
3	MIM_QS_WF	<b>35,61</b>	RIF_FEM_WF	<b>40,61</b>	-14,04 %	0,88
4	MIM_QS_WF	<b>35,61</b>	MIM_FEM_WF	<b>34,81</b>	2,25 %	1,02
5	MIM_FEM_WF	<b>34,81</b>	RIF_FEM_WF	<b>40,61</b>	-16,66 %	0,86
6	MIM_QS_LF	<b>182,76</b>	SIM_QS_LF	<b>184,43</b>	-0,91 %	0,99
7	SIM_QS_LF	<b>184,43</b>	RIF_FEM_LF	<b>189,31</b>	-2,65 %	0,97
8	MIM_QS_LF	<b>182,76</b>	RIF_FEM_LF	<b>189,31</b>	-3,58 %	0,97
9	MIM_QS_LF	<b>182,76</b>	MIM_FEM_LF	<b>182,76</b>	0,00 %	1,00
10	MIM_FEM_LF	<b>182,76</b>	RIF_FEM_LF	<b>189,31</b>	-3,58 %	0,97

Table 7.2: Main comparison results for line 1 and 7. All the values in the table are STD, and the table is sorted in the order of importance

In the table above the leeward line is presented first because this will be the main focus throughout the discussions. The windward line will be used to compare with the leeward line.

The first observation made is the difference in magnitude between LF tension for the windward and leeward line. The LF tension for line 1 is almost twice as large as for line 7. This difference will be discussed in the following section.

From table 7.2 and figure 7.1 we see that the difference between the STD of LF tension deviate less then -4% for all values that are compared for both windward and leeward line. We also have a verification that MIMOSA computes the STD of LF tension equally regardless of using QS or FEM (comparison 9 for both line 1 and 7), as was described in section 5.1.

For the windward line the largest observed difference for STD of WF tension is for comparison 5, which is -16,66%.

For the STD of WF tension for the leeward line there are significant differences observed for comparison 2 to 5, and the largest difference is found for comparison 3 which is -43,79%.

## 7.2 Windward vs. Leeward line

For the windward line (line 1) we see that the total STD tension is dominated by STD of LF tension, while the total STD tension for the leeward line (line 7) is dominated by STD of WF tension. To explain these differences we need to look at the motion for a turret moored FPSO.

Since the incoming environment propagate in the same direction, the motion of a turret moored FPSO will be elliptical in the  $xz$ -plane [Lone, 2009]. This means that the resulting force acting on the windward line will be larger then for the leeward line, which can be seen from the results. A illustration is made to show the elliptical motion for the turret moored FPSO and the resulting forces due to this motion. Note that figure 7.2 is a illustration so, resulting forces, depth and so on are not up to scale.

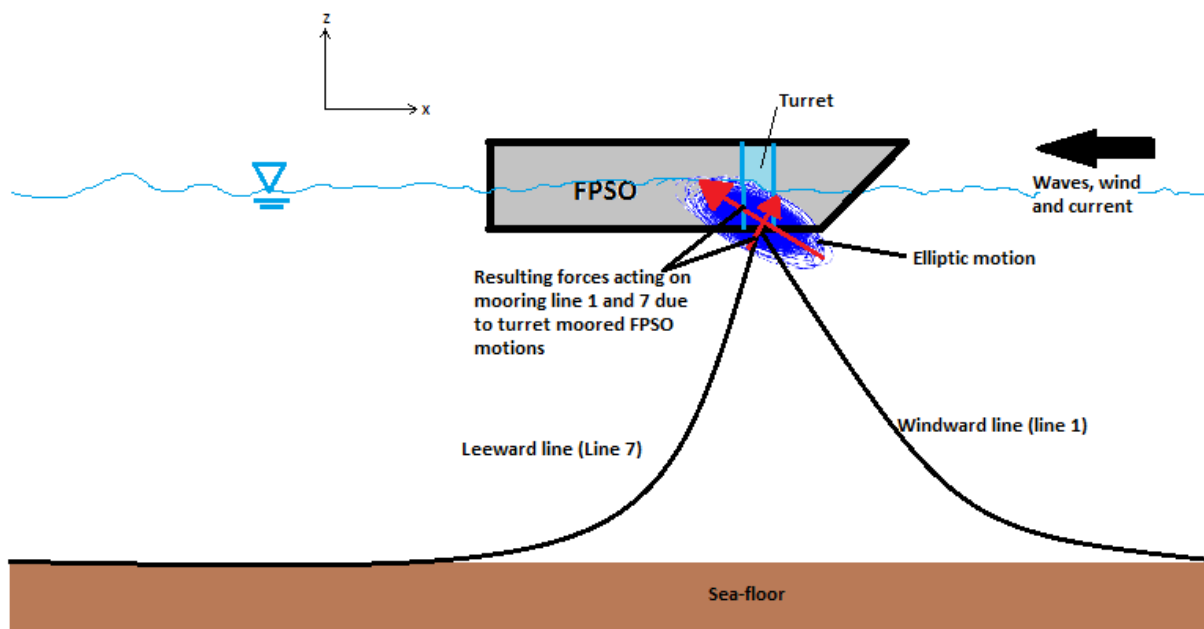


Figure 7.2: Illustration of a elliptical motion for a turret moored FPSO, and the resulting forces due to this motion (red arrows)

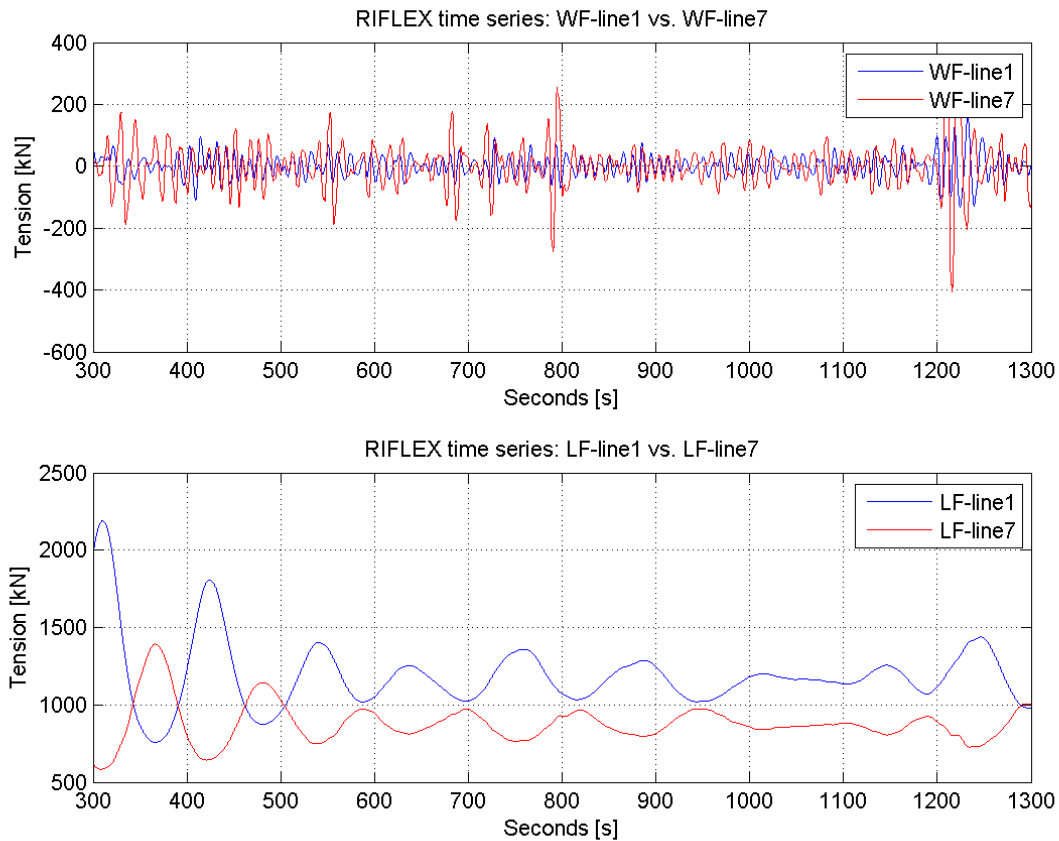


Figure 7.3: Comparing filtered WF and LF tension forces for windward (line 1) and leeward line (line 7) from RIFLEX time series. Plot: 300 s - 1300 s.

Figure 7.3 shows a plot from 300 s - 1300 s, and we can clearly see that the amplitudes for LF tension are larger for line 1 than for line 7. The opposite can be said for WF tension forces where the leeward line has larger WF tension contributions than the windward line. This trend continues throughout the whole 9 hour simulation. This was first observed in figure 6.6 in section 6.5.

Due to the elliptical motions for a turret moored FPSO, line 1 will be more tightened up, while line 7 will have a more non-linear slack configuration. Because line 1 is more taut, WF motions will not influence the total motion as much as they will for line 7. The combined WF and LF motions will therefore affect the total tension forces differently for the two mooring lines. This can be seen from the main results and on figure 7.3.



### 7.3 Comparison differences between methods: STD of WF tension

Table 7.2 is the basis for the discussions throughout this section. The main focus will be on the STD of WF tension for the leeward line since these comparison values deviate the most in the main results, and also because the leeward line is the critical line for fatigue damage.

The difference between MIM\_FEM\_WF and RIF\_FEM\_WF (comparison 5) for the leeward line is the main result which we are after. To be able to explain what causes the variation between them we need to rule out different effects with help from different computation methods. This is the reason for also performing the analysis in SIMO, and using these results to isolate different effects.

#### 7.3.1 Importance of updated line characteristics

For comparison 1 (QS-method for MIM and SIM), the only difference between the computation methods is that SIMO updates the line characteristics, as described in section 5.2. This means that the geometrical stiffness is properly accounted for in SIMO. A difference of -4,75 % shows that for a non-linear mooring line characteristic, this effect needs to be considered, and by using the QS-method in MIMOSA will not sufficiently handle this effect.

Comparing the comparison 1 differences between the leeward and windward line we see that windward line has a higher difference (-6,35%) in percent then for the leeward line (-4,75%).

The explanation of this difference for comparison 1 has to do with the non-linear mooring line characteristics. Let us now introduce a local axis system at the top end (fairled) of the mooring lines 1 and 7, respectfully. The x-axis for the two mooring lines will have opposite directions in the global axis system which has a positive x-axis towards north. The system is in initial position for  $x = 0,00m$ . When static equilibrium is found, about  $x = -2,00m$  in global axis system, the local x-coordinate for the windward line will be the same (orientated towards north). For the leeward line, which has the x-axis in the other direction (towards south) in the global axis system, the local x-coordinate will be  $x = 2,00m$ .

This means that we will move further down for the windward line, and further up for the leeward line in the line characteristics. Since MIMOSA and SIMO has the same line characteristics, the windward line will move to a area where the line characteristic is non-linear. The leeward line will then move to a location where the line characteristic is less non-linear. Since MIMOSA uses a linearised interpolation method for finding the STD of WF tension for the QS-method, the difference between MIMOSA and SIMO will be larger in a area where the line characteristics are more non-linear, and therefore the difference when comparing MIM\_QS\_WF with SIM\_QS\_WF for line 1 and 7.

If WF and LF combined (WF&LF) calculations had been carried out, then the STD of LF motions would be included in the calculation of the STD of WF tension. The difference between the methods used in comparison 1 would most likely be smaller. A suggestion for further work can be to verify if this is true.

### 7.3.2 Importance of dynamic effects

When dynamic effects are mentioned it means that drag and inertia forces on the mooring lines are included and accounted for in the computation method. We now want to assess the importance of dynamic effects on the windward and leeward lines.

The only difference between SIM-QS and RIF-FEM (comparison 2) is that the fully non-linear analysis in RIFLEX accounts for dynamic effects. By comparing these to methods we undoubtedly see that dynamic effects are of high importance for the leeward line. -37,27% difference for the leeward line indicates that dynamic effects must be included in the analysis to get accurate results when calculating the STD of WF tension. When drag forces are included, we know that the WF tension response will be phase shifted [Faltinsen, 1990]. This can clearly be seen from figure 7.4 where RIF-WF is phase shifted compared to SIM-WF because RIFLEX accounts for drag and inertia forces.

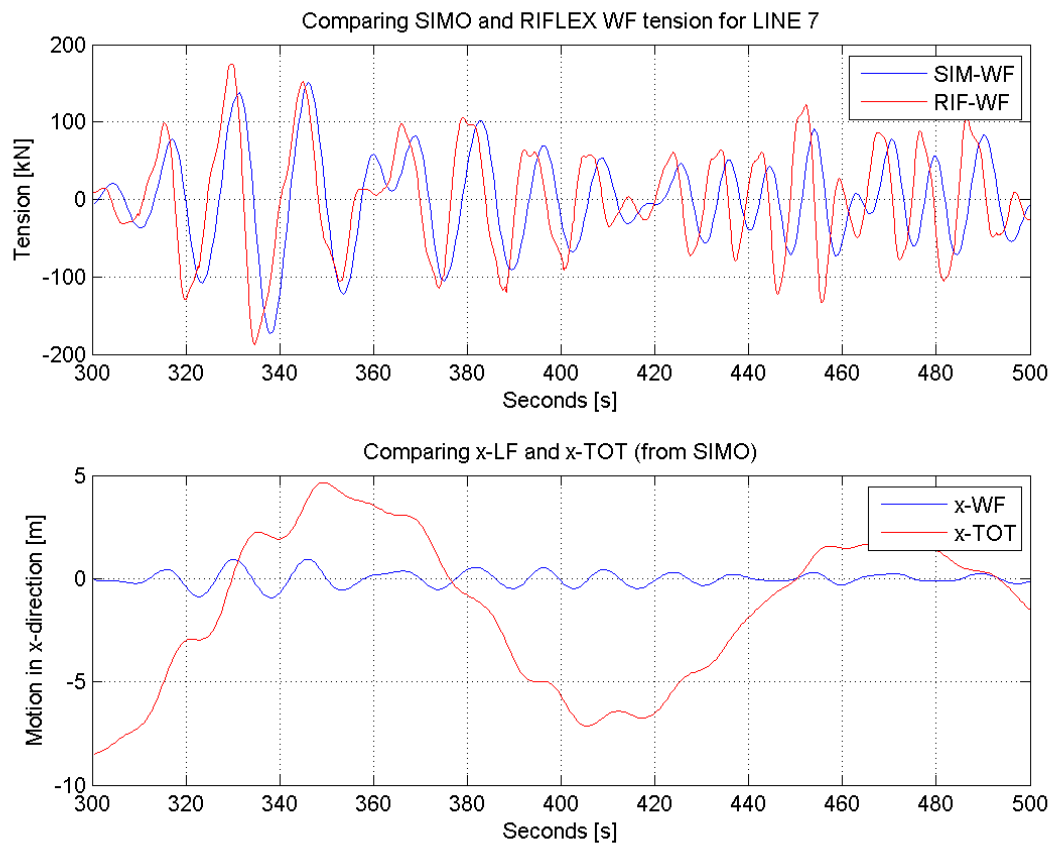


Figure 7.4: Comparing WF tension between SIMO and RIFLEX for leeward line (upper graph). Lower plot is the surge motion for the same time series. Plot: 300 s - 500 s

The windward line will on the other hand have less dynamic effects then the leeward line because this line is more taut. A difference of -7,24% is considerably less then for the leeward line. This is again a confirmation that the leeward line experiences large dynamics, and is the critical line for fatigue damage.

Comparison 3 is the difference between the MIM-QS and RIF-FEM. As previously discussed the fully non-linear analysis in RIFLEX accounts for geometrical stiffness and dynamic effects, see conclusion of program theory section 5.4. For MIM-QS non of these effects are accounted for. One would then expect that the difference for this comparison would increase for both the leeward and windward line. From the results we see that this is also the case, because two essential effects are not accounted for in MIM-QS: (i) updated line characteristics, (ii) dynamic effects.

### 7.3.3 STD of WF tension: MIM-QS vs MIM-FEM

MIM-QS and MIM-FEM are both computation methods that calculated in the FD. MIM-FEM is the method which uses a simplified method to account for dynamic effects, see section 5.1. This means that the difference of -17,39% for the leeward line in comparison 4 is mainly due to the simplified method for accounting dynamic effects in the MIM-FEM. Neither of these computation methods account for updated line characteristics, so this will be the same for both as well as the static offset.

The difference between comparison 3 and 4 is that RIF-FEM properly accounts for dynamic effects and updated line characteristic. Since the difference between comparison 3 and 4 should, theoretically, be the updated line characteristics, one would expect a small percent difference between comparison 3 and 4. The actual difference between comparison 3 (-43,79%) and 4 (-17,39%) for the leeward line is over 50%, which is larger then one would expect. This means that there are other effects which cause this difference.

From the MIMOSA theory section, section 5.1, we found that MIM-FEM linearises the touch-down point, or in other words, keeps the bottom node fixed. We also know that MIM-FEM uses a simplified method that accounts for dynamic effects. These two mentioned properties for MIM-FEM is what causes the difference in comparison 4. MIMOSA linearises all the non-linear effects. So for strongly non-linear effects, the linearisation of these effect may not be sufficient enough.

For the windward line the comparison difference is 2,25% (comparison 4), which is interesting. It is not quite clear what causes the MIM-QS to over predict the STD of WF tension. One possible explanation for the difference could be the vertical line characteristics. Because of the vessels elliptical motion, the reality would be that one also needs to account for line characteristics which varies in vertical direction ( $z$ -direction). The line characteristics that have been used throughout this master thesis is only considered for horizontal displacements ( $x$ -direction), because our main focus has been on the surge motion which is the critical motion for fatigue damage.

### 7.3.4 STD of WF tension: MIM-FEM vs RIF-FEM

Comparison 5 is the main goal of this master thesis. The difference found here is the difference between a simplified computation method in the FD, which computes quickly, and a fully non-linear TD analysis that uses significantly more computation time.

Lets now recapitulate what we know for these two methods:

**MIM-FEM** - dynamic effects are found by a simplified method

**RIF-FEM** - dynamic effects and updated line characteristic are properly accounted for

The main difference between these various methods should be the updated line characteristics. Because the difference is -22,47% there is a suspicion that the simplified method for accounting dynamic effects in MIM-FEM is not sufficient enough. This suspicion arises because the difference in comparison 1, where the difference only is updated line characteristics, is much less then the difference in comparison 5. This means that the simplified method used to account for dynamic effects in MIM-FEM contribute significantly to the difference between MIM-FEM and RIF-FEM.

On the other hand, if we look at comparison 4 (MIM-QS and MIM-FEM) we see that dynamic effects in MIMOSA give rise to a difference of -17,39%. When adding the updated line characteristics, which we get in comparison 5 (MIM-FEM and RIF-FEM), the percent difference increase to -22,47%. This increase is somewhat similar to the percent difference in comparison 1 (MIM-QS and SIM-QS).

It is hard to point out exactly what causes the difference in comparison 5, but we can now say that it most definitely has something to do with the linearisation process used in the line characteristics and in the simplified method used in accounting for dynamic effects in MIM-FEM. For mooring lines which are dominated by WF motion and has a non-linear configuration, the differences between MIM-FEM and RIF-FEM can be relatively large for turret moored FPSO in shallow waters. A table is made to summarize the different effects which are included in the different computation methods. This table gives an overview of what has been discussed throughout this chapter.

	Method 1 vs. Method 2		Differences between computation methods	Diff. leeward line
1	MIM_QS_WF	SIM_QS_WF	Updated line characteristic (SIM)	-4,75 %
2	SIM_QS_WF	RIF_FEM-WF	Dynamic effects (RIF)	-37,27 %
3	MIM_QS_WF	RIF_FEM-WF	Updated line characteristic (RIF) Dynamic effects (RIF)	-43,79 %
4	MIM_QS_WF	MIM_FEM_WF	Dynamic effects simplified (MIM_FEM)	-17,39 %
5	MIM_FEM_WF	RIF_FEM_WF	Dynamic effects (RIF) Dynamic effects simplified (MIM_FEM) Updated line characteristic (RIF)	-22,47 %

Table 7.3: STD of WF tension difference for leeward line (line 7)

# Chapter 8

## Conclusion

### 8.1 Conclusion from discussions and results

A quote from guidance note on page 40 in the offshore standard DNV-OS-E301, [DNV, 2010];

*"Catenary moorings without buoyancy elements or clump weights will have a quasi static behaviour in shallow waters (water depths < 100m)"*

It is seen from the results and discussions that simplified methods computed in the FD give satisfactory results for calculation the STD of LF tension. All the comparisons deviate less than -4% for both the windward and leeward line when comparing the calculations for STD LF tension. It is noted that some dynamic effects (drag and inertia forces) are present for both lines, and that the windward line deviate the most when MIM-FEM and RIF-FEM are compared. A quasi-static representation for computing the STD of LF tension is acceptable for both mooring lines.

The leeward line has been the main focus throughout this master thesis mainly because this line is dominated by WF motion and will therefore be the line which experience the largest line dynamics. The windward line was also modelled, and has been used to compare with the leeward line.

From the results and discussions one thing is quite clear, that dynamic effects and geometrical stiffness needs to be properly accounted for, especially for the leeward line. When comparing the STD of WF tension for SIMO QS method with RIFLEX fully non-linear analysis, both in time domain, the difference was -37,27%. The difference here gives an indication of how important it is to account for dynamic effects. The comparison between MIMOSA and SIMOs QS method showed that to account for geometrical stiffness, updated line characteristic is necessary.

For the turret moored FPSO analysed in this master thesis, a QS representation of the mooring lines is not recommended for the leeward and windward line because the STD of WF tension will be too conservative. The difference between the simplified FEM in MIMOSA and the fully non-linear TD analysis in RIFLEX was -22,48% for the leeward line, and -16,66% for the windward line. The difference here is mainly caused by the linearisation methods used in MIMOSA to account for geometrical stiffness and dynamic effects (drag and inertia forces acting on the mooring line). Using the simplified FEM in MIMOSA one will under predict the STD

of WF tension for the windward and leeward line, and therefore under predict the results in the estimation of fatigue life in the mooring lines.

## 8.2 Suggestions for further work

It would be interesting to perform a study that varies the environmental conditions for this turret moored FPSO, and to see what the differences in comparing the different computation methods would then be. It is obvious that for more calm sea-states the dynamic effect will decrease and perhaps not be of the same importance as shown in this study. Since our modified system is relatively stiff, it would also be interesting to see what would happen for a less stiff mooring system. By varying the mooring system properties for the same turret moored FPSO, and then comparing these results with the once found for this master thesis would also be interesting.

Performing a parameter study where pretension and turret horizontal position is varied would also be interesting. The interesting part here would be to see if the differences are of the same magnitude as shown for this master thesis.

Current forces acting on the mooring lines and bottom friction is disregarded for all the analysis performed in this master thesis. This was done because all the programs (MIM,SIM,RIF) model this differently, and to account for this would introduce more uncertainties in isolating the different effects between computation methods. It would therefore be interesting to see, if current forces and friction were included, how this would affect the comparison between MIM-FEM and RIF-FEM. A suggestion for including current forces on the mooring lines could be to include a linearly decreasing current profile. MIMOSA and RIFLEX can include current forces on the mooring lines, while in SIMO this possibility is not included.

Even though a small fatigue analysis was carried out, a more thorough fatigue analysis based on the results would be interesting. One could retrieve environmental data form a real location at a 100 m water depth, and then use these data in a similar analysis as conducted in section 6.5. It would also be very interesting to perform a comparison study between fatigue damage methods, e.g. comparing Rain-Flow counting (RFC) with the Combined Spectrum (CS) approach.

Another suggestion for further work would be to conduct a study where the main focus is on the differences in extreme value statistics for MIMOSA. This is because MIMOSA computes in the FD and uses extreme statistics to find max tension in the mooring lines. Conducting a study where the main focus is to see if there are any differences by running a Rayleigh or non-Rayleigh based analysis.

## 8.3 Practical improvement

Self made scripts can always be improved to reduce computation time. Even though the post-processing script made in Matlab only used 2 minutes, improvements can be done.

One practical improvement which could be done is to program everything in Matlab. Matlab can execute batch commands, and one of the advantages in coding everything in Matlab would be that the post-processing scripts and batch scripts would run simultaneously. In Matlab one could also create better defined directories for saving the analysis results for all programs. Because this

knowledge of Matlabs capabilities of execution batch commands came at the end of this master thesis, all the batch scripts created were kept.

Running different environmental conditions would on the other hand cause some problems when programming everything in Matlab. Matlab would have to create a new *sys.dat* file for SIMO every time the environmental conditions were changed, and to make a script that creates a new *sys* file for every environment would be quite time consuming.

All in all, the script which were made and used served there purposes, and did so quite well. A small drawback would be that if some changes were made to the model, for instance turret position, these changes needed to be done manually in the input files. This could be done differently by creating a script which creates input files as mentioned earlier.

# Bibliography

- [DNV, 2010] (2010). *DNV Offshore Standard, DNV-OS-E301 Position Mooring*.
- [MIM, 2012] (2012). *MIMOSA User's Documentation, Program version 6.3-06*. MARINTEK, Trondheim, Norway.
- [RIF, 2012a] (2012a). *RIFLEX Theory Manual Vertion 4.0 rev.0*. MARINTEK, Trondheim, Norway.
- [RIF, 2012b] (2012b). *RIFLEX User's Manual Vertion 4.0 rev.3*. MARINTEK, Trondheim, Norway.
- [SIM, 2012a] (2012a). *SIMO Theory Manual Version 4.0 rev.0*. MARINTEK, Trondheim, Norway.
- [SIM, 2012b] (2012b). *SIMO User's Manual Version 4.0 rev.0*. MARINTEK, Trondheim, Norway.
- [Faltinsen, 1990] Faltinsen, O. (1990). *Sea Loads on Ships and offshore structures*. Cambridge University Press.
- [Fylling and Larsen, 1982] Fylling, I. and Larsen, C. (1982). Dynamic behaviour of anchor lines. *Norwegian Maritime Research*, 3:18–32.
- [Kaasen, 2012] Kaasen, K. E. (2012). Mimoso: Interactive static and dynamic mooring system analysis. MIMOSA Course, 17.09.2012, MARINTEK.
- [Kaasen, 2013] Kaasen, K. E. (2013). 19.04.2013, Private communication.
- [Langen and Sigbjørnsson, 1999] Langen, I. and Sigbjørnsson, R. (1999). Dynamic response of marine structures (tmr4305).
- [Larsen, 1987] Larsen, C. (1987). Fatigue life analysis of production risers. In *OTC 5468 Offshore Thechnology Conference*.
- [Larsen and Sandvik, 1990] Larsen, K. and Sandvik, P. (1990). Efficient methods for the calculation of dynamic mooring line tension. *Proceedings of the First (1990) European Offshore Mechanics Symposium*, ISOPE:482–489.
- [Leira, 2013] Leira, B. (2013). 19.04.2013, Private communication.
- [Lone, 2009] Lone, E. N. (2009). Stochastic analysis of anchor line forces for floating production units. Master's thesis, Department of Marine Technology, NTNU.
- [Lone, 2013] Lone, E. N. (2013). Private communication.



- [Miedema, 2013] Miedema, S. (2013). Turret mooring. [http://www.offshoremoorings.org/moorings/2006/Groep6/Real%20page/Turret\\_main.htm](http://www.offshoremoorings.org/moorings/2006/Groep6/Real%20page/Turret_main.htm).
- [Mo, 2013] Mo, K. (2013). 25.04.2013, Private communication.
- [Moan, 2003] Moan, T. (2003). *TMR4190 Finite Element Modelling and Analysis of Marine Structures*. Department of Marine Technology.
- [Myrhaug, 2005] Myrhaug, D. (2005). *TMR4235 Stochastic Theory Of Sealoads*. Department of Marine Technology.
- [Newland, 1993] Newland, D. (1993). An introduction to random vibrations spectral and wave analysis. Lecture Notes from TMR4235 Stochastic Theory of Sealoads by Dag Myrhaug.
- [NTNU-Library, 2013] NTNU-Library (2013). <http://www.ntnu.edu/ub>.
- [Ormberg et al., 1997] Ormberg, H., Fylling, I., Larsen, K., and Sødahl, N. (1997). Coupled analysis of vessel motions and mooring and riser system dynamics. In *Proceedings of the International Conference on Offshore Mechanics and Arctic Engineering - OMAE*, pp. 91-100.
- [Ormberg and Larsen, 1998] Ormberg, H. and Larsen, K. (1998). Coupled analysis of floater motions and mooring dynamics for a turret-moored ship. *Applied Ocean Research*, 20:55–67.
- [SMB-Offshore, 2013] SMB-Offshore (2013). Turret mooring systems. <http://www.sbmoffshore.com/what-we-do/our-products/turret-mooring-systems/>.
- [Smith, 1999] Smith, S. W. (1999). *The Scientist and Engineer's Guide to Digital Signal Processing*. California Technical Publishing.
- [Storller, 2012] Storller, R. (2012). 27.09.2012, Course in Information Retrieval.
- [Webster, 1995] Webster, W. C. (1995). Mooring-induced damping. *Ocean Engineering*, 22:571–591.



# Appendix A

## Information Retrieval

When writing a scientific article, or a master thesis it is important to use information with good quality and that has been approved by scientists within the field of your study. What kind of databases that have been used is important to ensure that the quality of your product is good. In this small chapter it will be discussed how the information retrieval is carried out for this particular master thesis. The detail of the different search engines and what their advantages and disadvantages are, is not discussed here. It is just mentioned to show that this is taken into account when performing a literature search.

When performing a literature search different possibilities are given by the NTNU library. To ensure good quality of the articles found, the NTNU library website has only been used in this study [NTNU-Library, 2013]. NTNU library include a lot of different databases. Databases that were used for this master thesis were SCOPUS and COMPENDIX. Books that were being used are mainly purchased, and have been used in previous courses lectured at MTS.

Throughout this master thesis a lot of courses have been given, and the lecture notes from these courses have been used. Personal conversations and private lectures given by Erling Lone have also been used, but to ensure reliability of the content lectured, the theory given in these courses has been found in different books and articles.

The course in information retrieval was given by Roar Storller, [Storller, 2012].

# Appendix B

## Programlist

Program	Edition	Function
MIMOSA	6.3	MARINTEK program: Frequency Domain
SIMO	4.0 rev 0	MARINTEK program: Time Domain
RIFLEX	4.0.2	MARINTEK program: Time Domain
SIMA	0.10.0.43	MARINTEK program: Communication between programs
Matlab	R2012a (7.14.0.739)	Used for post processing data and calculations
Texmaker	3.5.2	L <sup>A</sup> T <sub>E</sub> X editor
JabRef	2.9.2	Helps with creating a reference list in L <sup>A</sup> T <sub>E</sub> X
TextPad	6.2.2	Editor used for scripts and batch codes
ConTEXT	0.98.6	Used for reading .res files from RIFLEX

## Appendix C

# Case Parameter Study in MIMOSA - Results

Case Description				
Case	Pretension [kN]	(Wd) [m]	xt [m]	Env.dir. [deg]
Base Case	1200	100	48,32	180
1	1000	100	48,32	180
2	800	100	48,32	180
3	1000	120	48,32	180
4a	1000	100	60,00	180
4b	1000	100	60,00	170
5	1000	100	70,00	180
6	1000	120	70,00	180

Table C.1: Case parameter study

*wd* - water depth

*xt* - turret *x* position

*Env.dir.* - environmental propagating direction (180 degrees; propagates towards south)

The ratio multiplied the power of 3 (next two tables) is only included to show how the difference will increase when used in fatigue damage, the slop parameter ( $m = 3$ ) from the S-N curve. See section 2.3.

Windward Line (line1)

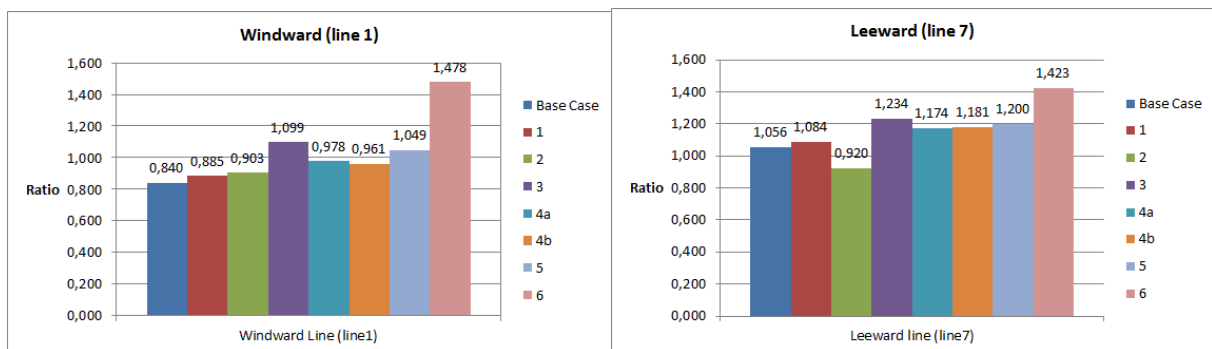
Case	STD FEM-WF [kN]	STD QS-WF [kN]	Ratio [-]	Ratio <sup>3</sup> [-]
Base Case	41,55	49,45	0,84	0,59
1	33,88	38,30	0,88	0,69
2	25,37	28,09	0,90	0,74
3	28,46	25,89	1,10	1,33
4a	34,81	35,61	0,98	0,93
4b	34,84	36,26	0,96	0,89
5	36,94	35,23	1,05	1,15
6	36,04	24,38	1,48	3,23

Table C.2: STD tension ratio for Windward line

Leeward Line (line7)

Case	STD FEM-WF [kN]	STD QS-WF [kN]	Ratio [-]	Ratio <sup>3</sup> [-]
Base Case	74,43	70,51	1,06	1,18
1	57,43	52,96	1,08	1,28
2	32,91	35,79	0,92	0,78
3	47,14	38,20	1,23	1,88
4a	66,49	56,64	1,17	1,62
4b	68,13	57,71	1,18	1,65
5	70,34	58,64	1,20	1,73
6	60,21	42,33	1,42	2,88

Table C.3: STD tension ratio for Leeward line



(a) Windward Line

(b) Leeward Line

Figure C.1: Bar-plot of the ratio for all cases

Each case was executed in MIMOSA and the results were automatically plotted in Matlab. These Matlab results were then extracted manually in tables for comparison. The Matlab bar plots are shown in following figures.

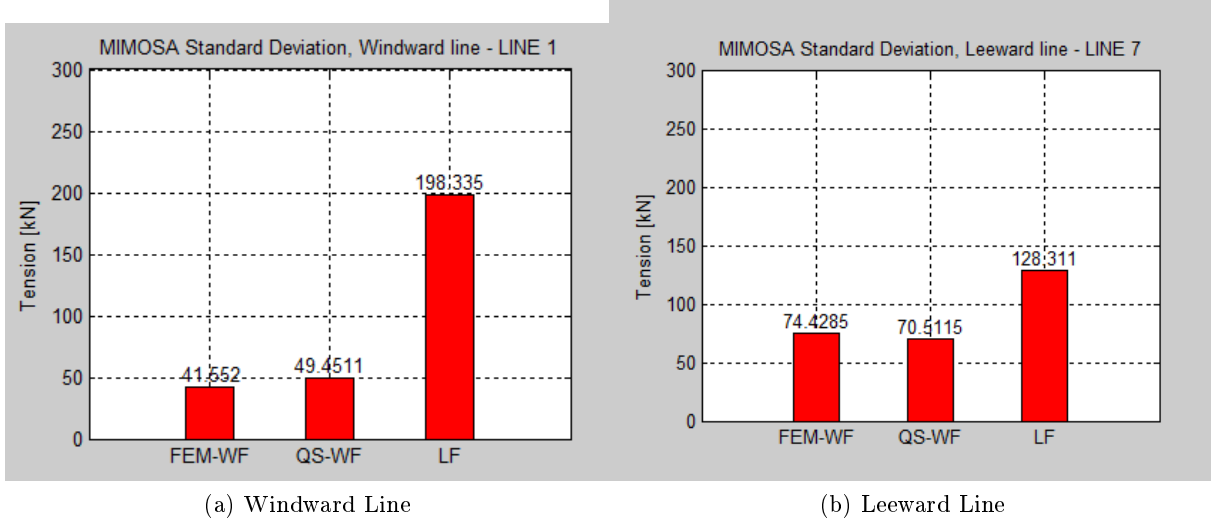


Figure C.2: Matlab results Base Case

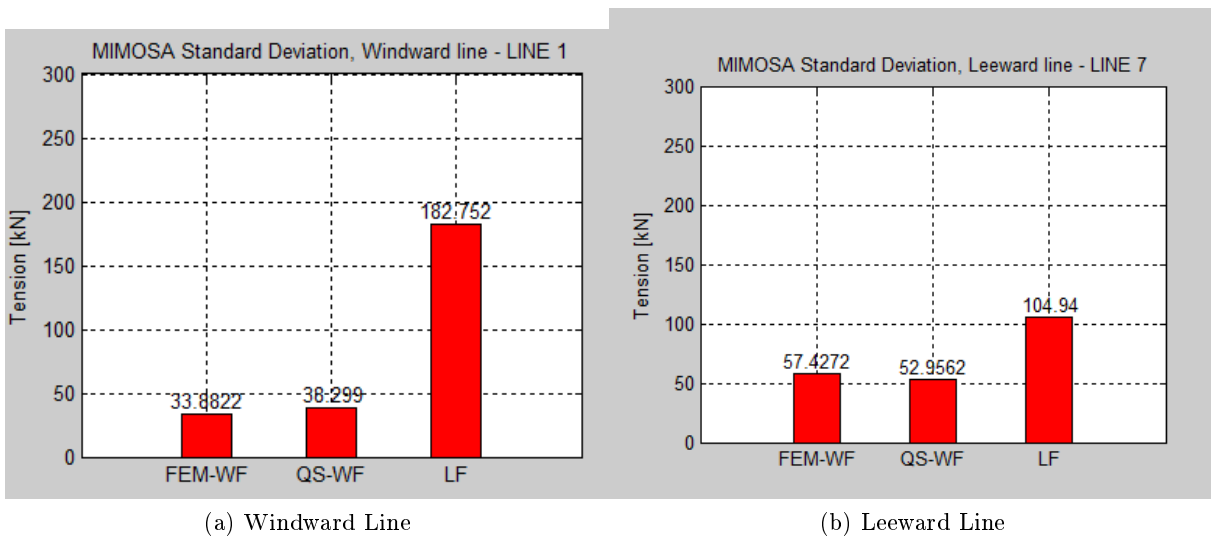


Figure C.3: Matlab results Case 1

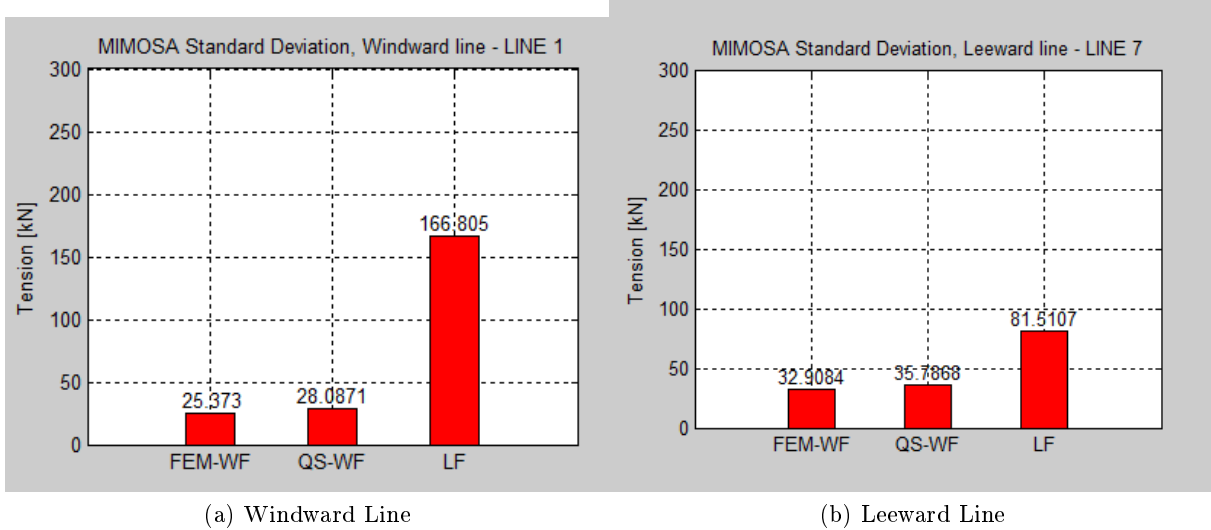


Figure C.4: Matlab results Case 2

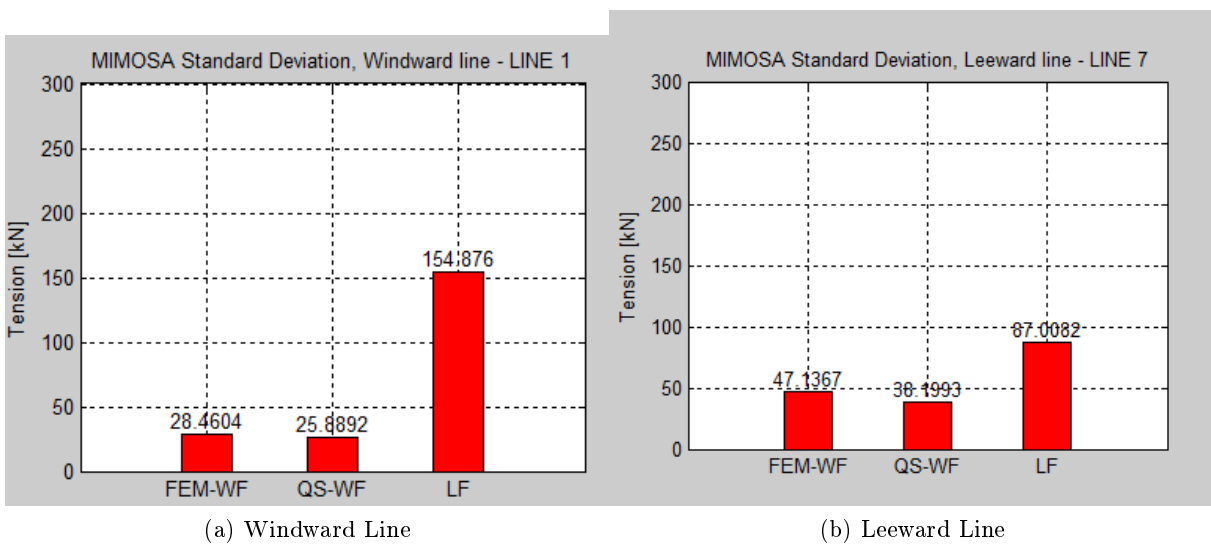


Figure C.5: Matlab results Case 3



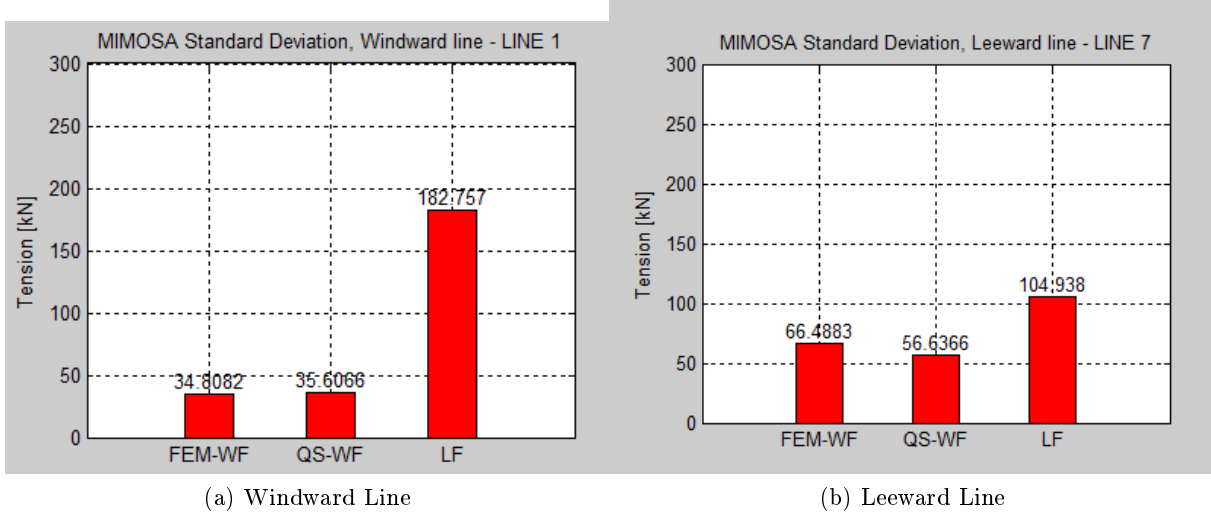


Figure C.6: Matlab results Case 4a

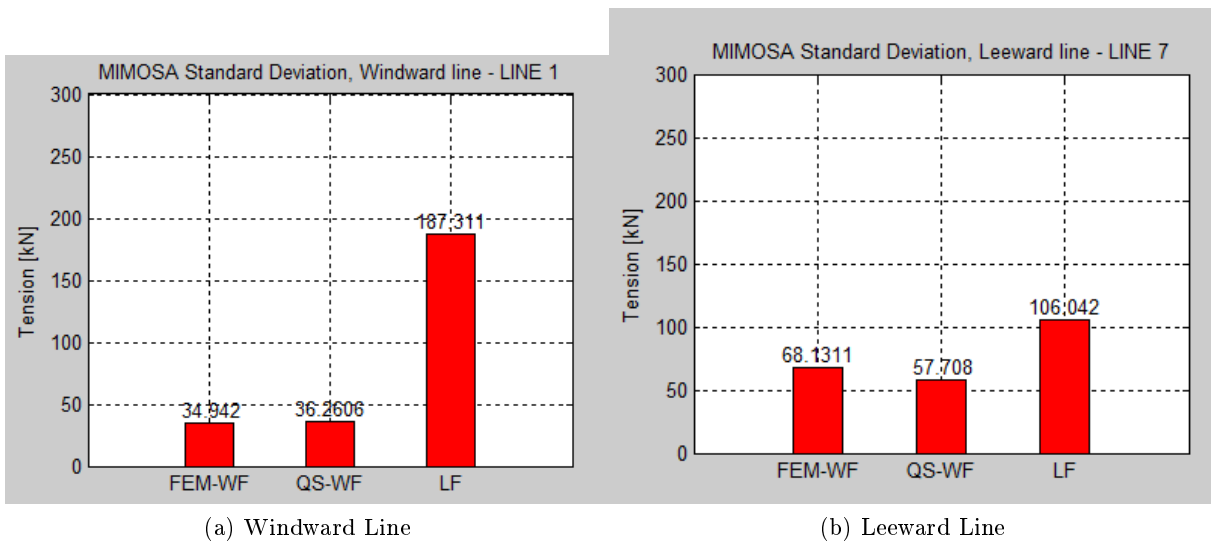


Figure C.7: Matlab results Case 4b

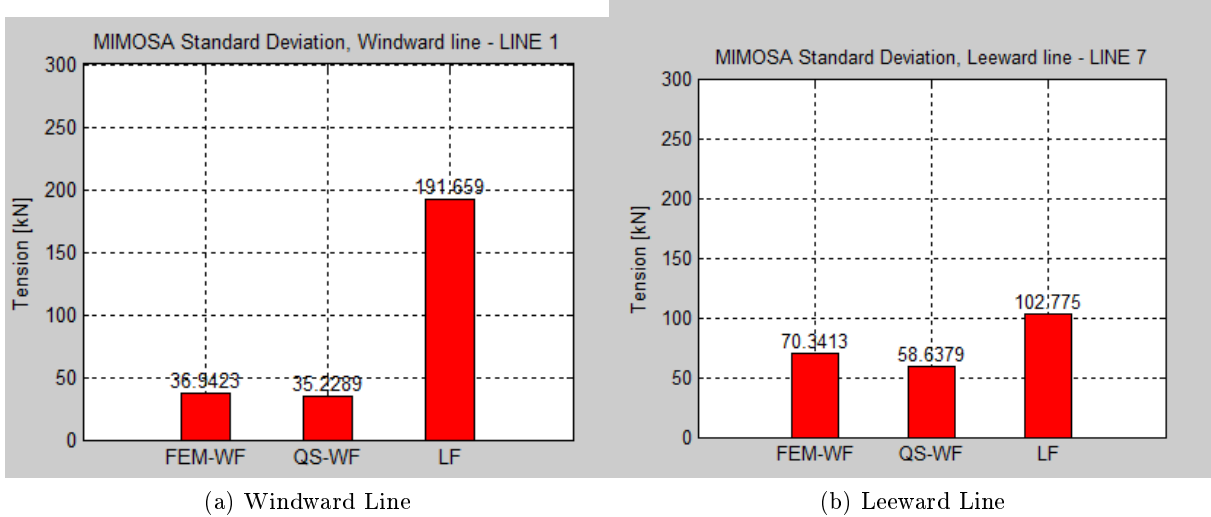


Figure C.8: Matlab results Case 5

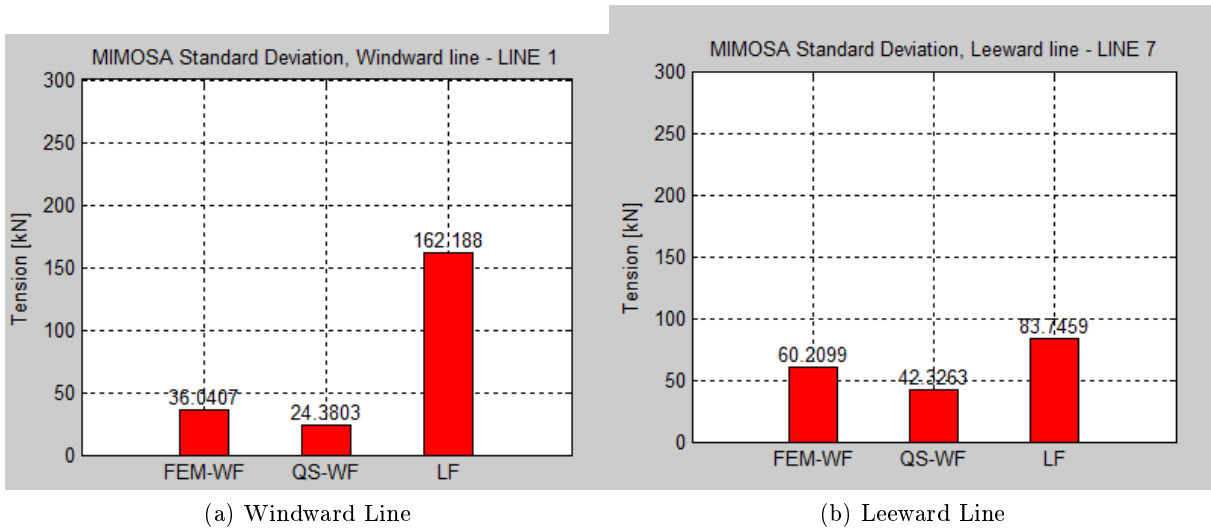


Figure C.9: Matlab results Case 6

## Matlab script: Case Parameter Study - read\_mimosa\_case4a

```

clear all
close all
clc

% MIMOSA case4a
=====
% Read Data
fem_wf_mim = (load('RES_FEM_WF.dat'))';
QS_wf_mim = (load('RES_QS_WF.dat'))';
LF_mim = (load('RES_QS_LF.dat'))';
=====
std_line1(1) = fem_wf_mim(4,1);
std_line1(2) = QS_wf_mim(4,1);
std_line1(3) = LF_mim(3);

tz_line1(1) = fem_wf_mim(7,1);
tz_line1(2) = QS_wf_mim(7,1);
tz_line1(3) = LF_mim(6,1);

std_line7(1) = fem_wf_mim(12,1);
std_line7(2) = QS_wf_mim(12,1);
std_line7(3) = LF_mim(10);

tz_line7(1) = fem_wf_mim(15,1);
tz_line7(2) = QS_wf_mim(15,1);
tz_line7(3) = LF_mim(13,1);

max_line1(1) = fem_wf_mim(6,1);
max_line1(2) = QS_wf_mim(6,1);
max_line1(3) = LF_mim(5,1);

max_line7(1) = fem_wf_mim(14,1);
max_line7(2) = QS_wf_mim(14,1);
max_line7(3) = LF_mim(12,1);
=====
% Figure Plots
scrsz = get(0,'ScreenSize');
figure('Position',[10 scrsz(4)/4 scrsz(3)/2 scrsz(4)/1.5])
x=1:3;

subplot(2,2,1);
bar(std_line1, 0.4, 'r');
text(x,std_line1',strcat(num2str(std_line1')),...
     'horiz','center','vert','bottom')
title('MIMOSA Standard Deviation, Windward line - LINE 1')
set(gca,'XTickLabel',{'FEM-WF', 'QS-WF', 'LF'});
ylabel('Tension [kN]');
axis([0 4 0 300]);
grid on

subplot(2,2,2);
bar(tz_line1, 0.4, 'b');
text(x,tz_line1',strcat(num2str(tz_line1')),...
     'horiz','center','vert','bottom')
title('MIMOSA Mean-up-crossing period, Windward line - LINE 1')

```

```

set(gca,'XTickLabel',{'FEM-WF','QS-WF','LF'});
ylabel('Tz [s]');
axis([0 4 0 150]);
grid on

subplot(2,2,3);
bar(std_line7, 0.4, 'r');
text(x,std_line7',strcat(num2str(std_line7')),...
     'horiz','center','vert','bottom')
title('MIMOSA Standard Deviation, Leeward line - LINE 7')
set(gca,'XTickLabel',{'FEM-WF','QS-WF','LF'});
ylabel('Tension [kN]');
axis([0 4 0 300]);
grid on

subplot(2,2,4);
bar(tz_line7, 0.4, 'b');
text(x,tz_line7',strcat(num2str(tz_line7')),...
     'horiz','center','vert','bottom')
title('MIMOSA Mean-up-crossing period, Leeward line - LINE 7')
set(gca,'XTickLabel',{'FEM-WF','QS-WF','LF'});
ylabel('Tz [s]');
axis([0 4 0 150]);
grid on
saveas(gcf,...
'C:\Users\Michael\Skole\Master-Var2013\MIMOSA-Var2013'...
'\ResultsMatlab\case4aa.1000.pdf')
%=====

scrsz = get(0,'ScreenSize');
figure('Position',[980 scrsz(4)/4 scrsz(3)/3 scrsz(4)/1.5])
x=1:3;

subplot(2,1,1);
bar(max_line1, 0.4, 'r');
text(x,max_line1',strcat(num2str(max_line1')),...
     'horiz','center','vert','bottom')
title('MIMOSA Max Tension, Windward line - LINE 1')
set(gca,'XTickLabel',{'FEM-WF','QS-WF','LF'});
ylabel('Tension [kN]');
axis([0 4 0 1000]);
grid on

subplot(2,1,2);
bar(max_line7, 0.4, 'b');
text(x,max_line7',strcat(num2str(max_line7')),...
     'horiz','center','vert','bottom')
title('MIMOSA Max Tension, Leeward line - LINE 7')
set(gca,'XTickLabel',{'FEM-WF','QS-WF','LF'});
ylabel('Tension [kN]');
axis([0 4 0 1000]);
grid on

```

# Appendix D

## Plots of Main Results

### Comparing SIMO and RIFLEX

Figure D.1 compares SIMO and RIFLEX simulations for WF and LF tension.

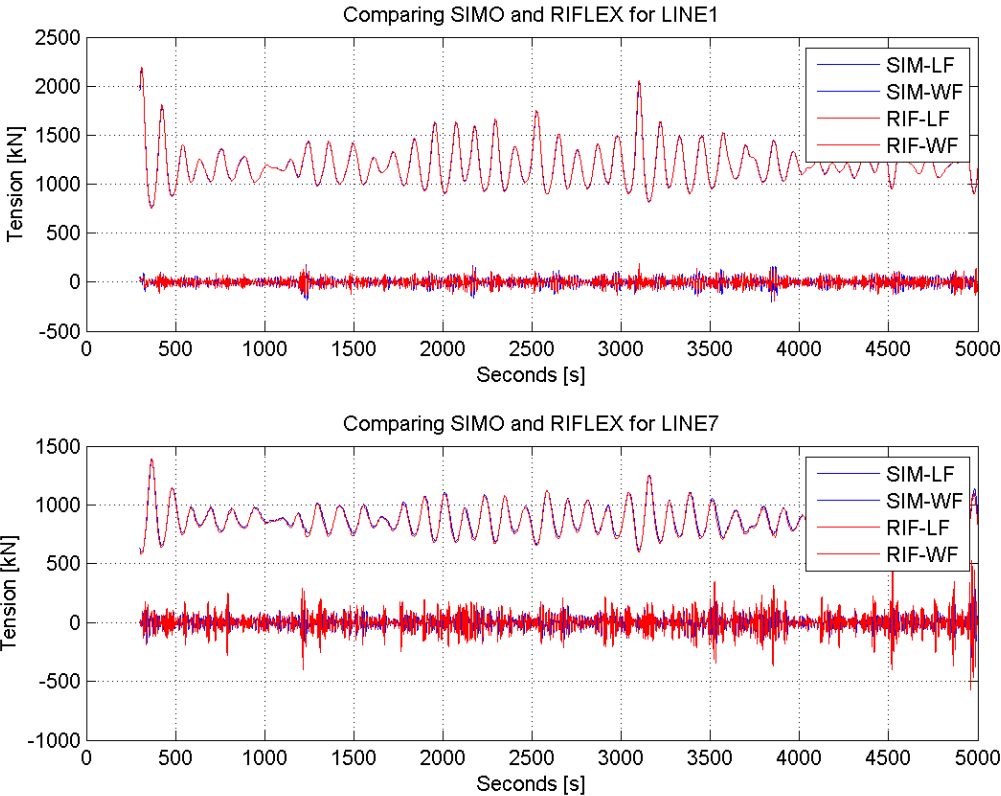


Figure D.1: Comparing WF and LF tension for RIFLEX and SIMO, 300 s - 5000 s. In both figures the upper graph compares LF tension, while the lower graph (around  $y = 0$ ) compares WF tension.

Figure D.2 and D.3 compares the LF tension for the whole 9 hour simulation.

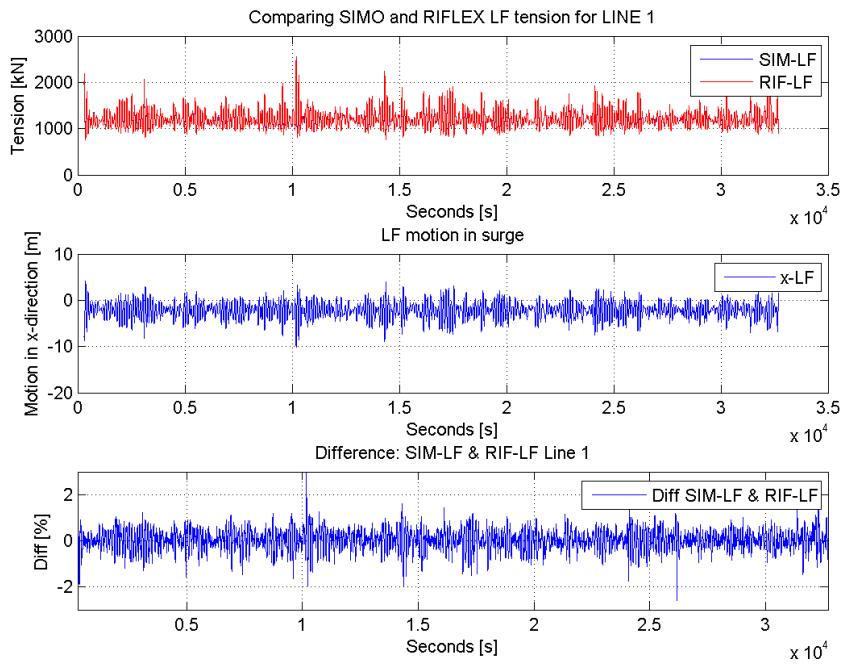


Figure D.2: Line 1: Compares LF tension for SIMO and RIFLEX, 9 hour simulation

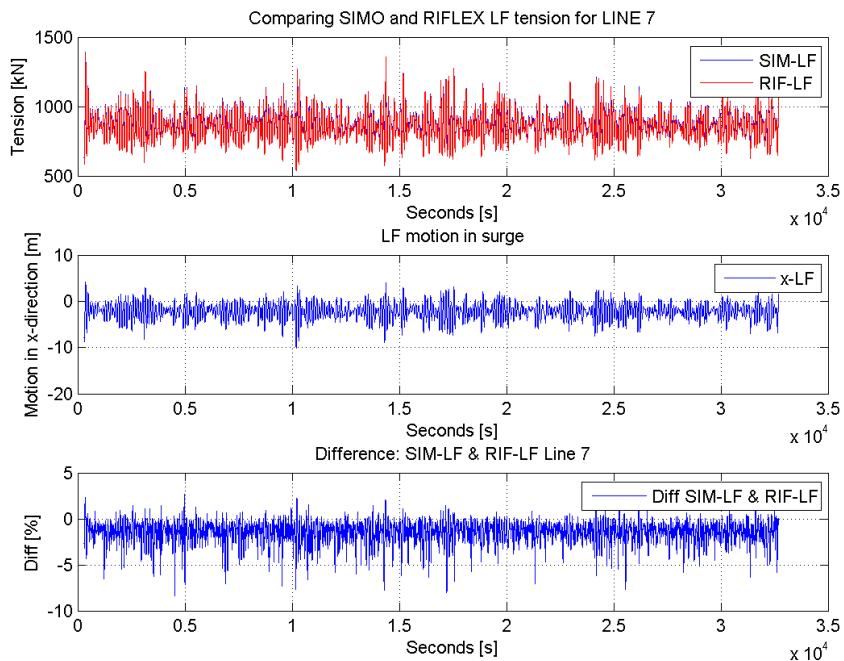


Figure D.3: Line 7: Compares LF tension for SIMO and RIFLEX, 9 hour simulation

## Appendix E

# Matlab Script for Post Processing

### Post\_processing.m

```
clc
clear all
close all
format short

%=====
%           Post processing script of the Results from
%           MIMOSA, SIMO, RIFLEX
%           by
%           Michael Chrolenko
%
%           Script: Post_processing.m
%           Functionality: Main matlab script for processing data
%=====

% Function that times the duration of the script,
% tic = start
% toc = end
tic

##### INPUT #####
turret_pos = 60;           % [m] Turret position (positive in x-direction)
% ----- FFT -----
fft_xs = 0.0;             % Fast Fourier Transform x start
fft_xe = 0.2;             % Fast Fourier Transform x end

% ----- SIMO -----
timestep_sim = 0.5;       % [s] timestep used in SIMO
red_SIMO = 600;           % Reduction of timeseries 1 = 0,5s, 600 = 300s
% Can chose the range of plot x-direction:
% Max: 64800 = 32400s (due to step in SIMO is 0,5) and removed 300s
% Min: 1 = 0,5s
x_start = 1 ;
x_end = 2000;
% X_start and X_end for comparing WF/LF for line1 and line7
x_s_comp = 1;
x_e_comp = 2000;         % Rule: (Seconds you what)*2 - 600
```

```

% ----- RIFLEX -----
timestep_rif = 0.1;      % [s] timestep used in RIFLEX
red_RIF = 3000;         % Reduction of timeseries 1 = 0,1s, 3000 = 300s
% Can chose the range of plot x-direction:
% Max: 324000 = 32400s (due to step in RIFLEX is 0,1) and removed 300s
% Min: 1 = 0,1s
XSR = 1;               % xsr - x Start Riflex
XER = 10000;           % xer - x End Riflex
% X_start and X_end for comparing WF/LF for line1 and line7
XSRC = 1;
XERC = 10000;          % Rule: (Seconds you what)*10 - 3000

% ----- Comparing/Diff -----
% Using SIMO timestep for comparing. So the rule above for SIMO is usable.
xscompdiff = 51700;
xecompdiff = 51800;    % Rule: (Seconds you what)*2 - 600
RIFxs = 258500;
RIFxe = 259000;        % Rule: (Seconds you what)*10 - 3000
#####

% Deleting previous saved files
% delete('Timeseries_simo_filter.png', 'RESULTS.txt');
% Creating a Result file which saves the results
fileID = fopen('RESULTS.txt','w');

% ----- read_dat.m -----
%=====
% Reads in tension forces from all the programs; MIM,SIM,RIF
% Line1 and 7 only, (windward and leewards line)
disp('... running read_dat.m')
[SIM1,SIM7,MSL1,MSL7,RIF,hs,tp,fem_wf_mim,LF_mim,TMOT] = read_data(...
    fileID,turret_pos);
%=====

% ----- filter_process.m -----
%=====
% Preforming and Tests the designed filter for
% SIM, RIF to check if it's good.
% For SIM and RIF one can insert how many seconds will be
% removed in the time series for statistical purposes.
disp('... running filter_process.m')
[RSIM1,RSIM7,RSHFL1,RSHFL7,RSLFL1,RSLFL7,RRIF,RRHFL1,...
    RRHFL7,RRLFL1,RRLFL7,RHFTMOT,RLFTMOT,RTMOT]=filter_process...
    (fileID,fft_xs,fft_xe,red_SIMO,red_RIF,SIM1,SIM7,RIF,TMOT);
%=====

% ----- plot_process.m -----
%=====

```



```

% Uses design filter to extract WF and LF tension forces from original
% WF&LF tension forces. This is only done for SIM and RIF because of
% the time series.
% Then the script plots WF&LF, WF, LF for comparison.

disp('... running plot_process.m')
plot_process(fileID,x_start,x_end,x_s_comp,x_e_comp,RSIM1,RSIM7,RSHFL1,...
    RSHFL7,RSLFL1,RSLFL7,RRIF,RRHFL1,RRHFL7,RRLFL1,RRLFL7,...
    XSR,XER,XSRC,XERC,RHFTMOT,RLFTMOT,RTMOT);
%=====

%----- comparison.m -----
%=====
% Compares results from MIM,SIM,RIF.
disp('... running comparison.m')
[RES,compLF_1]=comparison(fileID,RSHFL1,RSHFL7,RSLFL1,RSLFL7,MSL1,MSL7,...
    RRHFL1,RRHFL7,RRLFL1,RRLFL7,RSIM1,RSIM7,RRIF,hs,tp,xscompdiff,...
    xecompdiff,timestep_sim,timestep_rif,RHFTMOT,RLFTMOT,RTMOT,RIFxs,...
    RIFxe);
%=====

%----- fatigue_damage.m -----
%=====
% Preformes fatigue damage calculation using the Combined Spectrum (CS)
% approach, which is considered as an conservative approach.
disp('... running fatigue_damage.m')
fatigue_damage(fileID,fem_wf_mim,LF_mim);
%=====
fclose(fileID);
toc

```

## read\_data.m

```

function[SIM1,SIM7,MSL1,MSL7,RIF,hs,tp,fem_wf_mim,LF_mim,TMOT] = ...
    read_data(fileID,turret_pos)
%=====
%           Function: read_data.m
%           Functionality: Reads in tension forces from all the
%                           programs; MIM,SIM,RIF.
%                           Line1 and 7 only, (windward and leewards line)
%=====

fprintf(fileID,'\nINPUT FILES\n');
fprintf(fileID,'-----\n');
% ----- MIMOSA -----
%=====
fprintf(fileID,'MIMOSA:\n');
fprintf(fileID,'--> RES_FEM_WF.dat\n');
fprintf(fileID,'--> RES_QS_WF.dat\n');
fprintf(fileID,'--> RES_QS_LF.dat\n\n');
% Read Data

```

```

fem_wf_mim = (load('RES_FEM_WF.dat'))';
QS_wf_mim = (load('RES_QS_WF.dat'))';
LF_mim = (load('RES_QS_LF.dat'))';

% MSL - MIMOSA STD Line
% MTZL - MIMOSA tz Line
MSL1(1) = fem_wf_mim(6,1);
MSL1(2) = QS_wf_mim(6,1);
MSL1(3) = LF_mim(5,1);

MTZL1(1) = fem_wf_mim(9,1);
MTZL1(2) = QS_wf_mim(9,1);
MTZL1(3) = LF_mim(8,1);

MSL7(1) = fem_wf_mim(14,1);
MSL7(2) = QS_wf_mim(14,1);
MSL7(3) = LF_mim(12,1);

MTZL7(1) = fem_wf_mim(17,1);
MTZL7(2) = QS_wf_mim(17,1);
MTZL7(3) = LF_mim(15,1);

hs = fem_wf_mim(2,1);
tp = fem_wf_mim(3,1);

%=====

% ----- SIMO -----
%=====
fprintf(fileID, 'SIMO:\n');
fprintf(fileID, '--> B01r20c001\n');
fprintf(fileID, '--> B01r20c007\n\n');
fprintf(fileID, '--> B01r33c001\n\n');

% Channel name      : TotalforceElement1
tot1 = load('B01r20c001');
% Channel name      : TotalforceElement7
tot7 = load('B01r20c007');
% Channel name      : XGtranslationTotalmotion
tmot = load('B01r33c001');
% Because the time step is 0,5 in SIMO the matrix needs to be modified
for i = 1:length(tot1)
    SIM1(i,1) = tot1(i,1);
    SIM1(i,2) = i*0.5;
    SIM7(i,1) = tot7(i,1);
    SIM7(i,2) = i*0.5;
    TMOT(i,1) = turret_pos+tmot(i,1);
    TMOT(i,2) = i*0.5;
end
%=====

% ----- RIFLEX -----
%=====
fprintf(fileID, 'RIFLEX:\n');

```

```

fprintf(fileID, '--> moor_elmfor.asc\n\n');

RIF = load('moor_elmfor.asc');
=====

end

filter_process.m

function [RSIM1,RSIM7,RSHFL1,RSHFL7,RSLFL1,RSLFL7,RRIF,RRHFL1,...
        RRHFL7,RRLFL1,RRLFL7,RHFTMOT,RLFTMOT,RTMOT] = filter_process(fileID,...
        fft_xs,fft_xe,red_SIMO,red_RIF,SIM1,SIM7,RIF,TMOT)
=====
%
%           Function: filter_process.m
%   Functionality: Preforming and Tests the designed filter for
%                   SIM, RIF to check if it's good.
%                   For SIM and RIF one can insert how many
%                   seconds will be removed in the time series
%                   for statistical purposes.
=====

fprintf(fileID, '\nFILTER PROCESS\n');
fprintf(fileID, '-----\n');

%----- SIMO -----
%----- Highpass FILTER -----
% All frequency values are in Hz.
Fs = 2;      % Sampling Frequency
N = 4;      % Order
Fc = 0.03;  % Cutoff Frequency
% Construct an FDESIGN object and call its BUTTER method.
h = fdesign.highpass('N,F3dB', N, Fc, Fs);
Hd = design(h, 'butter');
% SHFL1 - Simo Highpass Filter Line1
SHFL1 = filter(Hd,SIM1(:,1));
% SHFL7 - Simo Highpass Filter Line7
SHFL7 = filter(Hd,SIM7(:,1));
% HFTMOT - Highpass Filtered Total Motion
HFTMOT = filter(Hd,TMOT(:,1));

%----- Lowpass FILTER -----
% Construct an FDESIGN object and call its BUTTER method.
h = fdesign.lowpass('N,F3dB', N, Fc, Fs);
Hd = design(h, 'butter');
% SLFL1 - Simo Lowpass Filter Line1
SLFL1 = filter(Hd,SIM1(:,1));
% SLFL7 - Simo Lowpass Filter Line7
SLFL7 = filter(Hd,SIM7(:,1));
% LFTMOT - Lowpass Filtered Total Motion
LFTMOT = filter(Hd,TMOT(:,1));
%-----

%----- RIFLEX -----
%----- Highpass FILTER -----

```

```

% All frequency values are in Hz.
Fs = 10;      % Sampling Frequency
N = 4;       % Order
Fc = 0.03;   % Cutoff Frequency
% Construct an FDESIGN object and call its BUTTER method.
h = fdesign.highpass('N,F3dB', N, Fc, Fs);
Hd = design(h, 'butter');
% RHFL1 - Riflex HIGHpass Filter Line 1
RHFL1 = filter(Hd,RIF(:,2));
% RHFL1 - Riflex HIGHpass Filter Line 7
RHFL7 = filter(Hd,RIF(:,3));

% ----- Lowpass FILTER -----
% Construct an FDESIGN object and call its BUTTER method.
h = fdesign.lowpass('N,F3dB', N, Fc, Fs);
Hd = design(h, 'butter');
% RLFL1 - Riflex LOWpass Filter Line 1
RLFL1 = filter(Hd,RIF(:,2));
% RLFL1 - Riflex LOWpass Filter Line 7
RLFL7 = filter(Hd,RIF(:,3));
%

% ----- Fast Fourier Transform -----
% ----- SIMO -----
% Sampling period
dtS1 = 1/2;
dtS7 = 1/2;
% Sampling Frequency
Fs = 10;
% Largest possible registred frequency
nyquist = 1/2;
% Fast Fourier Transform FFT
fft_SIM1=fft(SIM1(:,1));
amp_spec_SIM1=abs(fft_SIM1(1:floor(length(fft_SIM1)/2)));
freqS1 = (0:length(fft_SIM1)/2-1)/(length(fft_SIM1)/2*dtS1)*nyquist;

fft_SIM7=fft(SIM7(:,1));
amp_spec_SIM7=abs(fft_SIM7(1:floor(length(fft_SIM7)/2)));
freqS7 = (0:length(fft_SIM7)/2-1)/(length(fft_SIM7)/2*dtS7)*nyquist;

scrsz = get(0,'ScreenSize');
figure('Name','Fast Fourier Transform for SIMO, RIFLEX - Line1 and Line7',...
    'NumberTitle','off','Position',[100 scrsz(4)/12 scrsz(3)/2 scrsz(4)/1.2])

% Plotting Line1
subplot(2,2,1)
plot(freqS1(2:end),amp_spec_SIM1(2:end),'b')
title('FFT for LINE1 - SIMO')
%hleg1 = legend('WF-line1','WF-line7');
%set(hleg1,'Location','NorthEast')
ylabel('');
xlabel('Frequency [hz]');
axis([fft_xs fft_xe 0 max(amp_spec_SIM1(2:end))]);
grid on

% Plotting Line7

```

```

subplot(2,2,2)
plot(freqS7(2:end),amp_spec_SIM7(2:end),'b')
title('FFT for LINE7 - SIMO')
%hleg1 = legend('WF-line1','WF-line7');
%set(hleg1,'Location','NorthEast')
ylabel('');
xlabel('Frequency [hz]');
axis([fft_xs fft_xe 0 max(amp_spec_SIM7(2:end))]);
grid on

%----- RIFLEX -----
% Sampling period
dtR1 = 1/10;
dtR7 = 1/10;
% Sampling Frequency
Fs = 10;
% Largest possible registred frequency
nyquist = 1/2;
% Fast Fourier Transform FFT
fft_RIF1=fft(RIF(:,2));
amp_spec_RIF1=abs(fft_RIF1(1:floor(length(fft_RIF1)/2)));
freqR1 = (0:length(fft_RIF1)/2-1)/(length(fft_RIF1)/2*dtR1)*nyquist;

fft_RIF7=fft(RIF(:,3));
amp_spec_RIF7=abs(fft_RIF7(1:floor(length(fft_RIF7)/2)));
freqR7 = (0:length(fft_RIF7)/2-1)/(length(fft_RIF7)/2*dtR7)*nyquist;

% Plotting Line1
subplot(2,2,3)
plot(freqR1(2:end),amp_spec_RIF1(2:end),'b')
title('FFT for LINE1 - RIFLEX')
%hleg1 = legend('WF-line1','WF-line7');
%set(hleg1,'Location','NorthEast')
ylabel('');
xlabel('Frequency [hz]');
axis([fft_xs fft_xe 0 max(amp_spec_RIF1(2:end))]);
grid on

% Plotting Line7
subplot(2,2,4)
plot(freqR7(2:end),amp_spec_RIF7(2:end),'b')
title('FFT for LINE7 - RIFLEX')
%hleg1 = legend('WF-line1','WF-line7');
%set(hleg1,'Location','NorthEast')
ylabel('');
xlabel('Frequency [hz]');
axis([fft_xs fft_xe 0 max(amp_spec_RIF7(2:end))]);
grid on

saveas(gcf,'FFT_SR_LINE17.png')
saveas(gcf,...
'C:\Users\Michael\Skole\Master-Var2013\LaTeX-Master\Figures\FFT_SR_LINE17.png')
fprintf(fileID,'PLOT: --> FFT_SR_LINE17.png\n');
%-----

```

```

% ----- SIMO -----
fprintf(fileID, '===== SIMO =====\n');
%=====

% ----- Reducing DATA -----
% Original line1          % Original line7
SIM1(1:red_SIMO,:) = [] ; SIM7(1:red_SIMO,:) = [];
RSIM1 = SIM1           ; RSIM7 = SIM7;

% Filter line1          % Filter line7
SHFL1(1:red_SIMO,:) = [] ; SHFL7(1:red_SIMO,:) = [];
RSHFL1 = SHFL1        ; RSHFL7 = SHFL7;

SLFL1(1:red_SIMO,:) = [] ; SLFL7(1:red_SIMO,:) = [];
RSLFL1 = SLFL1        ; RSLFL7 = SLFL7;

% Original Motion
TMOT(1:red_SIMO,:) = [];
RTMOT = TMOT;

% Filtered Motion
HFTMOT(1:red_SIMO,:) = [];
RHFTMOT = HFTMOT;

LFTMOT(1:red_SIMO,:) = [];
RLFTMOT = LFTMOT;
%-----

% ----- CHECKING FILTER -----
fprintf(fileID, 'CHECKING FILTER \n\n');
% Line 1 - Windwards line

% SIMO STD Original Line1 (SSTD0) (WF&LF)
SSTD01 = std(RSIM1(:,1));
% SIMO STD WF (SSTDWF) from filter
SSTDWF1 = std(RSHFL1);
% SIMO STD LF (SSTDLF) from filter
SSTDLF1 = std(RSLFL1);
% Calculated TOTAL STD from WF and LF, used for comparing with SSTD0
SSTD_comp1 = sqrt(SSTDWF1^2 + SSTDLF1^2);
% Calculates the difference for SSTD_comp and SSTD0
S_diff1 = abs(100-((SSTD01/SSTD_comp1)*100));

fprintf(fileID, 'Testing Designed Filter for LINE 1 (windward line):\n');
fprintf(fileID, '-----\n');
fprintf(fileID, ['SIMO STD for WF&LF:          ' num2str(SSTD01) ' [kN]\n']);
fprintf(fileID, ['SIMO STD for sqrt(WF^2+LF^2): ' num2str(SSTD_comp1) ' [kN]\n']);
fprintf(fileID, ['Difference:                ' num2str(S_diff1) ' [percent]\n\n']);
fprintf(fileID, ['SIMO STD WF (filtered):          ' num2str(SSTDWF1) ' [kN]\n']);
fprintf(fileID, ['SIMO STD LF (filtered):          ' num2str(SSTDLF1) ' [kN]\n']);
fprintf(fileID, '-----\n\n');

% Line 7 - Leewards line

% SIMO STD Original Line7 (SSTD07) (WF&LF)
SSTD07 = std(RSIM7(:,1));
% SIMO STD WF Line7 (SSTDWF7) from filter

```

```

SSTDWF7 = std(RSHFL7);
% SIMO STD LF Line7 (SSTDLF7) from filter
SSTDLF7 = std(RSLFL7);
% Calculated TOTAL STD from WF and LF, used for comparing with SSTDO
SSTD_comp7 = sqrt(SSTDWF7^2 + SSTDLF7^2);
% Calculates the difference for SSTD_comp and SSTDO
S_diff7 = abs(100-((SSTD07/SSTD_comp7)*100));

fprintf(fileID, 'Testing Designed Filter for LINE 7 (leeward line):\n');
fprintf(fileID, '-----\n');
fprintf(fileID, ['SIMO STD for WF&LF:          ' num2str(SSTD07) ' [kN]\n']);
fprintf(fileID, ['SIMO STD for sqrt(WF^2+LF^2):      ' num2str(SSTD_comp7) ' [kN]\n']);
fprintf(fileID, ['Difference:                               ' num2str(S_diff7) ' [percent]\n\n']);
fprintf(fileID, ['SIMO STD WF (filtered):                   ' num2str(SSTDWF7) ' [kN]\n']);
fprintf(fileID, ['SIMO STD LF (filtered):                     ' num2str(SSTDLF7) ' [kN]\n']);
fprintf(fileID, '-----\n');

% Finding the Ratio between STD-WF-Line1 and -7, STD-LF-Line1 and -7
fprintf(fileID, '\nRatio between:\n');
STD_WF_RATIO_SIM = SSTDWF7/SSTDWF1;
STD_LF_RATIO_SIM = SSTDLF7/SSTDLF1;
fprintf(fileID, ['STD-WF-Line1 and -7:                   ' num2str(STD_WF_RATIO_SIM) ' [-]\n']);
fprintf(fileID, ['STD-LF-Line1 and -7:                   ' num2str(STD_LF_RATIO_SIM) ' [-]\n']);
%-----

% ----- RIFLEX -----
fprintf(fileID, '\n\n===== RIFLEX =====\n');
%-----

%----- Reducing DATA -----
% Original
RIF(1:red_RIF,:) = [];
RRIF = RIF;

% Filter Line1          % Filter Line7
RHFL1(1:red_RIF,:) = [] ; RHFL7(1:red_RIF,:) = [];
RRHFL1 = RHFL1        ; RRHFL7 = RHFL7;

RLFL1(1:red_RIF,:) = [] ; RLFL7(1:red_RIF,:) = [];
RRLFL1 = RLFL1        ; RRLFL7 = RLFL7;
%-----

%----- CHECKING FILTER -----
fprintf(fileID, 'CHECKING FILTER \n\n');
% Line 1 - Windwards line

% RIFLEX STD Original Line1 (RSTDO) (WF&LF)
RSTD01 = std(RRIF(:,2));
% RIFLEX STD WF (RSTDWF) from filter

```

```

RSTDWF1 = std(RRHFL1);
% RIFLEX STD LF (RSTDLF) from filter
RSTDLF1 = std(RRLFL1);
% Calculated TOTAL STD from WF and LF, used for comparing with RSTDO
RSTD_comp1 = sqrt(RSTDWF1^2 + RSTDLF1^2);
% Calculates the difference for RSTD_comp and RSTDO
R_diff1 = abs(100-((RSTDO1/RSTD_comp1)*100));

fprintf(fileID,'Testing Designed Filter for LINE 1 (windward line):\n');
fprintf(fileID,'-----\n');
fprintf(fileID,['RIFLEX STD for WF&LF:           ' num2str(RSTDO1) ' [kN]\n']);
fprintf(fileID,['RIFLEX STD for sqrt(WF^2+LF^2):   ' num2str(RSTD_comp1) ' [kN]\n']);
fprintf(fileID,['Difference:                           ' num2str(R_diff1) ' [percent]\n\n']);
fprintf(fileID,['RIFLEX STD WF (filtered):           ' num2str(RSTDWF1) ' [kN]\n']);
fprintf(fileID,['RIFLEX STD LF (filtered):           ' num2str(RSTDLF1) ' [kN]\n']);
fprintf(fileID,'-----\n\n');

% Line 7 - Leewards line

% RIFLEX STD Original Line7 (RSTDO7) (WF&LF)
RSTDO7 = std(RRIF(:,3));
% RIFLEX STD WF Line7 (RSTDWF7) from filter
RSTDWF7 = std(RRHFL7);
% RIFLEX STD LF Line7 (RSTDLF7) from filter
RSTDLF7 = std(RRLFL7);
% Calculated TOTAL STD from WF and LF, used for comparing with RSTDO
RSTD_comp7 = sqrt(RSTDWF7^2 + RSTDLF7^2);
% Calculates the difference for RSTD_comp and RSTDO
R_diff7 = abs(100-((RSTDO7/RSTD_comp7)*100));

fprintf(fileID,'Testing Designed Filter for LINE 7 (leeward line):\n');
fprintf(fileID,'-----\n');
fprintf(fileID,['RIFLEX STD for WF&LF:           ' num2str(RSTDO7) ' [kN]\n']);
fprintf(fileID,['RIFLEX STD for sqrt(WF^2+LF^2):   ' num2str(RSTD_comp7) ' [kN]\n']);
fprintf(fileID,['Difference:                           ' num2str(R_diff7) ' [percent]\n\n']);
fprintf(fileID,['RIFLEX STD WF (filtered):           ' num2str(RSTDWF7) ' [kN]\n']);
fprintf(fileID,['RIFLEX STD LF (filtered):           ' num2str(RSTDLF7) ' [kN]\n']);
fprintf(fileID,'-----\n\n');

% Finding the Ratio between STD-WF-Line1 and -7, STD-LF-Line1 and -7
fprintf(fileID,'\nRatio between:\n');
STD_WF_RATIO_RIF = RSTDWF7/RSTDWF1;
STD_LF_RATIO_RIF = RSTDLF1/RSTDLF7;
fprintf(fileID,['STD-WF-Line1 and -7:           ' num2str(STD_WF_RATIO_RIF) ' [-]\n']);
fprintf(fileID,['STD-LF-Line1 and -7:           ' num2str(STD_LF_RATIO_RIF) ' [-]\n']);
%
fprintf(fileID,'\n===== \n\n');
%=====

end

```

## plot\_process.m

```

function[] = plot_process(fileID,x_start,x_end,x_s_comp,x_e_comp,RSIM1,RSIM7,...
    RSHFL1,RSHFL7,RSLFL1,RSLFL7,RRIF,RRHFL1,RRHFL7,RRLFL1,RRLFL7,...
    XSR,XER,XSRC,XERC,RHFTMOT,RLFTMOT,RTMOT)
%=====

```



```

%           Function: plot_process.m
%           Functionality: Uses design filter to extract WF and LF tension
%                           forces from original WF&LF tension forces.
%                           This is only done for SIM and RIF because of
%                           the time series. Then the script plots WF&LF,
%                           WF, LF for comparison.
%=====

% ----- SIMO -----
%=====
% ----- Plotting Line 1 -----
mean1 = mean(RSIM1(:,1));
RSHFML1 = RSHFL1 + mean1;
pos1 = 900;

scrsz = get(0,'ScreenSize');
figure('Name','Plotting time series for SIMO, tension forces',...
       'NumberTitle','off','Position',[100 scrsz(4)/12 scrsz(3)/2 scrsz(4)/1.2])

% Plotting WF&LF, WF and LF
subplot(2,1,1)
plot(RSIM1(x_start:x_end,2),RSIM1(x_start:x_end,1),'g',...
     RSIM1(x_start:x_end,2),RSLFL1(x_start:x_end,1),'b',...
     RSIM1(x_start:x_end,2),RSHFL1(x_start:x_end),'r');
title('SIMO time series WF&LF, WF, LF - LINE1 (windward)')
hleg1 = legend('SIM-WF&LF','SIM-LF','SIM-WF');
set(hleg1,'Location','NorthEast')
ylabel('Tension [kN]');
xlabel('Seconds [s]');
grid on

% ----- Plotting Line 7 -----
% Plotting WF&LF, WF and LF
subplot(2,1,2)
plot(RSIM7(x_start:x_end,2),RSIM7(x_start:x_end,1),'g',...
     RSIM7(x_start:x_end,2),RSLFL7(x_start:x_end,1),'b',...
     RSIM7(x_start:x_end,2),RSHFL7(x_start:x_end),'r');
title('SIMO time series WF&LF, WF, LF - LINE7 (leeward)')
hleg1 = legend('SIM-WF&LF','SIM-LF','SIM-WF');
set(hleg1,'Location','NorthEast')
ylabel('Tension [kN]');
xlabel('Seconds [s]');
grid on

saveas(gcf,'Timeseries_SIMO_filter.png')
saveas(gcf,...
       'C:\Users\Michael\Skole\Master-Var2013\LaTeX-Master\Figures\Timeseries_SIMO_filter.png')
fprintf(fileID,'PLOT: --> Timeseries_SIMO_filter.png\n');

% ----- Comparing line 1 and line7 -----
% Comparing WF line 1 and line 7

scrsz = get(0,'ScreenSize');
figure('Name','Plotting time series for SIMO, WF-line1 vs. WF-line7',...
       'NumberTitle','off','Position',[100 scrsz(4)/12 scrsz(3)/2 scrsz(4)/1.2])

```

```

% Plotting WF-line1 vs WF-line7
subplot(2,1,1)
plot(RSIM1(x_s_comp:x_e_comp,2),RSHFL1(x_s_comp:x_e_comp),'b',...
      RSIM7(x_s_comp:x_e_comp,2),RSHFL7(x_s_comp:x_e_comp),'r');
title('SIMO time series: WF-line1 vs. WF-line7')
hleg1 = legend('WF-line1','WF-line7');
set(hleg1,'Location','NorthEast')
ylabel('Tension [kN]');
xlabel('Seconds [s]');
grid on

% Plotting LF-line1 vs. LF-line7
subplot(2,1,2)
plot(RSIM1(x_s_comp:x_e_comp,2),RSLFL1(x_s_comp:x_e_comp,1),'b',...
      RSIM7(x_s_comp:x_e_comp,2),RSLFL7(x_s_comp:x_e_comp,1),'r');
title('SIMO time series: LF-line1 vs. LF-line7')
hleg1 = legend('LF-line1','LF-line7');
set(hleg1,'Location','NorthEast')
ylabel('Tension [kN]');
xlabel('Seconds [s]');
grid on

saveas(gcf,'Comparing_WF_LF_line1_7_SIMO.png')
saveas(gcf,...
'C:\Users\Michael\Skole\Master-Var2013\LaTeX-Master\Figures\Comparing_WF_LF_line1_7_SIMO.png')
fprintf(fileID,'PLOT: --> Comparing_WF_LF_line1_7_SIMO.png\n');
%
%=====

% ----- RIFLEX -----
%=====
% ----- Plotting Line 1 -----
mean1 = mean(RSIM1(:,1));
RSHFML1 = RSHFL1 + mean1;
pos1 = 900;

scrsz = get(0,'ScreenSize');
figure('Name','Plotting time series for RIFLEX, tension forces',...
      'NumberTitle','off','Position',[100 scrsz(4)/12 scrsz(3)/2 scrsz(4)/1.2])

% Plotting WF&LF, WF and LF
subplot(2,1,1)
plot(RRIF(XSR:XER,1),RRIF(XSR:XER,2),'g',...
      RRIF(XSR:XER,1),RRLFL1(XSR:XER,1),'b',...
      RRIF(XSR:XER,1),RRHFL1(XSR:XER,1),'r');
title('RIFLEX time series WF&LF, WF, LF - LINE1 (windward)')
hleg1 = legend('RIF-WF&LF','RIF-LF','RIF-WF');
set(hleg1,'Location','NorthEast')
ylabel('Tension [kN]');
xlabel('Seconds [s]');
grid on

mean7 = mean(RSIM7(:,1));
RSHFML7 = RSHFL7 + mean7;
pos7 = 900;

```

```

% ----- Plotting Line 7 -----
% Plotting WF&LF, WF and LF
subplot(2,1,2)
plot(RRIF(XSR:XER,1),RRIF(XSR:XER,3),'g',...
      RRIF(XSR:XER,1),RRLFL7(XSR:XER,1),'b',...
      RRIF(XSR:XER,1),RRHFL7(XSR:XER,1),'r');
title('RIFLEX time series WF&LF, WF, LF - LINE7 (leeward)')
hleg1 = legend('RIF-WF&LF','RIF-LF','RIF-WF');
set(hleg1,'Location','NorthEast')
ylabel('Tension [kN]');
xlabel('Seconds [s]');
grid on

saveas(gcf,'Timeseries_RIFLEX_filter.png')
saveas(gcf,...
'C:\Users\Michael\Skole\Master-Var2013\LaTeX-Master\Figures\Timeseries_RIFLEX_filter.png')
fprintf(fileID,'PLOT: --> Timeseries_RIFLEX_filter.png\n');

% ----- Comparing line 1 and line7 -----
% Comparing WF line 1 and line 7

scrsz = get(0,'ScreenSize');
figure('Name','Plotting time series for RIFLEX, WF-line1 vs. WF-line7',...
      'NumberTitle','off','Position',[100 scrsz(4)/12 scrsz(3)/2 scrsz(4)/1.2])

% Plotting WF-line1 vs WF-line7
subplot(2,1,1)
plot(RRIF(XSRC:XERC,1),RRHFL1(XSRC:XERC,1),'b',...
      RRIF(XSRC:XERC,1),RRHFL7(XSRC:XERC,1),'r');
title('RIFLEX time series: WF-line1 vs. WF-line7')
hleg1 = legend('WF-line1','WF-line7');
set(hleg1,'Location','NorthEast')
ylabel('Tension [kN]');
xlabel('Seconds [s]');
grid on

% Plotting LF-line1 vs. LF-line7
subplot(2,1,2)
plot(RRIF(XSRC:XERC,1),RRLFL1(XSRC:XERC,1),'b',...
      RRIF(XSRC:XERC,1),RRLFL7(XSRC:XERC,1),'r');
title('RIFLEX time series: LF-line1 vs. LF-line7')
hleg1 = legend('LF-line1','LF-line7');
set(hleg1,'Location','NorthEast')
ylabel('Tension [kN]');
xlabel('Seconds [s]');
grid on

saveas(gcf,'Comparing_WF_LF_line1_7_RIFLEX.png')
saveas(gcf,...
'C:\Users\Michael\Skole\Master-Var2013\LaTeX-Master\Figures\Comparing_WF_LF_line1_7_RIFLEX.png')
fprintf(fileID,'PLOT: --> Comparing_WF_LF_line1_7_RIFLEX.png\n');
%
%=====

% ----- COMPARING SIMO & RIFLEX -----

```

```

=====
scrsz = get(0, 'ScreenSize');
figure('Name', 'Comparing SIMO and RIFLEX - WF, LF', ...
    'NumberTitle', 'off', 'Position', [100 scrsz(4)/12 scrsz(3)/2 scrsz(4)/1.2])

% Plotting SIMO/RIFLEX WF AND LF - LINE1
subplot(2,1,1)
plot(RSIM1(x_start:x_end,2),RSLFL1(x_start:x_end,1),'b',...
    RSIM1(x_start:x_end,2),RSHFL1(x_start:x_end),'b',...
    RRIF(XSR:XER,1),RRLFL1(XSR:XER,1),'r',...
    RRIF(XSR:XER,1),RRHFL1(XSR:XER,1),'r');
title('Comparing SIMO and RIFLEX for windward line (line 1)')
hleg1 = legend('SIM-LF', 'SIM-WF', 'RIF-LF', 'RIF-WF');
set(hleg1, 'Location', 'NorthEast')
ylabel('Tension [kN]');
xlabel('Seconds [s]');
grid on

% Plotting SIMO/RIFLEX WF AND LF - LINE7
subplot(2,1,2)
plot(RSIM7(x_start:x_end,2),RSLFL7(x_start:x_end,1),'b',...
    RSIM7(x_start:x_end,2),RSHFL7(x_start:x_end),'b',...
    RRIF(XSR:XER,1),RRLFL7(XSR:XER,1),'r',...
    RRIF(XSR:XER,1),RRHFL7(XSR:XER,1),'r');
title('Comparing SIMO and RIFLEX for Leeward line (line 7)')
hleg1 = legend('SIM-LF', 'SIM-WF', 'RIF-LF', 'RIF-WF');
set(hleg1, 'Location', 'NorthEast')
ylabel('Tension [kN]');
xlabel('Seconds [s]');
grid on

saveas(gcf, 'Comparing_SIMO_RIFLEX.png')
saveas(gcf, ...
    'C:\Users\Michael\Skole\Master-Var2013\LaTeX-Master\Figures\Comparing_SIMO_RIFLEX.png')
fprintf(fileID, 'PLOT: --> Comparing_SIMO_RIFLEX.png\n');
%
=====

% LINE 1: Plotting SIM-LF, RIF-LF and x-LF, x-tot
%
figure('Name', 'Comparing SIMO and RIFLEX - LINE 1 - LF', ...
    'NumberTitle', 'off', 'Position', [100 scrsz(4)/12 scrsz(3)/2 scrsz(4)/1.2])

% Comparing SIMO and RIFLEX LF tension for LINE1
subplot(2,1,1)
plot(RSIM1(x_s_comp:x_e_comp,2),RSLFL1(x_s_comp:x_e_comp,1),'b',...
    RRIF(XSRC:XERC,1),RRLFL1(XSRC:XERC,1),'r')
title('Comparing SIMO and RIFLEX LF tension for LINE 1')
hleg1 = legend('SIM-LF', 'RIF-LF');
set(hleg1, 'Location', 'NorthEast')
ylabel('Tension [kN]');
xlabel('Seconds [s]');
grid on

% Comparing x-LF and x-TOT (from SIMO)
subplot(2,1,2)
plot(RTMOT(x_s_comp:x_e_comp,2),RLFTMOT(x_s_comp:x_e_comp,1),'b',...

```

```

        RTMOT(x_s_comp:x_e_comp,2),RTMOT(x_s_comp:x_e_comp,1),'r')
title('Comparing x-LF and x-TOT (from SIMO)')
hleg1 = legend('x-LF','x-TOT');
set(hleg1,'Location','NorthEast')
ylabel('Motion in x-direction [m]');
xlabel('Seconds [s]');
grid on

saveas(gcf,'Comparing_LF_LINE1_SIMO_RIFLEX.png')
saveas(gcf,...
'C:\Users\Michael\Skole\Master-Var2013\LaTeX-Master\Figures\Comparing_LF_LINE1_SIMO_RIFLEX.png')
fprintf(fileID,'PLOT: --> Comparing_LF_LINE1_SIMO_RIFLEX.png\n');
%-----

% LINE 7: Plotting SIM-LF, RIF-LF and x-LF, x-tot
%-----
figure('Name','Comparing SIMO and RIFLEX - LINE 7 - LF',...
'NumberTitle','off','Position',[100 scrsz(4)/12 scrsz(3)/2 scrsz(4)/1.2])

% Comparing SIMO and RIFLEX LF tension for LINE 7
subplot(2,1,1)
plot(RSIM7(x_s_comp:x_e_comp,2),RSLFL7(x_s_comp:x_e_comp,1),'b',...
RRIF(XSRC:XERC,1),RRLFL7(XSRC:XERC,1),'r')
title('Comparing SIMO and RIFLEX LF tension for LINE 7')
hleg1 = legend('SIM-LF','RIF-LF');
set(hleg1,'Location','NorthEast')
ylabel('Tension [kN]');
xlabel('Seconds [s]');
grid on

% Comparing x-LF and x-TOT (from SIMO)
subplot(2,1,2)
plot(RTMOT(x_s_comp:x_e_comp,2),RLFTMOT(x_s_comp:x_e_comp,1),'b',...
RTMOT(x_s_comp:x_e_comp,2),RTMOT(x_s_comp:x_e_comp,1),'r')
title('Comparing x-LF and x-TOT (from SIMO)')
hleg1 = legend('x-LF','x-TOT');
set(hleg1,'Location','NorthEast')
ylabel('Motion in x-direction [m]');
xlabel('Seconds [s]');
grid on

saveas(gcf,'Comparing_LF_LINE7_SIMO_RIFLEX.png')
saveas(gcf,...
'C:\Users\Michael\Skole\Master-Var2013\LaTeX-Master\Figures\Comparing_LF_LINE7_SIMO_RIFLEX.png')
fprintf(fileID,'PLOT: --> Comparing_LF_LINE7_SIMO_RIFLEX.png\n');
%-----

% LINE 1: Plotting SIM-WF, RIF-WF and x-WF, x-tot
%-----
figure('Name','Comparing SIMO and RIFLEX - LINE 1 - WF',...
'NumberTitle','off','Position',[100 scrsz(4)/12 scrsz(3)/2 scrsz(4)/1.2])

% Comparing SIMO and RIFLEX WF tension for LINE 1
subplot(2,1,1)
plot(RSIM1(x_s_comp:x_e_comp,2),RSHFL1(x_s_comp:x_e_comp,1),'b',...

```

```

        RRIF(XSRC:XERC,1),RRHFL1(XSRC:XERC,1),'r')
title('Comparing SIMO and RIFLEX WF tension for LINE 1')
hleg1 = legend('SIM-WF','RIF-WF');
set(hleg1,'Location','NorthEast')
ylabel('Tension [kN]');
xlabel('Seconds [s]');
grid on

% Comparing x-WF and x-TOT (from SIMO)
subplot(2,1,2)
plot(RTMOT(x_s_comp:x_e_comp,2),RHFTMOT(x_s_comp:x_e_comp,1),'b',...
      RTMOT(x_s_comp:x_e_comp,2),RTMOT(x_s_comp:x_e_comp,1),'r')
title('Comparing x-LF and x-TOT (from SIMO)')
hleg1 = legend('x-WF','x-TOT');
set(hleg1,'Location','NorthEast')
ylabel('Motion in x-direction [m]');
xlabel('Seconds [s]');
grid on

saveas(gcf,'Comparing_WF_LINE1_SIMO_RIFLEX.png')
saveas(gcf,...
'C:\Users\Michael\Skole\Master-Var2013\LaTeX-Master\Figures\Comparing_WF_LINE1_SIMO_RIFLEX.png')
fprintf(fileID,'PLOT: --> Comparing_WF_LINE1_SIMO_RIFLEX.png\n');
%-----

% LINE 7: Plotting SIM-WF, RIF-WF and x-WF, x-tot
%-----
figure('Name','Comparing SIMO and RIFLEX - LINE 7 - WF',...
      'NumberTitle','off','Position',[100 scrsz(4)/12 scrsz(3)/2 scrsz(4)/1.2])

% Comparing SIMO and RIFLEX WF tension for LINE 7
subplot(2,1,1)
plot(RSIM7(x_s_comp:x_e_comp,2),RSHFL7(x_s_comp:x_e_comp,1),'b',...
      RRIF(XSRC:XERC,1),RRHFL7(XSRC:XERC,1),'r')
title('Comparing SIMO and RIFLEX WF tension for LINE 7')
hleg1 = legend('SIM-WF','RIF-WF');
set(hleg1,'Location','NorthEast')
ylabel('Tension [kN]');
xlabel('Seconds [s]');
grid on

% Comparing x-WF and x-TOT (from SIMO)
subplot(2,1,2)
plot(RTMOT(x_s_comp:x_e_comp,2),RHFTMOT(x_s_comp:x_e_comp,1),'b',...
      RTMOT(x_s_comp:x_e_comp,2),RTMOT(x_s_comp:x_e_comp,1),'r')
title('Comparing x-LF and x-TOT (from SIMO)')
hleg1 = legend('x-WF','x-TOT');
set(hleg1,'Location','NorthEast')
ylabel('Motion in x-direction [m]');
xlabel('Seconds [s]');
grid on

saveas(gcf,'Comparing_WF_LINE7_SIMO_RIFLEX.png')
saveas(gcf,...
'C:\Users\Michael\Skole\Master-Var2013\LaTeX-Master\Figures\Comparing_WF_LINE7_SIMO_RIFLEX.png')
fprintf(fileID,'PLOT: --> Comparing_WF_LINE7_SIMO_RIFLEX.png\n');
%-----
%=====

```

```
end
```

## comparison.m

```
function [RES, compLF_1] = comparison(fileID, RSHFL1, RSHFL7, RSLFL1, RSLFL7, MSL1, MSL7, ...
    RRHFL1, RRHFL7, RRLFL1, RRLFL7, RSIM1, RSIM7, RRIF, hs, tp, xscompdiff, ...
    xecompdiff, timestep_sim, timestep_rif, RHFTMOT, RLFTMOT, RTMOT, RIFxs, ...
    RIFxe)
%=====
%           Function: comparison.m
%           Functionality: Compares different values for MIM, SIM, RIF
%=====

fprintf(fileID, '\nCOMPARING\n');
fprintf(fileID, '-----\n');
% Comparing Tension STD for line 7; MIM, SIM, RIF
%----- MIMOSA -----
MIM_FEM_WF_STD_1 = MSL1(1);
MIM_FEM_WF_STD_7 = MSL7(1);

MIM_QS_WF_STD_1 = MSL1(2);
MIM_QS_WF_STD_7 = MSL7(2);

MIM_LF_STD_1 = MSL1(3);
MIM_LF_STD_7 = MSL7(3);

MIM_TOT_FEM_1 = sqrt((MIM_FEM_WF_STD_1)^2+(MIM_LF_STD_1)^2);
MIM_TOT_FEM_7 = sqrt((MIM_FEM_WF_STD_7)^2+(MIM_LF_STD_7)^2);

MIM_TOT_QS_1 = sqrt((MIM_QS_WF_STD_1)^2+(MIM_LF_STD_1)^2);
MIM_TOT_QS_7 = sqrt((MIM_QS_WF_STD_7)^2+(MIM_LF_STD_7)^2);

%----- SIMO -----
SIM_WF_STD_1 = std(RSHFL1(:,1));
SIM_WF_STD_7 = std(RSHFL7(:,1));

SIM_LF_STD_1 = std(RSLFL1(:,1));
SIM_LF_STD_7 = std(RSLFL7(:,1));

SIM_TOT_STD_1 = std(RSIM1(:,1));
SIM_TOT_STD_7 = std(RSIM7(:,1));

%----- RIFLEX -----
RIF_WF_STD_1 = std(RRHFL1(:,1));
RIF_WF_STD_7 = std(RRHFL7(:,1));

RIF_LF_STD_1 = std(RRLFL1(:,1));
RIF_LF_STD_7 = std(RRLFL7(:,1));

RIF_TOT_STD_1 = std(RRIF(:,2));
RIF_TOT_STD_7 = std(RRIF(:,3));

DIFF_WF_SR1 = 100-(SIM_WF_STD_1/RIF_WF_STD_1)*100;
DIFF_WF_SR7 = 100-(SIM_WF_STD_7/RIF_WF_STD_7)*100;

DIFF_LF_SR1 = 100-(SIM_LF_STD_1/RIF_LF_STD_1)*100;
DIFF_LF_SR7 = 100-(SIM_LF_STD_7/RIF_LF_STD_7)*100;
```

```

%----- Creating a RES matrix with all the results -----
RES = zeros(6,4);

RES(1,1)=MIM_QS_WF_STD_1;   RES(1,2)=MIM_FEM_WF_STD_1;
RES(2,1)=MIM_LF_STD_1;     RES(2,2)=MIM_LF_STD_1;
RES(3,1)=MIM_TOT_QS_1;     RES(3,2)=MIM_TOT_FEM_1;
RES(4,1)=MIM_QS_WF_STD_7;  RES(4,2)=MIM_FEM_WF_STD_7;
RES(5,1)=MIM_LF_STD_7;     RES(5,2)=MIM_LF_STD_7;
RES(6,1)=MIM_TOT_QS_7;     RES(6,2)=MIM_TOT_FEM_7;

RES(1,3)=SIM_WF_STD_1;     RES(1,4)=RIF_WF_STD_1;
RES(2,3)=SIM_LF_STD_1;     RES(2,4)=RIF_LF_STD_1;
RES(3,3)=SIM_TOT_STD_1;    RES(3,4)=RIF_TOT_STD_1;
RES(4,3)=SIM_WF_STD_7;    RES(4,4)=RIF_WF_STD_7;
RES(5,3)=SIM_LF_STD_7;    RES(5,4)=RIF_LF_STD_7;
RES(6,3)=SIM_TOT_STD_7;    RES(6,4)=RIF_TOT_STD_7;

%----- Creating a Table for comparison -----
fprintf(fileID, 'Comparing WF tension STD for SIMO and RIFLEX:\n');
fprintf(fileID, '-----\n');
fprintf(fileID, '      | RIF-STD-WF | SIM-STD-WF | Diff   |\n');
fprintf(fileID, '      |   [kN]   |   [kN]   | [percent] |\n');
fprintf(fileID, '-----\n');
fprintf(fileID, ['LINE1 | ' num2str(RIF_WF_STD_1) ' | ' ...
num2str(SIM_WF_STD_1) ' | ' num2str(DIFF_WF_SR1) ' |\n']);
fprintf(fileID, ['LINE7 | ' num2str(RIF_WF_STD_7) ' | ' ...
num2str(SIM_WF_STD_7) ' | ' num2str(DIFF_WF_SR7) ' |\n']);
fprintf(fileID, '-----\n\n');

fprintf(fileID, 'Comparing LF tension STD for SIMO and RIFLEX:\n');
fprintf(fileID, '-----\n');
fprintf(fileID, '      | RIF-STD-LF | SIM-STD-LF | Diff   |\n');
fprintf(fileID, '      |   [kN]   |   [kN]   | [percent] |\n');
fprintf(fileID, '-----\n');
fprintf(fileID, ['LINE1 | ' num2str(RIF_LF_STD_1) ' | ' ...
num2str(SIM_LF_STD_1) ' | ' num2str(DIFF_LF_SR1) ' |\n']);
fprintf(fileID, ['LINE7 | ' num2str(RIF_LF_STD_7) ' | ' ...
num2str(SIM_LF_STD_7) ' | ' num2str(DIFF_LF_SR7) ' |\n']);
fprintf(fileID, '-----\n\n');

fprintf(fileID, '\n\n===== TENSION STD RESULTS =====\n\n');
fprintf(fileID, '      MIM-QS      MIM-FEM      SIM-QS      RIF-FEM\n');
fprintf(fileID, '-----\n');
fprintf(fileID, ' LINE1-WF    %3.2f    %3.2f    %3.2f    %3.2f\n', RES(1, :));
fprintf(fileID, ' LINE1-LF    %3.2f    %3.2f    %3.2f    %3.2f\n', RES(2, :));
fprintf(fileID, ' LINE1-TOT    %3.2f    %3.2f    %3.2f    %3.2f\n', RES(3, :));
fprintf(fileID, '-----\n');
fprintf(fileID, ' LINE7-WF    %3.2f    %3.2f    %3.2f    %3.2f\n', RES(4, :));
fprintf(fileID, ' LINE7-LF    %3.2f    %3.2f    %3.2f    %3.2f\n', RES(5, :));
fprintf(fileID, ' LINE7-TOT    %3.2f    %3.2f    %3.2f    %3.2f\n', RES(6, :));
fprintf(fileID, '\n\n=====');
%----- Bar plot for TENSION STD; MIM, SIM, RIF -----
scrsz = get(0, 'ScreenSize');
figure('Name', 'BAR plot of TENSION STD for MIM, SIM, RIF', ...

```



```

    'NumberTitle','off','Position',[100 scrsz(4)/12 scrsz(3)/2 scrsz(4)/1.2])

subplot(2,1,1);
bar(RES(1:3,:));
title(['Tension: Standard Deviation - Line1 (windward). H_s=' num2str(hs) 'm, T_p=' num2str(tp) 'm]);
set(gca,'XTickLabel',{'WF','LF','TOT'});
hleg1 = legend('MIM-QS','MIM-FEM','SIM-QS','RIF-FEM');
set(hleg1,'Location','NorthWest');
ylabel('STD Tension [kN]');
axis([0 4 0 220]);
grid on

subplot(2,1,2);
bar(RES(4:6,:));
title(['Tension: Standard Deviation - Line7 (leeward). H_s=' num2str(hs) 'm, T_p=' num2str(tp) 'm']);
set(gca,'XTickLabel',{'WF','LF','TOT'});
hleg1 = legend('MIM-QS','MIM-FEM','SIM-QS','RIF-FEM');
set(hleg1,'Location','NorthWest');
ylabel('STD Tension [kN]');
axis([0 4 0 220]);
grid on

saveas(gcf,['BarPlot_MSR_results_' num2str(hs) '_' num2str(tp) '.png'])
saveas(gcf,...
['C:\Users\Michael\Skole\Master-Var2013\LaTeX-Master\Figures\BarPlot_MSR_results_' num2str(hs) '.png'])
fprintf(fileID,'PLOT: --> BarPlot_MSR_results.png\n');
%
%-----Comparing the difference SIM-LF & RIF-LF-----
step = timestep_sim/timestep_rif;
compLF_1(1,1) = ((RRLFL1(1,1)-(RSLFL1(1,1)))/(RRLFL1(1,1)))*100;
compWF_1(1,1) = ((RRHFL1(1,1)-(RSHFL1(1,1)))/(RRHFL1(1,1)))*100;
compLF_7(1,1) = ((RRLFL7(1,1)-(RSLFL7(1,1)))/(RRLFL7(1,1)))*100;
compWF_7(1,1) = ((RRHFL7(1,1)-(RSHFL7(1,1)))/(RRHFL7(1,1)))*100;
for i=1:length(RSIM1)-1
    compLF_1(i+1,1) = ((RRLFL1(i*step,1)-(RSLFL1(i+1,1)))/(RRLFL1(i*step,1)))*100;
    compWF_1(i+1,1) = ((RRHFL1(i*step,1)-(RSHFL1(i+1,1)))/(RRHFL1(i*step,1)))*100;
    compLF_7(i+1,1) = ((RRLFL7(i*step,1)-(RSLFL7(i+1,1)))/(RRLFL7(i*step,1)))*100;
    compWF_7(i+1,1) = ((RRHFL7(i*step,1)-(RSHFL7(i+1,1)))/(RRHFL7(i*step,1)))*100;
end

% Difference between SIM & RIF - LF
%
% ----- LINE 1 -----
scrsz = get(0,'ScreenSize');
figure('Name','Difference between SIM & RIF - LF- LINE 1',...
    'NumberTitle','off','Position',[100 scrsz(4)/12 scrsz(3)/2 scrsz(4)/1.2])

%Comparing SIMO and RIFLEX LF tension for LINE 1
subplot(3,1,1)
plot(RSIM1(xscmpdiff:xcompdiff,2),RSLFL1(xscmpdiff:xcompdiff,1),'b',...
    RRIF(RIFxs:RIFxe,1),RRLFL1(RIFxs:RIFxe,1),'r')
title('Comparing SIMO and RIFLEX LF tension for LINE 1')
hleg1 = legend('SIM-LF','RIF-LF');
set(hleg1,'Location','NorthEast')
ylabel('Tension [kN]');
xlabel('Seconds [s]');
grid on

```

```

% LF motion in surge (from SIMO)
subplot(3,1,2)
plot(RTMOT(xscmpdiff:xcompdiff,2),RLFTMOT(xscmpdiff:xcompdiff,1),'b')
title('LF motion in surge')
hleg1 = legend('x-LF');
set(hleg1,'Location','NorthEast')
ylabel('Motion in x-direction [m]');
xlabel('Seconds [s]');
grid on

% Difference: SIM-LF & RIF-LF Line 1
subplot(3,1,3)
plot(RSIM1(xscmpdiff:xcompdiff,2),compLF_1(xscmpdiff:xcompdiff,1),'b')
title('Difference: SIM-LF & RIF-LF Line 1')
hleg1 = legend('Diff SIM-LF & RIF-LF');
set(hleg1,'Location','NorthEast')
ylabel('Diff [%]');
xlabel('Seconds [s]');
axis([RSIM1(xscmpdiff,2) RSIM1(xcompdiff,2) -3 3])
grid on

saveas(gcf,['Diff_LF_SIM_RIF_Line1_' num2str(RSIM1(xscmpdiff,2)) '_' ...
num2str(RSIM1(xcompdiff,2)) '.png'])
saveas(gcf,...
['C:\Users\Michael\Skole\Master-Var2013\LaTeX-Master\Figures\Diff_LF_SIM_RIF_Line1_' ...
num2str(RSIM1(xscmpdiff,2)) '_' num2str(RSIM1(xcompdiff,2)) '.png'])
fprintf(fileID,['PLOT: --> Diff_LF_SIM_RIF_Line1_' num2str(RSIM1(xscmpdiff,2)) '_' ...
num2str(RSIM1(xcompdiff,2)) '.png\n']);

% ----- Line 7 -----
scrsz = get(0,'ScreenSize');
figure('Name','Difference between SIM & RIF - LF- LINE 7',...
'NumberTitle','off','Position',[100 scrsz(4)/12 scrsz(3)/2 scrsz(4)/1.2])

% Comparing SIMO and RIFLEX LF tension for LINE 7
subplot(3,1,1)
plot(RSIM7(xscmpdiff:xcompdiff,2),RSLFL7(xscmpdiff:xcompdiff,1),'b',...
RRIF(RIFxs:RIFxe,1),RRLFL7(RIFxs:RIFxe,1),'r')
title('Comparing SIMO and RIFLEX LF tension for LINE 7')
hleg1 = legend('SIM-LF','RIF-LF');
set(hleg1,'Location','NorthEast')
ylabel('Tension [kN]');
xlabel('Seconds [s]');
grid on

% LF motion in surge (from SIMO)
subplot(3,1,2)
plot(RTMOT(xscmpdiff:xcompdiff,2),RLFTMOT(xscmpdiff:xcompdiff,1),'b')
title('LF motion in surge')
hleg1 = legend('x-LF');
set(hleg1,'Location','NorthEast')
ylabel('Motion in x-direction [m]');
xlabel('Seconds [s]');
grid on

% Difference: SIM-LF & RIF-LF Line 7

```

```

subplot(3,1,3)
plot(RSIM7(xscmpdiff:xcompdiff,2),compLF_7(xscmpdiff:xcompdiff,1),'b')
title('Difference: SIM-LF & RIF-LF Line 7')
hleg1 = legend('Diff SIM-LF & RIF-LF');
set(hleg1,'Location','NorthEast')
ylabel('Diff [%]');
xlabel('Seconds [s]');
grid on

saveas(gcf,['Diff_LF_SIM_RIF_Line7_' num2str(RSIM1(xscmpdiff,2)) '_' num2str(RSIM1(xcompdiff,2))
saveas(gcf,...
['C:\Users\Michael\Skole\Master-Var2013\LaTeX-Master\Figures\Diff_LF_SIM_RIF_Line7_' ...
num2str(RSIM1(xscmpdiff,2)) '_' num2str(RSIM1(xcompdiff,2)) '.png'])
fprintf(fileID,['PLOT: --> Diff_LF_SIM_RIF_Line7_' num2str(RSIM1(xscmpdiff,2)) '_' ...
num2str(RSIM1(xcompdiff,2)) '.png\n']);
%
end

```

### fatigue\_damage.m

```

function[] = fatigue_damage(fileID,fem_wf_mim,LF_mim)
%=====
%           Function: fatigue_damage.m
%           Functionality: Preformes fatigue damage calculation using
%                           the Combined Spectrum (CS) approach, which is
%                           considered as an conservative approach.
%=====

[n1 n_wf] = size(fem_wf_mim);
[n2 n_lf] = size(LF_mim);

%----- Input -----
mim_env = 1;
% Since SIM and RIF are compared with MIM,
% the first line in the env.dat is the
% seastate wich is compared. Therefore one
% wishes to no include this line in the
% fatigue damage analysis. See env.dat for
% MIMOSA. This means that you give in the
% line which you like to skip.

d = 0.130;
A = (pi/4)*(d^2);
% [mm] Mooring line diameter
% [mm^2] Area of mooring line

ad = 6.0*10^(10);
m = 3;
gamma = 1.3293;
Lyear = 20;
Td = Lyear*365*24*60*60;
duration = 20*365*24;
% [-] the intercept parameter of S-N curve
% [-] the slope pf the S-N curve
% Gamma function for m = 3
% [years] Designed Life Time
% [seconds]Designed Life Time in seconds
% [hours] Duration of data. 20 years.
%-----

% Creating SEASTATE matrix from Larsen's article. See reference list.
%-----
seastate = zeros(17+mim_env,4);
teller = 0;
peakperiod(:,1) = [6.60 8.42 9.54 10.40 11.14 11.79 12.38 12.93 13.45 ...

```

```

13.94 14.40 14.85 15.28 15.69 16.09 16.47 16.85];

dur_hour(:,1) = [31828 45969 39119 26881 15968 8452 4055 1783 712 ...
                274 97 32 10 3 0.8 0.2 0.05];

format long
for i = 1+mim_env:length(seastate)
    seastate(i,1) = i-1;
    seastate(i,2) = 0.5 + teller;
    seastate(i,3) = peakperiod(i-mim_env,1);
    seastate(i,4) = dur_hour(i-mim_env,1);
    teller = teller + 1;
end
%
%
% Calculating fatigue damage for Line 1 and 7
%
d_CS = zeros(n_wf,3);           % Column 1: Fatigue damage for Line 1
                                % Column 2: Fatigue damage for Line 7
for j = 1+mim_env:n_wf

    d_CS(j,1) = fem_wf_mim(2,j);

    % Fatigue Damage for Line 1
    sigmay1 = sqrt((fem_wf_mim(6,j)^2) + (LF_mim(5,j)^2));
    lamda_LF1 = (LF_mim(5,j)^2)/((LF_mim(5,j)^2) + (fem_wf_mim(6,j)^2));
    lamda_WF1 = (fem_wf_mim(6,j)^2)/((LF_mim(5,j)^2) + (fem_wf_mim(6,j)^2));
    vLF1 = 1/LF_mim(8,j);
    vWF1 = 1/fem_wf_mim(9,j);
    v1 = sqrt((lamda_LF1*vLF1^2) + lamda_WF1*vWF1^2);
    Ti1 = (seastate(j,4)/duration) * Td;
    d_CS(j,2) = ((v1*Ti1)/ad)*((2*sqrt(2*sigmay1))^m)*gamma;

    % Fatigue Damage for Line 7
    sigmay7 = sqrt((fem_wf_mim(14,j)^2) + (LF_mim(12,j)^2));
    lamda_LF7 = (LF_mim(12,j)^2)/((LF_mim(12,j)^2) + (fem_wf_mim(14,j)^2));
    lamda_WF7 = (fem_wf_mim(14,j)^2)/((LF_mim(12,j)^2) + (fem_wf_mim(14,j)^2));
    vLF7 = 1/LF_mim(15,j);
    vWF7 = 1/fem_wf_mim(17,j);
    v7 = sqrt(lamda_LF7*(vLF7^2) + lamda_WF7*(vWF7^2));
    Ti7 = (seastate(j,4)/duration) * Td;
    d_CS(j,3) = ((v7*Ti7)/ad)*((2*sqrt(2*sigmay7))^m)*gamma;

    max_wf_line1(j-mim_env,1) = (fem_wf_mim(8,j))/(1000*A);
    max_lf_line1(j-mim_env,1) = (LF_mim(7,j))/(1000*A);
    max_wf_line7(j-mim_env,1) = (fem_wf_mim(16,j))/(1000*A);
    max_lf_line7(j-mim_env,1) = (LF_mim(14,j))/(1000*A);
end
%Removes the row which is skipped due to input
d_CS(1:mim_env,:) = [ ];
%

```

```

% Plotting maximum stress and fatigue damage
%
scrsz = get(0, 'ScreenSize');
figure('Name', 'Fatigue Damage', ...
    'NumberTitle', 'off', 'Position', [100 scrsz(4)/12 scrsz(3)/2 scrsz(4)/1.2])

x_start = 0;
x_end = 20;

y_s_FD = 0;
y_e_FD = 0.6;
y_s_max = 0;
y_e_max = 250;

% Plotting Max stress Line 1 (Wf and LF)
subplot(2,2,1)
plot(d_CS(:,1), max_wf_line1(:,1), 'r', ...
    d_CS(:,1), max_lf_line1(:,1), 'b')
title('Maximum Stress - Line 1 (windward)')
hleg1 = legend('WF-line1', 'LF-line1');
set(hleg1, 'Location', 'NorthWest')
ylabel('Maximum Stress [MPa]');
xlabel('H_s [m]');
axis([x_start x_end y_s_max y_e_max]);
grid on

% Plotting Fatigue Damage Line 1
subplot(2,2,2)
plot(d_CS(:,1), d_CS(:,2), 'black')
title('Fatigue Damage - Line 1 (windward)')
%hleg1 = legend('WF-line1', 'WF-line7');
%set(hleg1, 'Location', 'NorthEast')
ylabel('Damage during 20 years');
xlabel('H_s [m]');
axis([x_start x_end y_s_FD y_e_FD]);
grid on

% Plotting Max stress Line 7 (Wf and LF)
subplot(2,2,3)
plot(d_CS(:,1), max_wf_line7(:,1), 'r', ...
    d_CS(:,1), max_lf_line7(:,1), 'b')
title('Maximum Stress - Line 7 (leeward)')
hleg1 = legend('WF-line7', 'LF-line7');
set(hleg1, 'Location', 'NorthWest')
ylabel('Maximum Stress [MPa]');
xlabel('H_s [m]');
axis([x_start x_end y_s_max y_e_max]);
grid on

% Plotting Fatigue Damage Line 7
subplot(2,2,4)
plot(d_CS(:,1), d_CS(:,3), 'black')
title('Fatigue Damage - Line 7 (leeward)')
%hleg1 = legend('WF-line1', 'WF-line7');
%set(hleg1, 'Location', 'NorthEast')
ylabel('Damage during 20 years');
xlabel('H_s [m]');
axis([x_start x_end y_s_FD y_e_FD]);
grid on

```

```
saveas(gcf, 'Fatigue_damage_LINE17.png')
saveas(gcf, ...
'C:\Users\Michael\Skole\Master-Var2013\LaTeX-Master\Figures\Fatigue_damage_LINE17.png')
fprintf(fileID, 'PLOT: --> Fatigue_damage_LINE17.png\n');
%-----
end
```

**RESULTS.txt**

## INPUT FILES

-----  
MIMOSA:  
--> RES\_FEM\_WF.dat  
--> RES\_QS\_WF.dat  
--> RES\_QS\_LF.dat

SIMO:  
--> B01r20c001  
--> B01r20c007

RIFLEX:  
--> moor\_elmfor.asc

## FILTER PROCESS

-----  
PLOT: --> FFT\_SR\_LINE17.png  
===== SIMO =====

## CHECKING FILTER

Testing Designed Filter for LINE 1 (windward line):

-----  
SIMO STD for WF&LF: 187.3805 [kN]  
SIMO STD for sqrt(WF^2+LF^2): 188.2722 [kN]  
Difference: 0.47359 [percent]

SIMO STD WF (filtered): 37.8812 [kN]  
SIMO STD LF (filtered): 184.4219 [kN]  
-----

Testing Designed Filter for LINE 7 (leeward line):

-----  
SIMO STD for WF&LF: 117.8497 [kN]  
SIMO STD for sqrt(WF^2+LF^2): 117.9077 [kN]  
Difference: 0.049214 [percent]

SIMO STD WF (filtered): 59.3249 [kN]  
SIMO STD LF (filtered): 101.896 [kN]  
-----

Ratio between:  
STD-WF-Line1 and -7: 1.5661 [-]  
STD-LF-Line1 and -7: 1.8099 [-]

```

===== RIFLEX =====
CHECKING FILTER

Testing Designed Filter for LINE 1 (windward line):
-----
RIFLEX STD for WF&LF:      201.2811 [kN]
RIFLEX STD for sqrt(WF^2+LF^2): 202.2744 [kN]
Difference:                0.49103 [percent]

RIFLEX STD WF (filtered):  41.9024 [kN]
RIFLEX STD LF (filtered): 197.8866 [kN]
-----

Testing Designed Filter for LINE 7 (leeward line):
-----
RIFLEX STD for WF&LF:      135.418 [kN]
RIFLEX STD for sqrt(WF^2+LF^2): 135.4585 [kN]
Difference:                0.029895 [percent]

RIFLEX STD WF (filtered):  83.138 [kN]
RIFLEX STD LF (filtered): 106.9442 [kN]
-----

Ratio between:
STD-WF-Line1 and -7:      1.9841 [-]
STD-LF-Line1 and -7:      1.8504 [-]

=====

PLOT: --> Timeseries_SIMO_filter.png
PLOT: --> Comparing_WF_LF_line1_7_SIMO.png
PLOT: --> Timeseries_RIFLEX_filter.png
PLOT: --> Comparing_WF_LF_line1_7_RIFLEX.png
PLOT: --> Comparing_SIMO_RIFLEX.png

COMPARING
-----
Comparing WF tension STD for SIMO and RIFLEX:
-----
| RIF-STD-WF | SIM-STD-WF | Diff |
| [kN] | [kN] | [percent] |
-----
LINE1 | 41.9024 | 37.8812 | 9.5964 |
LINE7 | 83.138 | 59.3249 | 28.6429 |
-----

```



Comparing LF tension STD for SIMO and RIFLEX:

```
-----  
| RIF-STD-LF | SIM-STD-LF | Diff |  
| [kN] | [kN] | [percent] |  
-----  
LINE1 | 197.8866 | 184.4219 | 6.8043 |  
LINE7 | 83.138 | 101.896 | 4.7204 |  
-----
```

===== TENSION STD RESULTS =====

	MIM-QS	MIM-FEM	SIM-QS	RIF-FEM
LINE1-WF	35.61	34.81	37.88	41.90
LINE1-LF	182.76	182.76	184.42	197.89
LINE1-TOT	186.19	186.04	187.38	201.28
LINE7-WF	56.64	66.49	59.32	83.14
LINE7-LF	104.94	104.94	101.90	106.94
LINE7-TOT	119.25	124.23	117.85	135.42

=====

PLOT: --> BarPlot\_MSR\_results.png

## Appendix F

# Marginal Distribution for $H_s$ Based on Joint Probability Distribution of $H_s$ and $T_P$ (from article)

This table is taken from the article written by C.M. Larsen [Larsen, 1987] and used for fatigue analysis in section 6.5.

Sea State	$H_s$	$T_p$	Duration, 20 years
no	[m]	[s]	[hours]
1	0,5	6,60	31828
2	1,5	8,42	45969
3	2,5	9,54	39119
4	3,5	10,40	26881
5	4,5	11,14	15968
6	5,5	11,79	8452
7	6,5	12,38	4055
8	7,5	12,93	1783
9	8,5	13,45	712
10	9,5	13,94	274
11	10,5	14,40	97
12	11,5	14,85	32
13	12,5	15,28	10
14	13,5	15,69	3
15	14,5	16,09	0,8
16	15,5	16,47	0,2
17	16,5	16,85	0,05

Table F.1: Marginal distribution for  $H_s$  based on joint probability distribution of  $H_s$  and  $T_P$ , retrieved from [Larsen, 1987]

# Appendix G

## Attached CD: Description of content

Including all the files in the appendix would occupy a lot of space, and is unnecessary. It is therefore more useful to give a good description of the content found on the attached CD, and also a description of the files used. A folder overview and a detailed file description is therefore given in this appendix.

In the ('READ ME.txt') file there is a recommendation of what programs could be used for reading the different files. File descriptions and what kind of purpose they serve is tabulated and explained in the table at the end of this appendix. This table is also included in the attached CD, ('File and Folder Description.pdf').

If the different batch scripts want to be executed it is necessary to create a environmental variables that links to the MIMOSA, SIMO, and RIFLEX programs. A detailed description of how this was done in this master thesis is given in the ('Environmental variable.txt') file.

### **FOLDER: Analysis**

An overview of what can be found in the analysis folder is listed below.

NOTE: Do not change the names of the folders if you want to run the analysis yourself.

1. FOLDER: MATLAB
2. FOLDER: MIMOSA\_analysis
3. FOLDER: RESULTS (is created after all the analysis and the ('Create\_RESULTS.bat') file has been executed)
4. FOLDER: RIFLEX\_analysis
5. FOLDER: SIMO\_analysis

If you want to run the analysis batch script ('MSR-Program.bat') environmental variables must be set for MIMOSA, SIMO and RIFLEX. Otherwise it will not work. On the other hand if environmental variables have been set one can simply copy the ANALYSIS folder from the CD to a arbitrary location on you computer. Then the MSR batch script should work. It is not recommended to run the analysis from the CD. Try to avoid spacing in the directory path when you copy the ANALYSIS folder to your computer.

NOTE: It is time consuming to run all the analysis for every program. So all the analysis have been executed beforehand.

### **Main Batch files**

('MSR Program.bat') - When clicking on this file a command (cmd) window will appear and a set of choices are available.

('Create\_RESULTS.bat') - After ALL the analysis are executed this batch file can be clicked. This will only copy the result files from MATLAB to a RESULT folder.

### **FOLDER: Created Scripts and Files**

In the analysis folder it can be difficult to find all the self made files. This folder includes all the self made files, and they are sorted in folders for where they were used. Here you also find a folder for the; MSR batch script and the post processing scripts. List of sub-folder which are found in this folder are:

1. FOLDER: MIMOSA
2. FOLDER: MSR Program
3. FOLDER: Post Processing
4. FOLDER: RIFLEX
5. FOLDER: SIMO

### **FOLDER: Input-files**

Here you will find the input files for MIMOSA, SIMO and RIFLEX in corresponding sub-folders.

### **FOLDER: Report**

In this folder you find the master thesis in PDF-format with PDF-bookmarks. Since this master thesis was written in Latex, no Microsoft word document is available. Some pages are blank because of the book format it was written in. It is recommended to print out the report in color, because it will then be easier to see the differences in the different plots.

**FOLDER: Result-Files**

As mentioned before it can be hard to find the files which you are looking for in the analysis folder. So here I have sorted the analysis and post processing results in the corresponding sub-folders.

1. FOLDER: MIMOSA
2. FOLDER: MIMOSA Parameter Case Study
3. FOLDER: Post Processing
4. FOLDER: RIFLEX
5. FOLDER: SIMO

<b>MIMOSA</b>	
File name	Description
<b>Files used in MIMOSA</b>	
<b>G1_medium.sif</b>	Includes the mass matrix, motion RAOs, Wave drift coefficients.
<b>mossi.dat</b>	Current and wind –quadratic coefficients, and linear damping (represents damping of mooring lines).
<b>dp.dat</b>	Thruster system: Only used to control fixed heading.
<b>env.dat</b>	Environmental data; waves, wind, current .
<b>moorsys-(CASE).dat</b>	Mooring system data (see MIMOSA user's manual). (CASE) = different mooring cases.
<b>RES_CALC_(*)*.dat</b>	Result file of the analysis run. (CALC) = calculation method (QS or FEM). (*) = LF or WF.
<b>(name).MAC</b>	MAC scripts that are used in MIMOSA. (name) = named MAC file. All MAC files have different name.
<b>run_mimosa_all.bat</b>	The main batch-file to execute all the sub-batch files.
<b>run_mimosa_CALC_(*)*.bat</b>	Sub-batch scripts for running different calculation method. (CALC) = calculation method (QS or FEM). (*) = LF or WF.
<b>SIMO</b>	
File name	Description
<b>Files used in SIMO</b>	
<b>sys.dat</b>	Input files for SIMO STAMOD which includes system descriptions (See SIMO user's Manual).
<b>(name).MAC</b>	Different MAC files. (name) = STA (STAMOD), DYN (DYNMOD), OUT (OUTMOD), SZX (SZXMOD). (name) can also have a different name depending on the use of this MAC file.
<b>(xx)-QS-(ss).lis</b>	Report and Result files (xx) = prd, prs, psc, pro. (ss) = STA (STAMOD), DYN (DYNMOD), OUT (OUTMOD).
<b>Folder: Results</b>	Include all the line tension force data files for the SIMO analysis. Also a Matlab-script (created in SZX mode), which explains what the different results files are and what they include.
<b>B01r20c001:</b>	File containing tension force results for time series (9 hour simulation) for line 1 (windward).
<b>B01r20c007:</b>	File containing tension force results for time series (9 hour simulation) for line 7 (leeward).
<b>B01r02c001:</b>	File containing translation total motion in surge (x-direction)
<b>run_simo_analysis.bat</b>	Batch file for executing the SIMO analysis
<b>RIFLEX</b>	
File name	Description
<b>Files used in RIFLEX</b>	
<b>moor_(zz)mod.inp</b>	moor = mooring line. (zz) = inp (INPMOD), sta (STAMOD), dyn (DYNMOD). Input files for RIFLEX (See RIFLEX user's manual).
<b>moor_(zz)mod.res</b>	Report and Result files from the analysis.
<b>dummy.tra</b>	RAOs for support vessel. Need to be included in RIFLEX even though it is not used.
<b>moor_elmfor.asc</b>	Result file; Tension force data results for time series (9 hour simulation), line 1 (windward) and line 7 (leeward).
<b>run_riflex_analysis.bat</b>	Batch file that executes the RIFLEX analysis.

<b>MATLAB</b>	
<b>File name</b>	<b>Description</b>
<b>Post_processing.m</b>	(Matlab Script): Main Matlab file. Executes all Matlab function).
<b>read_data.m</b>	(Matlab Function): Reads in all the result files from MIM, SIM, and RIF.
<b>filter_process.m</b>	(Matlab Function): Performs a FFT and uses design filter to filter out LF and WF tension forces form time series. This function also tests the designed filter.
<b>plot_process.m</b>	(Matlab Function): Plots different graphs.
<b>comparison.m</b>	(Matlab Function): Compares MIM, SIM, and RIF STD tension forces for line 1 and line 7, creates a bar plot and graphs for comparison.
<b>fatigue_damage.m</b>	(Matlab Function): Conducts a small fatigue damage analysis based on an article written by C.M. Larsen.
<b>RESULT.txt</b>	Results given in a text file.